INTERACTIONS OF RODENT CORONAVIRUSES WITH CELLULAR RECEPTORS

1992

GAGNETEN

UNIFORMED SERVICES UNIVERSITY OF THE HEALTH SCIENCES
F. EDWARD HÉBERT SCHOOL OF MEDICINE
4301 JONES BRIDGE ROAD
BETHESDA, MARYLAND 20814-4799

GRADUATE EDUCATION

APPROVAL SHEET

TEACHING HOSPITALS
WALTER REED ARMY MEDICAL CENTER
NAVAL HOSPITAL, BETHESDA
MALCOLM GROW AIR FORCE MEDICAL CENTER
WILFORD HALL AIR FORCE MEDICAL CENTER

Title of Dissertation: "Interactions of Rodent Coronaviruses with Cellular Receptors"

Name of Candidate: Sara Gagneten
Doctor of Philosophy Degree
May 8, 1992

Dissertation and Abstract Approved:

Committee Chairperson	May 8 1992 Date
Committee Member	May 8, 1992 Date
Committee Member	May 8, 1992 Date
Committee Member	May 8, 1992 Date
Committee Member	Oct 26, 1992 Date

The author hereby certifies that the use of any copyrighted material in the dissertation manuscript entitled:

"Interactions of Rodent Coronavirus with Cellular Receptors"

beyond brief excerpts is with the permission of the copyright owner, and will save and hold harmless the Uniformed Services University of the Health Sciences from any damage which may arise from such copyright violations.

Sara E. Gagneten
Department of Pathology
Uniformed Services University
of the Health Sciences

ABSTRACT

Title of Dissertation: Interactions of Rodent Coronavirus with Cellular Receptors

Sara Esther Gagneten, Doctor of Philosophy, 1992

Dissertation directed by: Kathryn V. Holmes Ph.D., Professor, Department of Pathology

Coronaviruses express a spike glycoprotein (S) on the viral envelope and a subset of coronaviruses expresses an additional glycoprotein (HE), that binds to a sugar moiety and has hemagglutinating and acetylesterase activities. This dissertation focuses on how interactions of these membrane glycoproteins with cell surface molecules affects virus species specificity and tissue tropism.

To study the role of the HE glycoprotein in MHV infection we used the anti-receptor MAb-CC1 to block binding of S to its receptor on various mouse cell lines and then challenged these cells with an HE expressing strain of MHV to determine whether this virus could use the HE alone to initiate viral infection. When the S glycoprotein was prevented from binding to its receptor by MAb-CC1 an MHV

strain expressing, HE could not infect mouse fibroblast cell lines or primary brain cells.

Although murine coronavirus (MHV) and rat coronavirus both cause common infections in colonies of laboratory rodents and are related antigenically, each virus is restricted to a single host species and the target organs for the mouse and rat viruses are different. A solid phase virus-binding assay was used to investigate the tissue specificity of binding of rat coronavirus. Rat coronavirus bound to membranes isolated from rat parotid and lacrimal glands, correlating well with the natural target tissues of this virus.

Both rat coronavirus and MHV can infect the same murine cell line. The hypothesis that rat homologs of the MHV receptor (MHVR) serve as receptors for rat coronavirus was tested. Antibodies to the MHV receptor that protected these cells against MHV infection, did not protect them against infection with rat coronavirus suggesting that the rat virus does not use MHVR to infect these cells. Rat ecto-ATPase, a glycoprotein homologous to MHVR was expressed in non-permissive hamster cells, but the cells remained resistant to infection with rat coronavirus. These studies show that closely related rodent coronaviruses utilize different receptors and that the receptor specificities of the viruses are important determinants of the tissue tropism of viral infection.

INTERACTIONS OF RODENT CORONAVIRUS WITH CELLULAR RECEPTORS

by

SARA ESTHER GAGNETEN

Dissertation submitted to the Faculty of the Department of Pathology Graduate Program of the Uniformed Services University of the Health Sciences in partial fulfillment of the requirement for the degree of Doctor of Philosophy, 1992

To my father, Alfredo Gagneten

ACKNOWLEDGEMENTS

I would like to express my deepest gratitude to my advisor, Dr. Kathryn Holmes, for her generous support and guidance.

Special thanks to Dr. Carl Dieffenbach, Dr. Gabriela Dveksler and Dr. Pablo Gutman for their discussions and advice.

Thanks to the members of the Department of Pathology and the Department of Microbiology who have always been eager to provide help, and especially everyone in Dr. Holmes' lab for their assistance and friendship.

Lastly, I wish to thank my mother Catalina, my brother and sisters, and Michel and Amanda for their understanding and love.

TABLE OF CONTENTS

	Page
I INTRODUCTION	1
ISOLATION AND GROWTH OF CORONAVIRUSES	1
Murine coronaviruses	1
Rat coronaviruses	8
Coronaviruses of other species	11
CORONAVIRUS STRUCTURE AND REPLICATION	12
Virion structure	12
N protein	16
M glycoprotein	16
S glycoprotein	17
HE glycoprotein	19
Nonstructural proteins	20
Genome organization	20
Replication	21
RNA recombination	25
VIRUS RECEPTORS	26
Definitions	27
Virus Specificity	27
Identification of Virus Receptors	28
Carbohydrate Receptors for Influenza Viruses	31
Glycoproteins in the Immunoglobulin (Ig)	

Superfamily that Serve as Receptors for HIV, Poliovirus, and Rhinovirus..... 32
Coronavirus Receptors..... 34

II MATERIALS AND METHODS..... 37
Cell Cultures..... 37
Preparation of Mouse Primary Brain Cell Cultures.. 38
Virus Propagation and Purification..... 38
Plaque assay..... 39
Hemagglutination Assay..... 41
Hemadsorption Assay..... 41
Acetylesterase Assay..... 42
Immunoblot Analysis..... 42
Receptor Blockade Experiments..... 44
Detection of Viral and Cellular Antigens by Immunofluorescence..... 46
Preparation of Intestinal Brush Border Membranes.. 50
Preparation of Hepatocyte Membranes..... 51
Preparation of Lacrimal and Salivary Gland Membranes 51
Preparation of Membranes from Other Tissues and Cell Cultures..... 52
Virus Overlay Protein Blot Assay (VOPBA)..... 53
Subcloning of the Rat Ecto-ATPase cDNA into a Eukaryotic Expression Vector and Transient Expression in BHK Cells..... 54

III THE ROLE OF MOUSE CORONAVIRUS HEMAGGLUTININ IN

INFECTION OF HOST CELLS..... 56
INTRODUCTION..... 56
RESULTS..... 58
Hemagglutination and Hemadsorption..... 58
Acetylesterase activity..... 62
Comparison of Viral Structural Proteins..... 67
Receptor Blockade..... 70
Reduction of Plaque Formation..... 78
Fluorescent-Antibody Staining to Detect Infection of Single Cells..... 83
Challenge of BHK and MDCK Cells with MHV-DVIM.. 84
Infection of Mixed Glial Cell Cultures with MHV-DVIM, MHV-A59, and MHV-JHM..... 87
Virus Overlay Protein Blot Assay of MHV-DVIM and MHV-A59 Binding to Intestinal Brush Border Membranes from BALB/c Mice..... 103
DISCUSSION..... 106
IV CHARACTERIZATION OF RAT CORONAVIRUS STRUCTURAL PROTEINS AND STUDIES ON THE RAT CORONAVIRUS RECEPTOR..... 110
INTRODUCTION..... 110
RESULTS..... 111
Replication of SDAV and PRCV on L2(Percy) Cells 111
Viral Structural Proteins..... 119
Antibody Blockade of the MHV Receptor..... 127
Studies on Interaction of Rat Coronavirus with Rat Homologs of the MHV Receptor..... 131

Virus Overlay Protein Blot Assays (VOPBA) of RCV and MHV on membrane tissues of different organs..... 139

DISCUSSION..... 145

V FUTURE DIRECTIONS..... 150

VI BIBLIOGRAPHY..... 155

LIST OF TABLES

Table		Page
1.	Coronaviruses: Names, Natural Hosts and Diseases..	13
2.	Host Cell Receptors for DNA and RNA Viruses.....	30
3.	Inhibition of MHV Plaque Formation on DBT Cells by MAb-CC1.....	79
4.	Inhibition of MHV Plaque Formation on L2 Cells by MAb-CC1.....	80
5.	Identification of MHV-Infected Cells in Primary C57BL/6 Mouse Central Nervous System Cultures.....	98
6.	Plaque Assay of MHV-A59, and Rat Coronavirus Strains SDAV and PRCV on L2 Cells and on Four Subclones of L2(Percy) Cells.....	118

LIST OF FIGURES

Figure		Page
1.	Model of coronavirus structure.....	15
2.	Model of coronavirus replication.....	23
3.	Hemagglutination of mouse erythrocytes by MHV-DVIM, MHV-A59, and BCV.....	61
4.	Hemadsorption of mouse erythrocytes to murine fibroblasts infected with two different strains of MHV.....	64
5.	Acetylesterase activities of gradient purified BCV, MHV-DVIM, and MHV-A59.....	66
6.	Immunoblotting of MHV-DVIM, MHV-A59, and BCV with anti-DVIM antiserum.....	69
7.	Immunoblotting of MHV-DVIM, MHV-A59, and BCV with antiserum against gp65 protein of BCV.....	72
8.	Immunoblotting of MHV-DVIM, MHV-A59, and BCV with antiserum against the S glycoprotein of MHV-A59...	74
9.	Protection of DBT cells from infection with MHV-DVIM or MHV-A59 by pretreatment of cells with anti-receptor MAb-CC1.....	77
10.	Plaque assay of MHV-DVIM and MHV-A59 in the presence and absence of anti-receptor MAb-CC1.....	82
11.	Fluorescent-antibody staining of DBT cells protected with anti-receptor MAb-CC1 and challenged with MHV-DVIM, MHV-A59, or MHV-JHM.....	86
12.	MAb-CC1 protection of BHK cells transfected with	

MHV-R and challenged with MHV-DVIM..... 89
13. Viral and cellular antigens in primary mouse brain cultures infected with various MHV strains..... 92
14. Viral and cellular antigens in primary mouse brain cultures infected with various MHV strains..... 94
15. Phenotype of MHV infected glial cells..... 97
16. Protection of mouse primary brain cells with MAb-CC1 from infection with various MHV strains..... 100
17. Protection of mouse primary brain cells with MAb-CC1 from infection with MHV-DVIM and MHV-A59..... 102
18. Binding of MHV-DVIM and MHV-A59 to intestinal brush border membrane proteins from BALB/c mice..... 105
19. L2, L2(Percy), and L2(Percy) clonal cells infected with MHV-A59 or SDAV..... 114
20. Plaque assay of MHV-A59, SDAV, and PRCV on L2, L2(Percy) and L2(Percy) clonal cells..... 117
21. Immunoblotting of RCV-SDAV, MHV-A59, and BCV with anti-RCV-SDAV antiserum..... 121
22. Immunoblotting of RCV-SDAV, MHV-A59, and BCV with antiserum against the S glycoprotein of MHV-A59... 124
23. Immunoblotting of RCV-SDAV, MHV-A59, and BCV with anti-HE antiserum against HE glycoprotein of BCV.. 126
24. Blocking of coronavirus infection of L2(Percy) subclone 41.a by anti-receptor MAb-CC1..... 130
25. Immunoblotting of membrane preparations of mouse and rat tissues with anti-ectoATPase..... 133

26. COS cells transiently transfected with rat ecto-ATPase and challenged with SDAV..... 136
27. Immunoblotting of cellular extracts of COS cells transfected with ecto-ATPase..... 138
28. Virus overlay protein blot assay (VOPBA) of MHV-A59 binding to membrane preparations of mouse and rat tissues..... 141
29. Virus overlay protein blot assay (VOPBA) of RCV-SDAV binding to membrane preparations of mouse and rat tissues..... 144

I. INTRODUCTION

The research presented in this thesis concentrated on two subjects involving rodents and virus receptors. For the first subject, experiments were designed to determine whether the strains of MHV which express the HE glycoprotein can use this molecule to bind to cell surface molecules containing N-acetyl-9-O-acetylneuraminic acid and initiate infection without the involvement of the S glycoprotein and its receptor. The second subject was to attempt to identify the molecule that serves as a receptor for rat coronavirus. This introduction covers three topics related to our work. First we describe the isolation of different coronaviruses with an emphasis on rodent coronaviruses and some aspects of their growth in culture. Second, we present important aspects of coronavirus structure and replication which further the understanding of the molecules involved in virus attachment to cellular receptors. Finally we present aspects of virus tropism and summarize the strategies employed in the identification of a few virus receptors.

ISOLATION AND GROWTH OF CORONAVIRUSES

Murine coronaviruses

More than 20 strains of mouse hepatitis virus (MHV)

have been described, but of these only a few have been studied extensively: MHV-JHM, MHV-3, MHV-S, and MHV-A59.

The first murine coronavirus described, was isolated in 1947 from two mice with spontaneous flaccid paralysis of the hind legs (Cheever et al., 1949). This neurotropic murine virus, initially called JHM, was passaged in mouse brain and found to cause disseminated encephalomyelitis accompanied by extensive demyelination of brain and spinal cord. Focal necrosis in the liver was also described.

Following this first report, a number of murine coronavirus strains were isolated, and although they were found to differ in the diseases that they cause they were all antigenically related and were called mouse hepatitis virus (MHV). A hepatotropic strain, MHV-1, was isolated from laboratory mice suffering from acute fatal hepatitis (Gledhill and Andrewes, 1951). MHV-1 alone produces a mild hepatitis in weanling mice, but when such mice are simultaneously infected with Eperythrozoon coccoides (normally a harmless blood parasite of mice) fatal hepatitis results. With the discovery of additional hepatotropic strains, MHV-2 in 1952 (Nelson, 1952) and MHV-3 in 1956 (Dick et al., 1956), differences among the different MHV strains and differences in MHV susceptibility among different mouse strains started to be noted. MHV-2 causes acute hepatitis in weanling Princeton mice which are more susceptible to death from MHV-2 than adult Princeton mice or

weanlings of other mouse strains (Nelson, 1952). In 1960, Bang and Warwick discovered that the genetic differences in susceptibility of MHV-2 in different strains of mice is reflected on the behavior of macrophages from the corresponding strains in culture. Macrophages from resistant mice (e.g. C3H strain) showed no destruction, whereas macrophages from susceptible mice were destroyed upon infection with MHV-2 in vitro. Furthermore, resistance to MHV-2 was found to depend on a single recessive gene. The clinical and histologic aspects of MHV-3, also depend on the strain of the host (Le Prevost et al., 1975a). After testing several mouse strains, three levels of viral sensitivity were observed upon intraperitoneal infection (i.p.) of adult mice with MHV-3 infection: susceptibility, semisusceptibility, and resistance (Le Prevost et al., 1975b). Twelve week old susceptible mice (e.g. DBA/2 and BALB/c strains) die 4 to 6 days after infection, but mice of the A/J and A/orl strain resist infection after the age of 6 weeks. In the semisusceptible group (e.g. C3H strain), 50% of the mice resist the acute disease at 12 weeks of age, but most of the surviving animals develop a chronic disease and paralysis.

MHV-A59, a hepatotropic strain that has been used extensively in our lab, was isolated in 1961 during the course of studies with the Moloney murine leukemia virus from a colony of BALB/c mice in which hepatitis was

frequently observed (Manaker et al., 1961). Via most routes of inoculation on ICR mice, MHV-A59 causes acute fatal hepatitis due to destruction of liver parenchymal and Kupffer cells (Hirano et al., 1981). When MHV-A59 is inoculated intracerebrally, it causes acute hepatitis and mild encephalitis followed by subacute spastic paralysis with demyelinating lesions in the brain and spinal cord (Lavi et al., 1984b). Early studies on the growth of MHV-A59 on normal and transformed cell lines, done with the purpose of identifying cell lines that would support the growth of MHV in culture, showed that growth of MHV-A59 was enhanced on transformed cell lines. Plaquing efficiency was higher and plaques were larger in spontaneously transformed cell lines such as AL/N and 17 Cl 1 than in untransformed cell lines (Sturman and Takemoto, 1972).

Ever since they were isolated, the MHV-JHM and MHV-A59 strains have been used extensively in research on the biology of coronaviruses and the pathogenesis of virus-induced demyelination. Most mouse strains are susceptible to infection by MHV-JHM and MHV-A59 (e.g. C57Bl/6, BALB/c, Pri, C3H) except for SJL/J mice which are resistant to viral infection (Stohlman and Frelinger, 1978; Smith et al., 1984). However, when SJL/J mice up to six weeks of age are inoculated intracerebrally with MHV-JHM, they are susceptible to viral infection and die (Stohlman et al., 1980). Therefore, there is a change with age in SJL mice

that protects them from central nervous disease. Genetically controlled resistance of mice to MHV infection may be due to lack of a receptor for virus attachment or to inappropriate intracellular virus replication, assembly and release. Host genetic control of MHV-A59 and MHV-JHM replication which imparts resistance to productive infection on SJL/J mice has been mapped to a single locus on chromosome 7 expressed in a recessive fashion (Knobler et al., 1981; Smith et al., 1984). Genetic resistance to MHV replication of SJL/J mice appears to be due to the lack of a functional virus binding receptor on the cellular membranes of these resistant mice (Boyle et al., 1987).

The experimental infection of the mouse central nervous system (CNS) by MHV-A59 and MHV-JHM has been used extensively as a model for the mechanism of viral induced-demyelination and the process of remyelination. Both MHV-A59 and MHV-JHM can induce acute encephalomyelitis and demyelination, although the outcome of the disease depends on the dose and the route of inoculation (Woyciechowska et al., 1984; Lavi et al., 1984c; Lucas et al., 1977). Using immunolabeling and electron microscopy Dubois-Dalcq et. al.(1982) showed that, in the CNS MHV-JHM infects neurons and non-neuronal cells, but MHV-A59 infects primarily non-neuronal cells. Considerable work has also been done on CNS infection of MHV-JHM in rats. Intracerebral inoculation of rats with MHV-JHM causes acute encephalomyelitis in 2-3 day

old rats or paralytic demyelinating disease at 10 days of age (Nagashima et al., 1978; Sorensen et al., 1980). Studies on primary rat brain cultures have shown that MHV-JHM can infect both neurons and oligodendrocyte-type-2 astrocytes (Pasick and Dales, 1991). However, no strain of MHV is known to infect rats under natural conditions.

Several enterotropic strains of MHV have also been identified. The first one to be described was isolated from infant C57BL mice and was designated lethal intestinal virus of infant mice (LIVIM) (Kraft, 1962). The agent is confined mainly to the intestinal tract and causes diarrhea and death in infant mice and inapparent infection in adults. LIVIM as well as other enterotropic MHV strains (e.g. MHV-Y) do not replicate in conventional cell cultures. Additional MHV strains that have been identified are MHV-D, MHV-S/CDC, MHV-Y (Barthold et al., 1982), and a strain called diarrhea virus of infant mice (MHV-DVIM). We will summarize here what is known about MHV-DVIM in greater detail since part of our research involved this MHV strain.

MHV-DVIM was isolated from an infant mouse with diarrhea. An important characteristic about MHV-DVIM is that it has hemagglutination (HA) and receptor destroying enzyme (RDE) activities which are not present in most MHV strains. MHV-DVIM agglutinates mouse red blood cells (RBC) at 4 °C. At 37 °C the hemagglutination is reversed (Sugiyama and Amano, 1980). MHV-DVIM-induced syncytia in DBT cell cultures

adsorb erythrocytes at 4 °C (Sugiyama and Amano, 1981).

Although the different MHV strains are generally described as neurotropic, hepatotropic, or enterotropic, this classification is relative and disease patterns overlap. For example, the neurotropic strain MHV-JHM also causes hepatitis (Bailey et al., 1949), the hepatotropic strain MHV-A59 can cause disease of the CNS following intracerebral inoculation (Lavi et al., 1984a; Woyciechowska et al., 1984), and some enterotropic MHV strains also cause hepatitis in infant mice (Barthold and Smith, 1984).

As we have described above, the pathogenesis of MHV is influenced by virus factors such as MHV strain, and host factors such as mouse strain. Route of inoculation also greatly affects the severity of disease of different MHV strains (Hirano et al., 1981). Intraperitoneal inoculation of C57BL/6 mice with MHV-A59 produces only hepatitis without involvement of the CNS (Lavi et al., 1984c), but when MHV-A59 is inoculated intracerebrally on C57BL/6 or C3H mice, it causes severe hepatitis and meningoencephalitis followed by demyelination (Lavi et al., 1984b; Woyciechowska et al., 1984).

Additional important host factors are age and immune status of the mouse. As for most viral infections, suckling mice are more susceptible to MHV infection than weanling or adult mice. Experimental inoculation of outbred Swiss mice at four weeks of age or younger causes demyelinative lesions

but inoculation of older animals (8-12 weeks) rarely causes lesions (Weiner, 1973). In adult BALB/c immunocompetent mice, MHV infection is not persistent, but in immunosuppressed mice the acute phase of the disease is more severe and the infection is more likely to disseminate to multiple organs.

In mice, MHV infection is the most prevalent of viral infections. In a survey that included 13 commercial facilities, 85% of these sites were found to be infected with MHV (Lindsey, 1986).

Rat coronaviruses

Rat coronaviruses were isolated much more recently than MHV and have been studied much less than MHV. Because a large part of my research was done on rat coronaviruses and their receptors, I will describe the diseases that they cause in detail. A coronavirus from rats was first isolated by Parker and coworkers (1970) from the lung of Fischer rats. Their isolate was called rat coronavirus (PRCV). Bhatt and coworkers (1972) isolated a second rat coronavirus from the salivary glands of rats with sialodacryoadenitis. This strain was designated sialodacryoadenitis virus (SDAV). A third rat coronavirus isolated from rats with inflamed salivary glands by Maru and Sato (1982) was called causative agent of rat sialoadenitis (CARS).

Although the rat coronaviruses were isolated fairly recently the disease was first described in 1961 (Innes and Stanton, 1961). Rat coronaviruses are highly infectious but the disease they cause is self limiting and rarely causes death. Characteristic signs include swelling of the neck from inflamed enlarged salivary glands and cervical lymph nodes, reddish nasal and ocular porphyrin discharges from inflamed lacrimal glands, and sneezing caused by acute rhinitis and photophobia. Other changes caused by rat coronaviruses are weight loss and reduced reproductive performance (Jacoby, 1986). Based on serological surveys, the incidence of endemic rat coronavirus infection in rat colonies is of 50 to 75% (Lindsey, 1986).

There have only been a few attempts to determine the influence of virus and host factors on rat coronavirus pathogenicity. Comparison of the incidence and distribution of lesions caused by PRCV and SDAV on SPF Wistar rats revealed that both strains have similar tissue tropisms causing inflammatory lesions in the respiratory tract and in the salivary and lacrimal glands (Percy and Williams, 1990). In one study, the immune state of the host was found to affect the outcome of the disease (Weir et al., 1990). Whereas rat coronavirus infection of immunocompetent rats is acute and self limited and infectious virus is eliminated by 7 days post inoculation (p.i.), in immunodeficient athymic rats, chronic active inflammation of salivary and lacrimal

glands persisted through day 90 p.i., indicating that normal T cell function is required for elimination of SDAV. Comparison of four rat strains (Wistar, Sprague-Dawly, and Long-Evans outbred rats and the Fischer344 inbred strain) for susceptibility to sialodacryoadenitis showed that the course of the disease was similar in these four strains (Percy et al., 1984).

The study of rat coronaviruses has been relatively slow because the diseases they cause are not devastating and, until recently, rat coronavirus could not be propagated in any continuous cell line. After testing a variety of continuous cell lines and primary cell cultures, Bhatt and coworkers (Bhatt et al., 1972) observed replication and CPE only in primary rat kidney (PRK) cells, and the virus titers obtained were low. Recently, replication of rat coronavirus on the LBC continuous cell line derived from a primary tumor in a Lewis rat (Hirano et al., 1986) and on the L2 mouse *fibroblast cell line* was reported (Percy et al., 1989; Percy et al., 1990). Comparison of the growth of SDAV on the LBC and L2 cells showed that on these cells SDAV can grow to fairly high titers (10^6-10^8 PFU/ml) and CPE was observed in both cell lines (Percy et al., 1989). PRCV was also found to grow to high titers on L929 and L2 mouse cells (Percy et al., 1990). My work on the cellular receptor for SDAV was made possible by Dr. Percy's discovery of an L2 cell line that propagates SDAV and PRCV at high titers.

Coronaviruses of other species

In 1968, a group of virologists proposed to the International Committee of Nomenclature of Viruses that a few viruses that had been recovered from man, namely strains 229E and B814, and mouse hepatitis virus which share the same appearance in negative stains, recalling a solar corona, should be included in a group which they suggested should be called the coronaviruses (Tyrrell et al., 1968). The coronaviridae family was officially recognized in 1975 (Tyrrell et al., 1975) and by then a great number of coronaviruses had been described. The first description of a disease caused by a coronavirus, dating from 1931, was avian infectious bronchitis virus infection of chickens (Schalk and Hawn, 1931). The causative agent, IBV, was isolated in 1937 by Beaudette and Hudson. The agent of transmissible gastroenteritis (TGEV) in swine was isolated in 1946 (Doyle and Hutchings, 1946), though the disease had been recognized several years earlier. As we mentioned above, MHV was also identified at about this time. In the years that followed, a great number of coronaviruses was described, including viruses that cause diseases in humans (human coronavirus, HCV-229E and HCV-OC43), turkeys (turkey coronavirus, TCV), dogs (canine coronavirus, CCV), cats (feline coronavirus, FIPV and FeCV), cattle (bovine coronavirus, BCV), and rats

(rat coronavirus, PRCV, SDAV and CARS). Most of these infect enteric or respiratory epithelium of their host species.

The family Coronaviridae now comprises 13 acknowledged coronaviruses of mammals and birds, grouped into 4 antigenic clusters (Wege et al., 1982). Table 1 lists some characteristics of these viruses.

CORONAVIRUS STRUCTURE AND REPLICATION

Virion structure

The coronaviridae are a family of enveloped viruses with a positive sense RNA genome and a characteristic morphology in negatively stained preparations with large petal spikes or peplomers that project from the viral membrane or envelope (Sturman et al., 1980). The general structure of the virions is shown in Figure 1. The virion contains an infectious RNA molecule of about 30,000 nucleotides (Boursnell et al., 1987) which is associated with the nucleocapsid proteins (N) to form a helical nucleocapsid which lies within a lipoprotein envelope (Sturman et al., 1980; Macnaughton et al., 1978). The envelope contains a lipid bilayer and two or three viral glycoproteins depending on the coronavirus. These are membrane protein (M), peplomer protein (S) and hemagglutinin esterase (HE). In all coronaviruses both the membrane

TABLE 1

Coronaviruses: Names, Natural Hosts, and Diseases

Antigenic group	Virus[a]	Host	Respiratory infection	Enteric infection	Hepatitis	Neurologic infection	Other[b]
I	HCV-229E	Human	X				
	TGEV	Pig	X	X			X
	CCV	Dog		X			
	FECV	Cat		X			
	FIPV	Cat	X	X	X	X	X
II	HCV-OC43	Human	X	?			
	MHV	Mouse	X	X	X	X	
	SDAV	Rat	X				X
	HEV	Pig	X	X		X	
	BCV	Cow		X			
	RbCV	Rabbit		X			X
III	IBV	Chicken	X				X
IV	TCV	Turkey	X	X			

a. Abbreviations: HCV-229E, human respiratory coronavirus; TGEV, porcine transmissible gastroenteris virus; CCV, canine coronavirus; FECV, feline enteric coronavirus; FIPV, feline infectious peritonitis virus; HCV-OC43, human respiratory coronavirus; MHV, mouse hepatitis virus; SDAV, sialodacryadentis virus; HEV, porcine hemagglutinating encephalomyelitis virus; BCV, bovine coronavirus; RbCV, rabbit coronavirus; IBV, avian infectious bronchitis virus; TCV, turkey coronavirus (turkey bluecomb disease).

b. Other diseases caused by coronaviruses include infectious peritonitis, runting, nephritis, pancreatitis, parotitis, and adenitis.

Adapted from Holmes, 1989. Used with permission.

Figure 1. Model of coronavirus structure. The viral nucleocapsid is composed of genomic RNA and nucleocapsid protein, N. The viral envelope bears the membrane glycoprotein, M, the spike glycoprotein, S, and the hemagglutinin-esterase glycoprotein, HE. Adapted from Holmes, 1989. Used with permission.

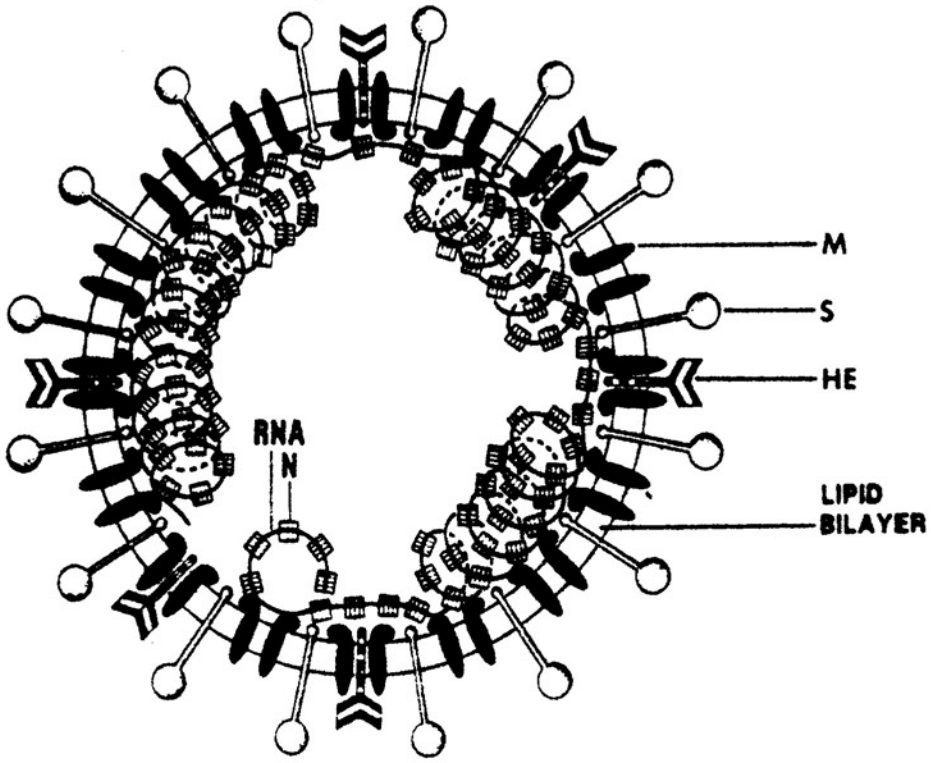
M
S
HE
RNA
N
LIPID
BILAYER

protein and the S glycoprotein span the lipid bilayer. In addition, the S glycoprotein forms the large surface projections. In coronaviruses from antigenic group II, a second surface projection is present which is shorter than the peplomer and has hemagglutinin and esterase activities. The characteristics of these virion components and the replication of coronaviruses are summarized below. The nomenclature for coronavirus proteins adopted in 1990 will be used (Cavanagh et al., 1990).

N protein. The nucleocapsid protein (N) is a phosphoprotein of 50-60 kDa. N is the major structural protein translated from coronavirus mRNA (Siddell, 1983). N undergoes phosphorylation at serine residues and it associates with newly synthesized genomic RNA molecules (Siddell et al., 1982). The encapsidated genomic RNA forms a long flexible nucleocapsid with helical symmetry. The nucleocapsid protein is probably involved in transcription, as antibodies against N of MHV inhibit in vitro synthesis of genomic RNA (Compton et al., 1987).

M glycoprotein. The small integral membrane glycoprotein (M) of 20-30 kDa becomes O-glycosylated in MHV and BCV (Holmes et al., 1981; Lapps et al., 1987) or N-glycosylated in IBV and TGEV (Stern and Sefton, 1982; Laude et al., 1987). Amino acid sequencing of M led to computer predictions of its

secondary structure in which the N-terminal part of the molecule is exposed on the outer surface of the virus membrane (Rottier et al., 1986). The next one third of the molecule forms hydrophobic α-helices which span the membrane three times. The C- terminal half of the molecule is located in the interior of the virus particle. Since M glycoprotein of MHV binds to isolated nucleocapsid *in vitro* (Sturman et al., 1980), it has been proposed that during virus assembly M may participate in binding nucleocapsid to the viral envelope.

S glycoprotein. The peplomer or spike glycoprotein S, with a size of 180-200 kDa forms the large club shaped surface projections typical of coronaviruses. S proteins are cotranslationally N-glycosylated and then acylated, possibly at cysteine residues. The peplomer proteins oligomerize into trimers before undergoing terminal glycosylation (Delmas and Laude, 1990). S proteins contain an N terminal signal sequence and a C-terminal hydrophobic domain by which they are most likely anchored in the membrane. A very important host dependent modification of some but not all coronaviruses is host proteolytic cleavage into two subunits (S1 and S2) of approximately equal molecular weight in MHV (Frana et al., 1985). The peplomer proteins of FIPV and TGEV are not cleaved.

The peplomer glycoprotein is crucial for virus

infectivity. In those coronaviruses where it is the only type of surface projection (e.g. MHV and FIPV), it binds to the host cell receptor and mediates fusion of viral and cellular membranes (Pfleiderer et al., 1990). Expression of the S gene of MHV on a vaccinia virus vector demonstrated that the S protein alone is sufficient to cause fusion of the membranes of recombinant vaccinia infected murine DBT cells. Fusion of the viral envelope of MHV and BCV with cellular membranes and infectivity of BCV are strongly enhanced by proteolytic cleavage of S (Sturman et al., 1985; Storz et al., 1981). S glycoproteins can be transported to the cell surface were they can participate in cell fusion which is an important mode of cell to cell spread of coronaviruses (Sturman and Holmes, 1983).

Protection against infection is obtained mainly with antibodies against the S glycoprotein. Experiments with monoclonal antibodies have enabled a better understanding of the functions of S. Since monoclonal antibodies directed against the S glycoprotein neutralize MHV and block fusion of infected cells, S probably contains both attachment and fusion activities (Collins et al., 1982). MHV strains with mutations on the S peplomer were obtained by selection for resistance to neutralization by monoclonal antibodies and these variants with small changes in S show important changes in neurovirulence (Dalziel et al., 1986; Fleming et al., 1986; Wege et al., 1988; Stuhler et al., 1991).

HE glycoprotein. The hemagglutinin esterase (HE) glycoprotein expressed on some coronaviruses (e.g. MHV-DVIM, MHV-JHM, BCV, HCV-OC43, HEV) is an additional surface protein which is cotranslationally N-glycosylated (Deregt et al., 1987). These 65 to 70 kDa glycoproteins appear as dimers on the surface of the virions (130-140 kDa) held together by disulfide bonds (King et al., 1985; Deregt et al., 1987). For several coronaviruses the gene encoding HE has been sequenced (Parker et al., 1989; Luytjes et al., 1988). Although MHV-A59 does not express HE, its genome contains the sequences encoding this protein but it lacks an initiator methionine for the correct translation of the protein. A 30% amino acid sequence homology has been found between the HE sequence of MHV-A59 and that of the HA1 subunit of the single glycoprotein of influenza C (Luytjes et al., 1988).

HE of BCV and HCV-OC43 like that of influenza C bind to N-acetyl-9-O-acetylneuraminic acid (Neu5,9Ac_2) residues on the membranes of erythrocytes and other cells (Vlasak et al., 1988a; Vlasak et al., 1988b). Viruses that express HE cause hemagglutination and hemadsorption which can be used to identify infected tissue culture cells. HE also has acetylesterase activity, which can permit elution of virus adsorbed to erythrocytes and destroy Neu5,9Ac_2 on the cell membranes (Vlasak et al., 1988a). Expression of the HE glycoprotein in vaccinia demonstrated that this protein has

both receptor destroying (esterase) and receptor binding (hemagglutination) activities (Pfleiderer et al., 1991).

Nonstructural proteins. The viral genome includes 5 or more open reading frames (ORF), depending on the coronavirus, that encode nonstructural proteins. Translation products of mRNAs which are believed to encode nonstructural proteins have been detected by in vitro translation or by using antisera against expression products in infected cells. These include a p28 protein expressed by MHV-JHM mRNA1 (Denison and Perlman, 1987) which is apparently the N-terminal cleavage product of the large polymerase polyprotein (Soe et al., 1987). Additional virus-specific peptides detected in MHV infected cells include a 15 kDa protein product of mRNA 4 (Ebner et al., 1988) and a 9.6 kDa product of the second ORF of mRNA 5 (Leibowitz et al., 1988). The functions of these proteins are not known.

Genome organization

The genomic RNA of coronaviruses is the largest of the RNA viruses (27-30 kb). The genome is organized into six or seven regions, each containing one or more ORFs which are separated by junction sequences that contain the signals for the transcription of subgenomic mRNAs (Budzilowicz et al., 1985).

Recently, extensive sequencing data has been obtained for several coronaviruses, including the complete genome of IBV and MHV. The 5' two thirds of the IBV genome encode non-structural proteins, probably the polymerase (Boursnell et al., 1987). The order of the ORFs encoding the structural viral proteins is 5'-HE-S-M-N-3'. The order remains the same for all coronaviruses except for the HE gene which is not present in the nonhemagglutinating coronaviruses. The number and location of additional ORFs encoding small nonstructural proteins varies among different coronaviruses (Spaan et al., 1988).

Replication

Coronaviruses attach to receptors on the membranes of the host cells. Coronaviruses that lack the HE surface glycoprotein bind to the cellular receptors by means of the S glycoprotein (Collins et al., 1982). For coronaviruses that bear two surface glycoproteins, S and HE, it is not yet known whether infection of host cells is initiated by binding of the S or HE glycoproteins to receptors on plasma membranes or if both interactions are required (Figure 2). After penetration, the plus strand genomic RNA, which is capped and polyadenylated, binds to ribosomes. The viral RNA-dependent RNA polymerase, is the first molecule to be translated on the ribosomes from viral genomes. This

Figure 2. Model of coronavirus replication. The subgenomic RNAs 2a, 3, 6, and 7 encode the HE, S, M glycoproteins, and the N phosphoproteins. Nonstructural proteins (NS) are translated from several mRNAs. Adapted from Holmes, 1989. Used with permission.

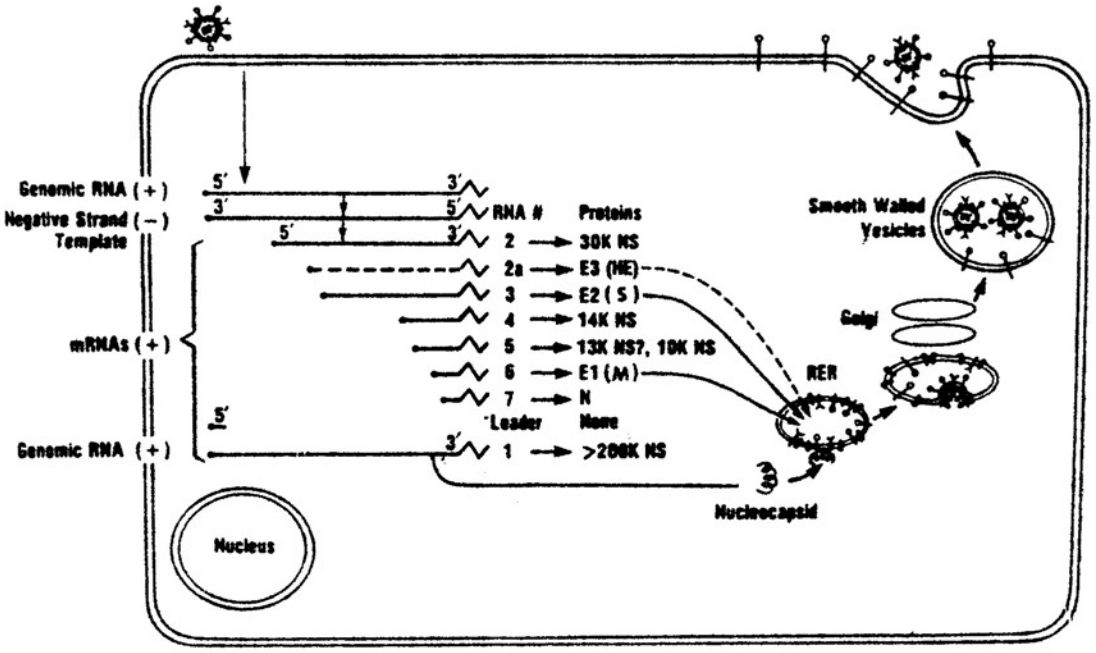
Genomic RNA (+)
Negative Strand (−) Template
mRNAs (+)
Genomic RNA (+)
5′
3′
RNA #
Proteins
2 → 30K NS
2a → E3 (NE)
3 → E2 (S)
4 → 14K NS
5 → 13K NS?, 10K NS
6 → E1 (M)
7 → N
Leader
None
1 → >200K NS
Nucleus
RER
Golgi
Smooth Walled Vesicles
Nucleocapsid

polymerase transcribes the genomic RNA into a full length negative strand RNA (Sawicki and Sawicki, 1986) which serves as a template for the synthesis of genomic RNA and a set of subgenomic messenger RNAs (Jacobs et al., 1981; Sethna et al., 1989).

The subgenomic mRNAs consist of a set of capped and polyadenylated RNA molecules which have common 3' ends. At the 5' end, each larger RNA contains an additional gene not found in the next smaller RNA. In addition, each mRNA contains an identical 5' leader sequence that is encoded in the 5' end of the genomic RNA and includes a short nucleotide sequence complementary to the junction sequences in the intergenic regions. This intergenic regions on the negative strand RNA template provides a complementary sequence for the leader RNA to bind to the initiation sites of the various subgenomic RNAs. The presence of the common leader on the nested set of mRNAs is explained by a mechanism in which mRNA synthesis is primed by leader transcripts which bind to one of the complementary junction sequences on the negative strand template (Baric et al., 1985; Lai et al., 1987). The genomic RNA gets incorporated into the newly assembled virions as the structural proteins are synthesized.

The mRNAs from which each protein is translated are shown in Figure 2. Most mRNAs are translated to yield one protein encoded by the ORF at the 5' end, e.g. mRNAs 3, 6,

and 7 yield the S, M, and N proteins, respectively (Siddell, 1983). The N protein and probably some nonstructural proteins are synthesized on polysomes in the cytoplasmic matrix. Synthesis of the M, S, and HE glycoproteins occurs on polysomes bound to the RER but they undergo different cotranslational and posttranslational modifications.

To form the helical nucleocapsid, the N proteins associate in the cytoplasm with the newly synthesized genomic RNA. The nucleocapsid, in turn, probably interacts with M glycoproteins on the membranes of the Golgi apparatus where both M and S have accumulated (Swift and Machamer, 1991). Virions then acquire their lipid bilayer when they bud into these intracellular membranes between the ER and the Golgi apparatus (Tooze et al., 1988). These newly formed virions are transported in cytoplasmic vesicles to the cell surface and released by exocytosis.

RNA recombination

High frequencies of coronavirus recombination and mutation are important features of coronavirus evolution. The recombination frequency between two coronaviruses in a single cell can be extremely high, approaching 10% in some cases (Makino et al., 1986). RNA-RNA recombination between MHV strains has been shown to occur both *in vitro* and *in vivo*. Recombination has been studied *in vitro* by performing

a cross between the fusion negative MHV-2, and a temperature-sensitive mutant of MHV-A59, which is fusion positive at the permissive temperature. By selecting fusion positive viruses at the nonpermissive temperature, recombinants containing multiple cross overs were isolated (Keck et al., 1988b). Recombination has also been demonstrated during replication of the virus in the animal host. By using two selectable markers, recombinant viruses were isolated from the brains of mice inoculated with two different strains of MHV (Keck et al., 1988a). This finding suggests that RNA-RNA recombination may play an important role in evolution. Recombination could possibly occur between coronaviruses and RNA viruses of other families. Nucleotide sequence analysis revealed a high similarity between the predicted amino acid sequence of the second ORF of mRNA 2 and the HA1 subunit of the influenza C spike protein (Luytjes et al., 1988).

VIRUS RECEPTORS

Since our work concentrated on two aspects of receptor recognition for two rodent coronaviruses, I will describe important concepts on virus receptors that were known at the beginning of my research.

Definitions

Attachment of a virus to a host cell is the first step in the virus infection. Attachment is mediated by the binding of a viral attachment protein (VAP) to a molecule on the cell surface that acts as a virus receptor. The VAPs are polypeptides on the membranes of enveloped viruses and on the capsid of non-enveloped viruses. Virus receptors are the structures on the surface membrane of cells to which virus binds prior to entering the cell (Tardieu et al., 1982). Binding of virus particles to receptors brings them into close physical contact with the cell surface which leads to fusion of the viral envelope with host cell membranes, introducing viral nucleocapsid into the cytoplasm.

Virus Specificity

An important feature of certain viral infections is the selective infection of specific tissues or of specific cells within a tissue. A classic example is poliovirus infection of anterior horn cells in the spinal cord (Jubelt et al., 1980). For some but not all viruses, cellular receptors determine the species-, tissue-, and cell-tropisms of the virus. An example of determination of tissue tropism by expression of cellular receptors is the infection of T lymphocytes and monocytes, epidermal Langerhans cells and

brain cells by human immunodeficiency virus (HIV1) (Klatzmann et al., 1984a; Tschachler et al., 1987; Maddon et al., 1986).

For productive virus infection, following binding of the virus to its receptor, the nucleocapsid must be internalized, the genome must be replicated, transcribed and translated, and new virions must be assembled and released. In different types of cells viral replication may be blocked at any stage of the virus life cycle. Therefore, cell receptors are not the only determinants of cell and tissue tropism. For example, it has been shown using immunofluorescence and electron microscopy, that Epstein Barr Virus (EBV) can attach to a particular human T lymphocyte cell line (Molt4), in which virus penetration does not occur (Menezes et al., 1977).

Identification of Virus Receptors

Though virologists have been interested in virus receptors for as long as they have been interested in other aspects of virus structure and replication, except for the early identification of sialic acid as the receptor for influenza A, until recently few virus receptors had been identified. Identification of virus receptors has proved difficult for many reasons. An important technical reason for the late development of this field has been the

difficulty of purifying cell membrane molecules. Biological aspects inherent to viruses and receptors have also hampered the progress of receptor studies. Virus particles may adhere nonspecifically to many substances, including inert materials as well as various cell surface molecules through electrostatic interactions (Tardieu et al., 1982). Therefore it may be very difficult to distinguish between nonspecific and biologically relevant binding. Specific virus receptors may be present on the cell surface in very small quantities. In addition some viruses may be able to utilize more than one type of cell membrane component as receptors. Viruses can also bind via intermediate molecules to cell surface components. For example, anti-virus antibodies bound to viruses, may interact with Fc receptors on cell surfaces which may lead to uptake of the virus-antibody complex (Homsy et al., 1989).

Table 2 shows some examples of well characterized virus receptors (Lentz, 1990). Two criteria have been used to confirm the identification of a virus receptor: 1) to show that purified receptor binds virus and 2) to show virus infection of cells transfected with the gene encoding the receptor and which prior to the transfection did not bind virus.

TABLE 2

Host Cell Receptors for DNA and RNA Viruses

Virus Family	Virus	Host Cell Receptor	References
Paramyxoviridae	Sendai Virus	Sialyloligosaccharides	Paulson et.al., 1979
	Newcastle Disease Virus	Sialyloligosaccharides	Paulson et.al., 1979
Orthomyxoviridae	Influenza Virus	Sialyloligosaccharides	Paulson, 1979; Paulson, 1985
Lentivirinae	HIV-1	CD4 Molecule of T lymphocyte	Dalgleish et.al., 1984; Klatzmann et.al.,1984b; McDougal et.al., 1986
Picornaviridae	Poliovirus	PVR member of immunoglobulin Superfamily	Mendelsohn et.al., 1989
	Human Rhinovirus	Intercellular adhesion molecule-1 (ICAM-1)	Greve et.al., 1989; Staunton et.al., 1989; Tomassini et.al., 1989
Herpesviridae	Epstein-Barr Virus	C3d receptor CR2 (CD21) of B Lymphocyte	Fingeroth et.al., 1984

Carbohydrate Receptors for Influenza Viruses

The hemagglutinin glycoproteins (HA) of influenza A and B viruses bind to sialic acid containing oligosaccharides on cell surface glycoproteins and/or glycolipids. Treatment of cultured cells with neuraminidase destroys their susceptibility to influenza virus infection and reintroduction of the sialic acid to oligosaccharides by cloned siacyl transferases restores the capacity of the cells to bind virus and initiate infection (Paulson et al., 1979). Recent X-ray crystallography studies, determined the three dimensional structure of HA complexed to cell receptor analogs containing sialic acid. The sialic acid residue fills the conserved receptor binding pocket on the HA glycoprotein (Weis et al., 1988).

Influenza viruses A and B bind via hemagglutinin (HA) to receptors on erythrocytes causing hemagglutination and possess neuraminidase glycoprotein (NA) with receptor-destroying enzyme activity. Influenza C virus carries only one surface protein, a hemagglutinin-esterase (HE) (Palese and Schulman, 1976; Nakada et al., 1984) that has both receptor-binding (hemagglutinin) and receptor-destroying activity (Vlasak et al., 1987), an acetylesterase which releases acetyl residues from position C-9 of 9-O-acetyl-N-acetylneuraminic acid (Neu5,9AC_2) (Herrler et al., 1985). This carbohydrate is the receptor determinant for influenza

C on tissue culture cells (Herrler and Klenk, 1987; Rogers et al., 1986).

Glycoproteins in the Immunoglobulin (Ig) Superfamily that Serve as Receptors for HIV, Poliovirus, and Rhinovirus

The receptor for HIV, CD4 is expressed on helper T lymphocytes and cells of the monocyte/macrophage lineage. Anti-CD4 antibodies block HIV1 infection of CD4+ cells *in vitro* (Klatzmann et al., 1984b). When CD4+ or T4+ T lymphocytes were exposed to HIV1, the viral envelope glycoprotein, gp120, was found to associate with the CD4 molecule (McDougal et al., 1986). Confirmation that CD4 functions as the receptor for HIV was obtained with the demonstration that cells resistant to HIV infection, became susceptible to infection after they were transfected with a cDNA encoding CD4 (Maddon et al., 1986).

The receptors for poliovirus and the major groups of human rhinoviruses, are also members of the immunoglobulin superfamily. Ninety percent of rhinovirus serotypes (the major group) share a single receptor on the surface of human cells. The major group rhinovirus receptor was isolated using two different approaches. Greve and coworkers (1989) isolated the receptor by transfecting human DNA into rodent cells and screening for virus susceptibility. A second approach, similar to the strategy our laboratory is

considering for the identification of the rat coronavirus receptor, identified the major group rhinovirus receptor by the use of monoclonal antibodies that blocked infection with the majority of the rhinovirus serotypes which recognized a 90 kDa protein on HeLa cells (Colonno et al., 1986). A protective monoclonal antibody was used to purify the receptor glycoprotein. Amino acid sequence information of the purified protein was used to clone the receptor. Murine cells transfected with the receptor cDNA, acquired the ability to bind rhinovirus as well as anti-receptor monoclonal antibody. Sequencing of the receptor cDNA showed that the receptor is the cell adhesion molecule ICAM-1 (Greve et al., 1989; Tomassini et al., 1989), a member of the Ig superfamily whose natural ligand is the lymphocyte integrin LFA-1. Subsequently purified human ICAM-1 binds specifically to the major rhinovirus serotypes (Staunton et al., 1989).

The strategy to isolate the poliovirus receptor gene used DNA mediated transformation. Receptor-negative mouse L cells were transformed with DNA from HeLa cells which are susceptible to infection (Mendelsohn et al., 1989). Transformants that bound an anti-receptor monoclonal antibody and were susceptible to poliovirus infection were isolated. Screening of genomic libraries prepared from the L cells transformants using the human Alu repeat sequence yielded clones encoding the cell receptor for poliovirus.

Subsequent isolation of cDNA clones from a HeLa cell library and sequencing of the receptor cDNA revealed that the poliovirus receptor is also a member of the immunoglobulin superfamily (Mendelsohn et al., 1989).

Coronavirus Receptors

At the time I started this work, our group was working on the identification and cloning of the MHV and HCV receptors. Experiments using an *in vitro* binding assay developed in our lab, the virus overlay protein blot assay (VOPBA), had shown that MHV-A59 bound to a 110-120 kDa glycoprotein on intestine and liver membranes of susceptible BALB/c mice, while membrane proteins of MHV resistant adult SJL/J mice did not bind virus (Boyle et al., 1987). This result suggested that the resistance of SJL/J mice to MHV infection may be due to the absence of a functional receptor on the cellular membranes of these mice.

Monoclonal anti-receptor antibodies which protect cells from MHV infection were prepared by immunizing receptor-negative SJL/J mice with intestinal brush border membrane preparations from MHV-susceptible BALB/c mice. An anti-receptor monoclonal antibody, MAb-CC1, was identified which blocks MHV-A59 infection of cultured mouse fibroblasts and recognizes a 110-120 kDa glycoprotein on hepatocyte and intestinal brush border membranes of susceptible BALB/c

mice. This monoclonal antibody was used for the immunoaffinity purification of the 110-120 kDa MHV receptor from livers of susceptible mice (Williams, et al., 1990).

As explained above, some MHV strains, including MHV-DVIM and MHV-JHM (Siddell, 1982; Sugiyama and Amano, 1981), in addition to the S glycoprotein, bear on their envelopes an HE glycoprotein that has hemagglutinating activity. We thought that it could be possible, as it occurs for influenza C virus, that binding of HE to molecules containing Neu5,9Ac_2 serves as an alternative route of infection for these HE+ strains of MHV. To attempt to answer this question I used the anti-receptor MAb-CC1, to block binding of S to its receptor, to determine whether MHV-DVIM and MHV-JHM could use HE alone to bind to receptors and initiate infection.

A second major goal of my work on rodent coronavirus receptors was to identify a molecule that serves as a receptor for rat coronavirus. Since the L2(Percy) mouse fibroblast cell line is susceptible to both MHV and rat coronavirus infections, I was interested in determining whether these two viruses share the same receptor on these cells. I also used the anti-receptor MAb-CC1 to determine whether it could protect L2(Percy) cells from both MHV and rat coronavirus infection. In addition we used membrane preparations of different organs and animal species on virus binding assays to investigate the species specificity and

the tissue tropism of rat coronavirus.

II. MATERIALS AND METHODS

Cell Cultures

L2 cells derived from C3H murine fibroblasts, and the 17 CL 1 cells derived from spontaneously transformed BALB/c 3T3 cells were obtained from Dr. L. Sturman, State Department of Health, Albany, NY. L2(Percy) cells were obtained from Dr. D. Percy, University of Guelph, Ontario, Canada. DBT cells were established from a brain tumor in a CDF1 mouse inoculated intracerebrally with Rous sarcoma virus. Human rectal tumor cells (HRT18) were obtained from Dr. D. Brian, University of Tennessee, Knoxville, TN. These cell lines were propagated in Dulbecco's modified Eagle medium (DMEM) with 10% fetal bovine serum (FBS) and 2% penicillin-streptomycin-fungizone (PSF) mix (all culture reagents were from GIBCO laboratories). BHK21 cells, derived from baby hamster kidney and MDCK cells derived from canine kidney were obtained from the American Type Culture Collection (ATCC), Rockville, MD. BHK and MDCK cells were propagated in minimum essential medium (Eagle) with Earle's BSS, 10% FBS, and 2% PSF mix. Medium for BHK cells contained, in addition, 1% tryptose phosphate broth. COS cells transfected with the rat ecto-ATPase gene were obtained from Dr. S. H. Lin, M.D. Anderson Cancer Center, Houston, TX and propagated in DMEM with 10% FBS and 2% PSF.

Single cell clones of L2(Percy) cells were obtained by preparing a cell suspension of 10 cells/10 ml medium and plating in 96 well plates using 100 μl cell suspension/well. Forty five single cell clones were grown and tested for virus susceptibility. Of these, six were chosen and subcloned one more time.

Preparation of Mouse Primary Brain Cell Cultures

Primary brain cultures were prepared from 2 day old C57Bl/6 mice as described by Dyer and Benjamins (1988). After the meninges were carefully dissected from the surface of the cerebral hemispheres, the brain was digested in MEM containing 0.25% trypsin and 10 μg of DNase/ml, for 10 minutes at 37°C. After centrifugation for 10 minutes at 150 xg the tissues were further disrupted by passing through a 25 gauge needle and through a 60 μm sieve. Cells were centrifuged for 10 minutes at 150 xg and resuspended in DMEM containing 10% FCS, 25 μg/ml of gentamycin (GIBCO) and 1 mM sodium pyruvate and plated on poly-L lysine coated coverslips. Cells were refed every three days, and at twelve days after plating they were used for experiments.

Virus Propagation and Purification

MHV-A59 was obtained from Dr. L. Sturman, State

Department of Health, Albany, NY and MHV-DVIM was provided by Dr. Maru, Shionogi Research Laboratories, Osaka, Japan. MHV-JHM was obtained from the ATCC. MHV-A59 and MHV-JHM were grown on 17 Cl 1, and MHV-DVIM was grown on DBT cells. Sialodacryoadenitis virus (SDAV) and Parker's rat coronavirus (PRCV) obtained from Dr. D. Percy were propagated on L2(Percy) cells. Bovine coronavirus (BCV) was obtained from Dr. D. Brian and was grown on HRT18 cells.

For some experiments, density gradient purified virus was used. It was prepared as described for MHV-A59 (Sturman et al.1980). Briefly, supernatant medium from virus infected cultures was harvested, clarified by centrifugation at 150 xg, precipitated with 30% polyethylene glycol and purified by discontinuous followed by continuous sucrose density gradients. Virus recovered from a 1.17 g/cc band in the continuous sucrose gradients was pelleted for 2 hours at 24,000 rpm in a Beckman SW28 rotor and resuspended in TMS (0.05 M Tris, 0.05 M maleic acid, 0.1 M sodium chloride pH 6) with or without 1% BSA.

Plaque assay

MHV-A59 and MHV-JHM were titered on L2 cells; MHV-DVIM was titered on DBT cells; SDAV and PRCV were titered on L2(Percy) cells according to the following protocol. Virus supernatants from infected cells or gradient purified

viruses were diluted in a 10-fold series in DMEM with 10% FBS. From each dilution, 0.5 ml/plate was used to inoculate each of three 60 mm tissue culture plates with confluent cell monolayers. Virus was adsorbed for 1 hour at 37°C with rocking every 20 minutes. The inoculum was removed and 5 ml/plate of agar overlay (MEM with 4% FBS, 2% PSF, and 0.95% Noble agar) were added. Plates were inverted and incubated at 37°C. After 2 days plaques were developed with the addition of 3 ml/plate agar with the above medium and 0.02% neutral red. When plaque assays were done in the presence of trypsin, 3 μg/ml trypsin (Sigma) was added to the agar overlay.

We measured the ability of anti-receptor MAb-CC1 (hybridoma culture supernatant) to inhibit plaque formation of MHV-A59 and MHV-DVIM. L2 and DBT cell monolayers on 60 mm plates were pretreated with 1 ml of MAb-CC1 or an irrelevant control MAb of the same isotype directed against cholera toxin (MAb-CT) diluted 1:2 in culture media for 1 hour at 37°C. Monoclonal antibodies were then removed and cells were challenged with 0.5 ml/plate of each of the ten fold virus dilutions and the plaque assay proceeded as described above.

Plaque assays were also done in the continuous presence of MAb-CC1 and control MAb. After 1 hour pretreatment with monoclonal antibodies as described above, cells were challenged with 0.5 ml/plate of each virus dilution containing 50% MAb-CC1 or control MAb for 1 hour at 37°C.

The inoculum was then removed and monolayers were overlaid with an agar solution containing MAb-CC1 or control MAb (10% MAb-CC1 or control MAb in MEM with 4% FBS, 2% PSF and 0.95% Noble agar). Plates were incubated for two days at 37°C and plaques were developed with an agar overlay containing neutral red.

Hemagglutination Assay

Red blood cells (RBC's) were harvested from BALB/c mice and stored in Alsver's solution (Gibco-BRL) at 4°C for not more than 4 days. Before use in the hemagglutination assay or the hemadsorption assay, cells were washed twice with cold phosphate buffered saline (PBS).

Hemagglutination test was done on a 96 well microtiter dish. Equal volumes (100 μl) of serial 2 fold dilutions of gradient purified virions and a suspension of 0.4% v/v mouse RBC's in PBS with Ca^{++} and Mg^{++} were used. Plates were incubated at 4°C for 2 hours and hemagglutination was recorded as the reciprocal of the highest virus dilution causing a detectable hemagglutination.

Hemadsorption Assay

Hemadsorption tests were performed on MHV-infected DBT cell monolayers grown on 60 mm tissue culture plates. After

the infection had produced syncytia (20 hours p.i. for MHV-A59 and 26 hours p.i. for MHV-DVIM), a 0.5% suspension of mouse RBC's was allowed to adsorb for 2 hours at 4°C. Monolayers were fixed with 2% paraformaldehyde in PBS for 15 minutes at room temperature and unattached erythrocytes were removed with 4 gentle washes of 5 ml PBS. Adsorption of RBC's was confirmed by light microscopy.

Acetylesterase Assay

Acetylesterase assays were done as previously described (Vlasak, et al., 1988a). Five micrograms of gradient purified virion preparations were incubated at room temperature in 1 ml of PBS containing 1 mM p-nitrophenyl acetate. A 100 mM stock solution was prepared by dissolving p-nitrophenylacetate in acetonitrile in such a way that the final acetonitrile concentration in the assay was 1%. Hydrolysis of the substrate was measured at 400 nm with a Beckman DU-7 spectrophotometer at 1 minute intervals.

Immunoblot Analysis

Glycoproteins from purified virions were separated by sodium dodecyl sulfate-polyacrylamide gel electrophoresis (SDS-PAGE) on 8% gels. Six micrograms of purified virions was loaded per lane. After electrophoresis, gels were

transferred onto nitrocellulose paper by electroblotting with a Trans-blot apparatus (Biorad Laboratories, Richmond, CA) for 16 hours at 150 mA in 25 mM Tris pH 8.6, 0.192 M glycine and 20% methanol. Nitrocellulose sheets were blocked for at least 24 hours at 4°C in 2% bovine serum albumin (BSA) in dilution buffer (50 mM Tris HCl pH 7.4, 150 mM NaCl, 1 mM EDTA, 0.05% Tween 20, and 0.1% BSA) to reduce non-specific binding. Nitrocellulose sheets were then incubated for 1 hour with mouse polyclonal antibody to MHV-DVIM, goat antibody to the S glycoprotein of MHV-A59, rabbit antibody to the HE glycoprotein of BCV (kindly provided by Dr. D. Brian), or mouse (ascites) polyclonal antibody to SDAV (kindly provided by Dr A. Smith, University of Yale, New Haven, CT). The four antisera were diluted 1:100 in dilution buffer. After five washes in dilution buffer, sheets were incubated for 1 hour with radioiodinated staphylococcal protein A ^{125}I-SPA (New England Nuclear Corp.); specific activity approximately 8 μCi/μg, 10^5 cpm/ml; 25 ml per 3 by 5 inches nitrocellulose sheet). After five washes with dilution buffer the nitrocellulose sheets were air dried and exposed to Kodak XAR-5 film at -70°C.

Immunoblot of membrane preparations of mouse and rat was done following similar procedures except, 200 μg protein/lane were separated on a 8% SDS-PAGE gel. After transfer to nitrocellulose blots were incubated with rabbit antibody to the denatured form of ecto-ATPase diluted 1:500

in dilution buffer.

Receptor Blockade Experiments

Monoclonal antibodies were used in the receptor blockade experiments. These were anti-MHV-receptor monoclonal antibody-CC1 (MAb-CC1) and a control monoclonal antibody of the same isotype (MAb-CT). Both were hybridoma culture supernatants. Cells in 96 well microtiter plates were incubated with serial 2 fold dilutions of monoclonal antibodies for 1 hour at 37°C. Antibodies were removed and the cells were challenged with 10^5 PFUs of virus per well. The inoculum was removed and cultures were incubated at 37°C. When the infection had advanced sufficiently (16 hours for MHV-A59, 36 hours for MHV-DVIM, and 20 hours for SDAV), cell survival was measured using the MTT colorimetric assay or cells were fixed and stained with crystal violet.

The MTT colorimetric assay (Chemicon, Temecula, CA) was performed to measure cell viability following the instructions of the manufacturer. MTT (3-(4,5-dimethylthiazol-2-yl)-2,5-diphenyl tetrazolium bromide) is a yellow substrate that is cleaved in the mitochondria of living cells to yield a dark blue formazan product whereas in dead cells MTT does not undergo cleavage. 0.01 ml MTT solution was added to each well. The plate was incubated at 37°C for 4 hours to permit cleavage of MTT. 0.1 ml

isopropanol/HCl was added to each well and mixed thoroughly by repeated pipetting with a multichannel pipettor. The isopropanol dissolves the formazan to give a homogeneous blue solution suitable for adsorbance measurement. The adsorbance was measured immediately on an ELISA plate reader (Dynatech Laboratories Inc.) at a wavelength of 570 nm.

For experiments in which the CPE on the monolayers was the endpoint, supernatants were removed and wells were rinsed twice with PBS. Cells were fixed with 0.1 ml normal buffered formalin for 15 minutes at room temperature. Formalin was removed and cells were stained with 0.05 ml of crystal violet at 25°C. Intact monolayers take on a uniform dark violet coloration while infected monolayers show holes where cells were killed by the virus and/or detached.

BHK cells expressing the MHV receptor or DBT cells were plated on coverslips. When the cells were confluent they were pretreated at 37°C for 1 hour with monoclonal antibody CC1 (MAb-CC1) or with control MAb (MAb-CT) diluted in an equal volume of culture medium. Cells were challenged with MHV-A59, MHV-DVIM, or MHV-JHM. The inocula contained 10^6 PFU/ml with 50% monoclonal antibody supernatant. After 1 hour at 37°C the inoculum was removed and fresh medium with 10% monoclonal antibody CC1 or control monoclonal antibody was added. At 10 hours post infection (p.i.) cells were fixed and intracellular viral antigens were detected by immunofluorescence as described below.

COS cells transiently transfected with the ecto-ATPase cDNA (Lin and Guidotti, 1989) in a cdm8 vector were kindly provided by Dr. S. H. Lin, MD Anderson Cancer Center, Houston, TX, and BHK cells transiently transfected with the ecto-ATPase cDNA in a RSVneo vector were plated on coverslips. COS cells were inoculated with 1 ml SDAV (MOI=5) five days after the transfection, and BHK cells were inoculated with 1 ml SDAV ($5x10^5$ PFU/ml or MOI=0.5) or PRCV ($4.4x10^6$ or approximate MOI=4.4) 3 days after the transfection. The inoculum was replaced with fresh medium and cultures were incubated at 37°C. Cells were fixed 8 and 24 hours p.i. in acetone as explained above.

L2(Percy) cell monolayers on coverslips on 24 well plates were pretreated with rabbit anti-MHV-receptor antibody, or rabbit antibody against undenatured ecto-ATPase purified from rat liver, diluted 1:2 in culture medium. After 1 hour at 37°C, antibodies were removed and cells were challenged with 0.5 ml SDAV or PRCV ($5x10^5$ and $4.4x10^6$ PFU/ml respectively) for 1 hour at 37°C. The inoculum was then replaced by fresh media, cells were incubated at 37°C, and fixed in acetone 8 and 24 hours p.i. as explained above.

Detection of Viral and Cellular Antigens by Immunofluorescence

Eight or 10 hours p.i. cells on coverslips were washed

with PBS, fixed in acetone at -20°C for 10 minutes, air dried and stored at -20°C. Acetone fixed coverslips were rehydrated for 10 minutes in PBS containing 2% normal goat serum (NGS), incubated with 0.05 ml of a 1:100 dilution of mouse polyclonal anti-MHV-DVIM convalescent serum in PBS for 30 minutes at 37°C. After 4 washes in PBS the coverslips were incubated with 1:100 rhodamine-labeled goat anti-mouse immunoglobulin G (IgG) (CAPPEL) at 37°C for 30 minutes, washed four times with PBS and examined with a Zeiss fluorescence microscope. Antibody dilutions and washes were done with PBS containing 2% normal goat serum.

COS cells and BHK cells transiently transfected with ecto-ATPase were stained using two-color immunofluorescence for the detection of rat coronavirus antigens and ecto-ATPase expression. Two primary antibodies mouse anti-SDAV ascites (kindly provided by Dr. Smith, Yale University, New Haven, CT) and rabbit polyclonal against the native form of purified ecto-ATPase were mixed and diluted 1:100 in PBS. The secondary antibodies, rhodamine conjugated goat anti-mouse IgG to visualize SDAV antigens and fluorescein conjugated goat anti-rabbit IgG (CAPPEL) to visualize ecto-ATPase were mixed in 1:100 and 1:40 in PBS respectively.

Primary brain cells prepared as described above were pretreated with 0.5 ml/well anti-receptor MAb-CC1 or a control MAb of the same IgG isotype for 1 hour at 37°C. The cells were challenged with 1 ml of inoculum containing 50%

MAb-CC1 or control MAb and $1x10^6$ PFU/ml MHV-DVIM, MHV-A59, or MHV-JHM. After 1 hour at 37°C the inoculum was removed and fresh medium with 10% MAb-CC1 or control MAb was added. Ten hours p.i. brain cells were fixed with 1 ml/well of 2% paraformaldehyde dissolved in PBS without Ca^{++} and Mg^{++}, for 10 minutes. Cells were rinsed twice with PBS and immunofluorescence staining was performed.

The phenotype of infected cells and the presence of viral antigens were identified using three color immunofluorescence which enabled simultaneous visualization of oligodendrocytes with anti-galactocerebroside (GC), astrocytes with anti-glial fibrillary acidic protein (GFAP), and MHV with anti-MHV-DVIM. A second set of cells was stained to allow the simultaneous identification of oligodendrocyte-type 2 astrocyte (O-2A) progenitor cells with the O4 antibody, astrocytes with anti-GFAP, and MHV antigens with anti-MHV-A59. Anti-GC is a rabbit polyclonal, O4 is a mouse monoclonal IgM, anti-GFAP is a rat polyclonal, anti-MHV-DVIM is a mouse convalescent serum, and anti-MHV-A59 is a rabbit polyclonal. All antibodies used for the labeling of primary brain cells (except for anti-MHV antibodies) were kindly provided by Dr. M. Dubois-Dalcq, NIH, Bethesda, MD.

For one set of cells, anti-GC was diluted 1:50 in PBS and applied to the cells for 30 minutes. Anti-GC was visualized with fluorescein conjugated donkey anti-rabbit.

After three washes the secondary antibody was diluted 1:50 in PBS and applied for 30 minutes. After three washes, the cultures were permeabilized with 100% ethanol for 10 minutes at -20°C to expose internal antigens. After three washes, anti-GFAP and anti-MHV-DVIM were mixed, diluted 1:50 in PBS and applied to cells for 30 minutes. Anti-GFAP was visualized with biotinylated donkey anti-rat IgG diluted 1:50 in PBS and applied for 30 minutes followed by 3 washes and streptavidin conjugated 7-amino-4-methyl-coumarin-3-acetic acid diluted 1:40 in PBS and applied for 1 hour. Anti-MHV-DVIM was visualized with rhodamine conjugated anti-mouse IgG diluted 1:50 in PBS and applied for 30 minutes. After three washes, coverslips were mounted on glass slides with 20% 0.02 M tris buffer pH 8.2 and 80% glycerol. All incubations with antibody were done at room temperature and all washes were done with PBS.

A second set of cells was stained following the same steps as described above but using different primary and secondary antibodies. O4 MAb was diluted 1:20 and applied for 30 minutes. O4 was visualized with rhodamine conjugated goat anti-mouse diluted 1:50 and applied for 30 minutes. After permeabilization with ethanol anti-GFAP and anti-MHV-A59 were mixed, diluted 1:50 and applied for 30 minutes. Anti-GFAP was visualized with biotinylated donkey anti-rat IgG followed by streptavidin conjugated 7-amino-4-methyl-coumarin-3-acetic acid. Anti-MHV-A59 was visualized with

fluorescein conjugated donkey anti-rabbit diluted 1:50.

Stained cells were observed in a immunofluorescence microscope equipped with three filter sets to view rhodamine, fluorescein, and coumarin (Zeiss Axiophot).

Preparation of Intestinal Brush Border Membranes

The method of Kessler and coworkers, (1978) was followed for the preparation of intestinal brush border membranes (BBM). Mouse and rat intestines were flushed with ice-cold PBS and frozen in liquid nitrogen. Tissues were stored at -70°C until needed. Fifteen milliliters of homogenization buffer (300 mM mannitol, 2 mM Tris HCl, pH 7.1) per gram of intestine was used to homogenize the tissue in a Tekmar Tissumizer (Cincinnati, Ohio). Calcium chloride was added to a final concentration of 10 mM and particulates were removed from the homogenate by centrifugation at 4000 xg for 15 minutes at 4°C. The supernatant was centrifuged at 15,000 rpm for 45 minutes at 4°C in a SW28 rotor. Pellets were resuspended in TE (10 mM Tris HCl pH 7.4 and 1 mM EDTA pH 8.0) and stored at -70°C. Protein concentrations were determined on all membrane preparations by the Bradford method (Bradford, 1976).

Preparation of Hepatocyte Membranes

Hepatocyte plasma membranes were prepared as previously described (Neville, 1976). Briefly, livers were harvested from BALB/c mice or Wistar-Furth rats, frozen in liquid nitrogen and stored at -70°C. Liver homogenates (0.5 g/ml of buffer) were prepared in 1 mM sodium carbonate buffer, pH 7.5 using a Dounce homogenizer and filtered to remove debris. Homogenates were centrifuged at 1500 xg for 30 minutes at 4°C. Pellets were homogenized again, resuspended until sucrose concentration was 44%, overlaid with 42.3% sucrose and centrifuged in a Beckman SW28 rotor at 22,340 rpm for 2 hours at 4°C. The material on top of the sucrose cushion was harvested, diluted in sodium carbonate buffer a discontinuous 3, 27, and 50% sucrose gradient and centrifuged in a SW28 rotor at 1746 rpm for 1 hour at 4°C. Material at 27-50% interface was harvested, diluted in TE, pelleted in SW28 rotor at 15,000 rpm for 45 minutes, and finally resuspended in TE and stored at -70°C.

Preparation of Lacrimal and Salivary Gland Membranes

Lacrimal exorbital and intraorbital glands and salivary submandibular and parotid glands were removed from Wistar-Furth rats, dissected free of fat, frozen in liquid nitrogen and stored at -70°C. Glands were thawed and 1 ml cold

homogenization buffer (0.25 M sucrose, 1 mM EDTA, and 1 mM DTT) per gram tissue was added. Tissues were homogenized in a Tekmar Tissumizer. Equal volumes of buffer and homogenate were mixed and then centrifuged at 2000 xg for 10 minutes at 4°C. The supernatant was centrifuged at 17,000 rpm for 15 minutes at 4°C in a SW28 rotor. Pellets were resuspended in buffer (10 mM Tris pH 7.4, 1 mM DTT, and 1 mM EDTA) and placed in a discontinuous sucrose gradient of 38 over 42% sucrose, and centrifuged at 25,000 rpm for 1 hour at 4°C in a SW28 rotor. Material on top of the 38% sucrose interface was harvested, diluted 1:2 in Tris-DTT-EDTA buffer and centrifuged at 17,000 rpm for 15 minutes at 4°C in a SW28 rotor. The resulting pellet was rinsed with Tris-DTT-EDTA buffer and finally resuspended in this buffer and stored at -70°C.

Preparation of Membranes from Other Tissues and Cell Cultures

Lungs were removed from Wistar-Furth rats, frozen in liquid nitrogen and stored at -70°C. Tissues were thawed and homogenized in 10 ml PBS without Ca^{++} and Mg^{++} per gram tissue in a Tekmar Tissumizer. One volume of PBS was added and the homogenate was spun at 700 xg for 5 minutes at 4°C. The resulting supernatant was centrifuged in a SW28 Beckman rotor at 25,000 rpm for 15 minutes at 4°C, and the pellet

was resuspended in cold PBS and then centrifuged. The final pellet, a crude preparation containing membranes, was resuspended in PBS and stored at -70°C.

Cultured cells grown in 150 cm^2 flasks were washed twice with PBS without calcium and magnesium. Ten milliliters of cold PBS with EDTA were added to each flask. After 10 minutes the cell monolayer was scraped and the cells were transferred to 50 ml conical tubes and centrifuged at 150 xg for 5 minutes. The cell pellets were washed twice in PBS with EDTA and resuspended in cell disruption buffer (10 mM potassium phosphate, pH 7.4 and 0.1 mg/ml of phenylmethyl-sulfonyl fluoride [Sigma]). Cells were allowed to swell on ice for 5 minutes and then homogenized with a Dounce homogenizer ('A' pestle). The homogenate was then centrifuged at 1000 xg for 5 minutes and the supernatant obtained was further centrifuged in an SW 28 rotor at 25,000 rpm for 1 hour at 4°C. Pelleted membranes were resuspended in cold TE (10 mM Tris HCl pH 7.4 and 1 mM EDTA pH 8.0) and stored at -70°C.

Virus Overlay Protein Blot Assay (VOPBA).

Membrane proteins (200 μg protein/lane) were separated on 8% SDS-PAGE, and transferred onto nitrocellulose paper as described above under the immunoblot analysis section. After blocking with 2% BSA in blocking buffer, the nitrocellulose

sheets were incubated for 1 hour with virus supernatant (MHV-DVIM, MHV-A59 or SDAV) containing 10 mM HEPES pH 7.4 or with medium alone. Unbound virus was removed by washing five times for five minutes each with dilution buffer. Bound virus was detected using anti-viral antibody (1:50 dilution of mouse anti-MHV-DVIM or anti-MHV-A59 convalescent sera; a 1:50 dilution of goat anti-S glycoprotein of MHV-A59 or a 1:500 dilution of mouse anti-SDAV ascites fluid) followed by detection with radioiodinated Staphylococcal protein A, with five washes after each incubation. The dried nitrocellulose sheets were then exposed to Kodak XAR-5 film for autoradiography.

Subcloning of the Rat Ecto-ATPase cDNA into a Eukaryotic Expression Vector and Transient Expression in BHK Cells

The rat ecto-ATPase cDNA subcloned in the expression vector cdm 8 was a gift from Dr. Sue-Hwa Lin, Houston, TX (Lin and Guidotti, 1989). To achieve high levels of expression, the ecto-ATPase cDNA was subcloned behind the Rous Sarcoma virus long terminal repeat. The insert was excised from the cdm 8 plasmid by digestion with Hind III and Not I. After digestion, the insert was separated from the plasmid by electrophoresis on a 1% agarose gel. The insert was recovered from the gel by incubation with glass milk beads under the recommendations in the geneclean kit

(Bio 101). pRSVneo was digested with Hind III and Eag I and ligated to the ecto-ATPase cDNA in a 10 μl reaction in the presence T4 DNA ligase, for 12 hours at 4°C. Two microliters of the ligation reaction were used to transform DH5α competent cells (GIBCO-BRL, Gaithersburg, MD) and plasmids containing the desired insert were selected by hybridization with an oligonucleotide probe complementary to the ecto-ATPase sequence labelled with gamma ^{32}P ATP in the presence of T4 polynucleotide kinase. The selected colony was grown in 500 ml of Super broth (0.089 M $KHPO_4$, bacto-yeast extract 24 g, bacto-tryptone 12 g, glycerol 4 ml, pH7.5) with ampicillin (Sigma) at a concentration of 50 μg/ml. Plasmid DNA was prepared by detergent lysis followed by double cesium chloride (Life Technologies) density gradient centrifugation.

Transfection of the plasmid containing the rat ecto-ATPase into the BHK line of baby hamster kidney fibroblasts was done with an electroporator (BRL Cell Porator at 330 capacitance and 300 volts) using 10 μg plasmid/10^7 cells in culture medium. Cells were plated on cover slips. Seventy two hours after the electroporation, cells were inoculated with SDAV or PRCV and incubated for 1 hour at 37°C. Inoculum was replaced with fresh media and cells were fixed 8 and 24 hours p.i. with acetone for 15 minutes at -20°C. Cover slips were stored at -20°C and immunofluorescence staining was performed after rehydration with PBS.

III. THE ROLE OF MOUSE CORONAVIRUS HEMAGGLUTININ IN INFECTION OF HOST CELLS

INTRODUCTION

Coronaviruses, such as HCV-OC43, BCV, HEV, and some strains of MHV, express hemagglutinin-esterase glycoproteins which have hemagglutination (receptor binding) and acetylesterase (receptor destroying) activities (Vlasak et al., 1988a; Vlasak et al., 1988b; Parker et al., 1989; Schultze et al., 1990; Yokomori et al., 1989; Sugiyama and Amano, 1980) like the HE glycoprotein of influenza C virus (Vlasak et al., 1987). The acetylesterase of these HE glycoproteins removes acetyl residues from position C-9 of N-acetyl-9-0-acetylneuraminic acid (Neu5,9Ac_2) (Herrler et al., 1985). Influenza C virus uses this molecule as a receptor determinant for virus attachment to cell membranes and for initiation of infection (Herrler and Klenk, 1987).

Although the S, N, and M structural proteins are present in all MHV strains, the HE glycoprotein is expressed only in some strains. The genome of MHV-A59 contains the gene coding for the HE protein, but MHV-A59 does not express this protein because its ORF lacks a translation initiation codon (Luytjes et al., 1988). The MHV-JHM strain expresses variable levels of HE depending on the passage history of different isolates (Yokomori et al., 1991). MHV-DVIM was

isolated from the intestine of infant mice with diarrhea and its biological and morphological properties were examined. Unlike most MHV strains, but like BCV, MHV-DVIM expresses a 69 kDa glycoprotein (Sugiyama et al., 1986), agglutinates mouse RBC's (Sugiyama and Amano, 1980), and the syncytia induced in MHV-DVIM-infected mouse fibroblasts hemadsorb mouse RBC's (Sugiyama and Amano, 1981).

The experiments in this section were designed to determine whether the HE glycoprotein of MHV is capable of binding to cell surface receptors containing N-acetyl-9-O-acetylneuraminic acid (Neu5,9Ac_2) and infecting host cells independently of the S glycoprotein. Since HE may bind to glycoprotein receptors containing sialic acid of any animal species, expression of HE may help a virus overcome the species specificity barrier and infect cells which would be nonpermissive for binding of the S glycoprotein. Our general strategy was to use the anti-receptor MAb-CC1 to block binding of S to its receptor on cultured cells and then challenge these cells with HE-bearing virus to test the capacity of these strains to use the HE to infect cells.

It is also possible that HE bearing viruses might have an advantage when replicating <u>in vivo</u>, or in a particular organ system rather than in tissue culture. We therefore investigated whether viruses that express HE have an advantage over viruses that do not, when replicating in primary brain cells. MHV-A59 and MHV-JHM cause infection of

oligodendroglia leading to acute encephalomyelitis and/or subacute demyelination (Lavi et al., 1984c; Weiner, 1973). After MHV-JHM inoculation of 4 to 5 week old Lewis rat brains in vivo, virus variants have been isolated which express a larger S glycoprotein (Taguchi et al., 1985). Inoculation of 10-day-old Wistar Furth rat pups with MHV-JHM, yielded a smaller S protein (Morris et al., 1989; La Monica et al., 1991) and expression of HE could not be detected (La Monica et al., 1991). On the other hand, variants expressing a 65 kDa glycoprotein, possibly HE, have been isolated from rat primary glial cell cultures after inoculation with wt-JHMV (Taguchi et al., 1986). Because these results suggested that strong selective processes favoring virus variants may occur in the brain, we used primary mouse brain cell cultures to determine whether HE of MHV-DVIM could use and alternative receptor on these cells, leading to infection without the need for the S glycoprotein.

RESULTS

Hemagglutination and Hemadsorption

Prior to investigating the role of the hemagglutinin in attachment to host cells, we performed four preliminary assays to confirm that the MHV-DVIM strain of mouse

coronavirus received from Dr. Maru, Shionogi Research Laboratories, Osaka, Japan, expresses a functional HE glycoprotein. These assays were immunoblot analysis, hemadsorption, hemagglutination, and acetylesterase activity. We compared the biological properties of MHV-DVIM to those of MHV-A59, which does not express HE (Luytjes et al., 1988), and to BCV which expresses HE (King et al., 1985; King and Brian, 1982).

The hemagglutination titer of MHV-DVIM was compared to the titer of MHV-A59 and BCV (Figure 3). Since MHV-DVIM grows to very low titers on cultured cells, for this experiment we had to use gradient purified virus to concentrate the virus supernatant of infected cultures about 1000 fold. To determine the hemagglutination titers for the three viruses on the same plate, the concentration of the purified virions used in the assay was adjusted so the initial protein concentration of BCV was 1/10 that of MHV-DVIM and MHV-A59. While mouse RBC's incubated with BCV or MHV-DVIM showed a hemagglutination titer of 512 HAU/5μg and 32 HAU/50μg respectively, RBC's incubated with MHV-A59 did not hemagglutinate.

The hemadsorption activity of MHV-DVIM was also compared to that of MHV-A59. MHV-DVIM or MHV-A59 infected DBT cells were assayed after extensive syncytia had formed in the infected cultures; 20 hours p.i. for MHV-A59 and 26 hours p.i. for MHV-DVIM because MHV-A59 is a faster growing

Figure 3. Hemagglutination of mouse erythrocytes by MHV-DVIM, MHV-A59, and BCV. Hemagglutination assay was performed at 4°C for two hours using a suspension of 0.4% BALB/c mouse erythrocytes and serial two fold dilutions of MHV-DVIM, MHV-A59, and BCV. The initial protein concentrations of the purified virion preparations was 50 μg for MHV-DVIM and MHV-A59 and 5 μg for BCV. Numbers at the top of the figure indicate the reciprocal of the virus dilution.

4096
2048
1024
512
256
128
64
32
16
8
4
2
MHV-DVIM
MHV-A59
BCV
Buffer

virus than MHV-DVIM. Hemadsorption of mouse erythrocytes was observed on syncytia of MHV-DVIM infected cells but not on syncytia caused by MHV-A59 (Figure 4, B and C). In the MHV-DVIM infected culture the cells which did not show signs of CPE and were not recruited into the syncytia did not adsorb erythrocytes. The specificity of the hemadsorption by MHV-DVIM was further demonstrated when we incubated MHV-DVIM infected DBT cells with polyclonal anti-MHV-DVIM antibody for one hour before exposing the monolayer to the suspension of mouse RBC's. In this case, the anti-MHV-DVIM antibody masked the HE glycoprotein on the surface of infected cells and prevented binding of RBC's (Figure 4 D).

Acetylesterase activity

The acetylesterase activities of BCV, MHV-DVIM, and MHV-A59 virions have been compared using a colorimetric assay that measures the ability of the viral enzyme to release acetate from p-nitrophenyl acetate (Vlasak et al., 1988a). We compared the acetylestarase activity of MHV-DVIM with that of MHV-A59 and BCV (Figure 5). Both purified MHV-DVIM and BCV showed high esterase activity compared to MHV-A59. When we compared the hemagglutination titer and the acetylesterase activity of MHV-DVIM in relation to BCV, we found that the acetylesterase activity of MHV-DVIM is high relative to its hemagglutination titer.

Figure 4. Hemadsorption of mouse erythrocytes to murine fibroblasts infected with two different strains of MHV. The mouse cell line DBT was inoculated with 1 ml of control medium (A), MHV-A59 (B), and MHV-DVIM (C and D) and incubated for 1 hour at 37°C. Virus inoculum was removed, and plates were refed with 5 ml of medium and incubated at 37°C. Virus-induced cell fusion developed at different rates in cultures infected with MHV-A59 and MHV-DVIM. Twenty hours p.i. the mock-infected culture (A) and the MHV-A59-infected culture (B) were exposed to a 5 ml suspension of 0.4% RBCs from BALB/c mice in PBS and incubated at 4°C for 2 hours. Cultures were then fixed with 2% glutaraldehyde in PBS for 15 minutes and unattached erythrocytes were washed off with PBS. The same procedure was repeated for MHV-DVIM at 26 hours p.i. (C). One MHV-DVIM-infected culture (D) was treated with anti-DVIM antibody at a dilution of 1:40 in culture media for 1 hour at 37°C before hemadsorption was performed as described above. * indicates multinucleate syncytia. Arrow indicates erythrocytes adsorbed to a large syncytium.

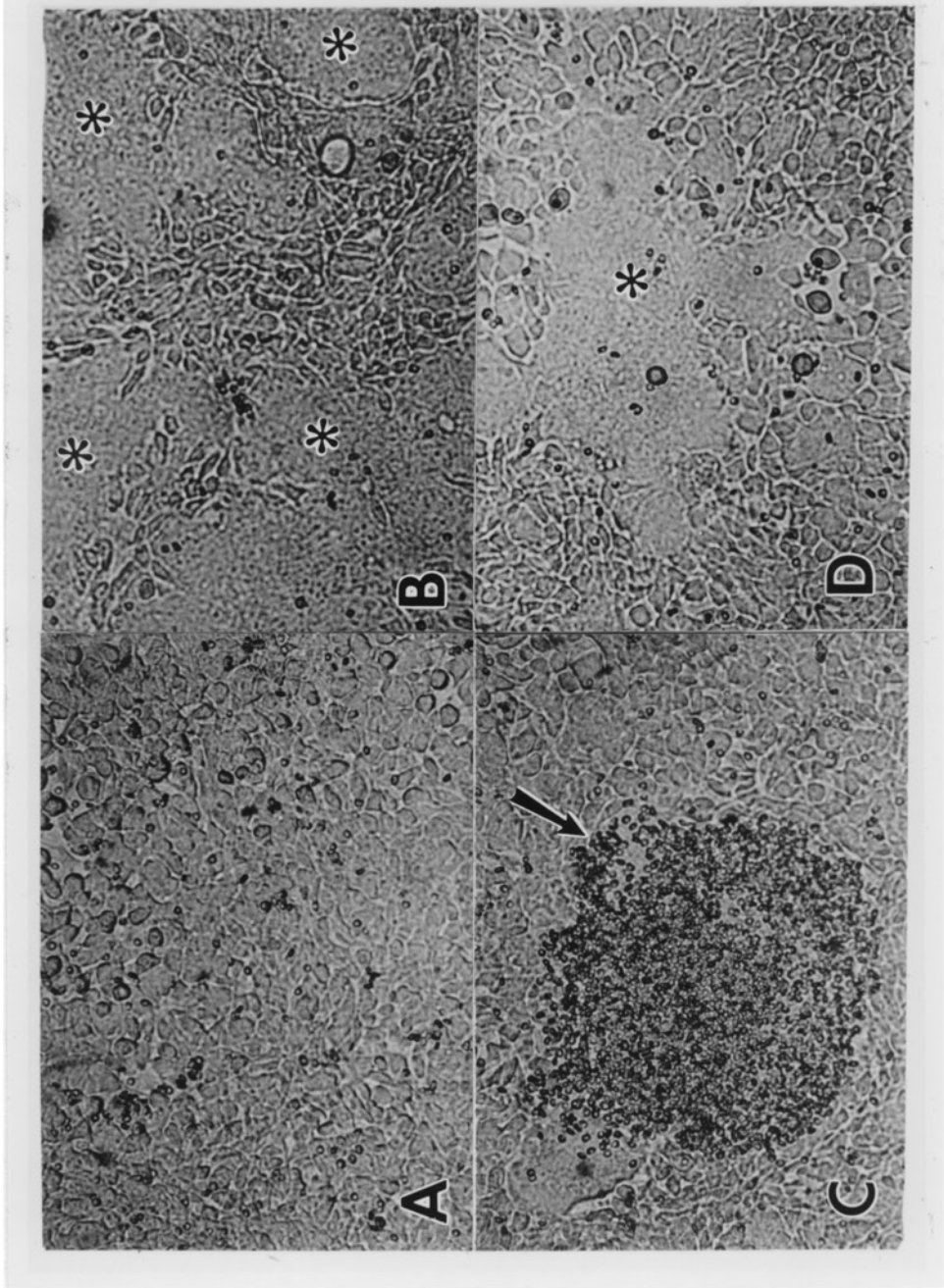
A
B
C
D

Figure 5. Acetylesterase activities of gradient purified BCV, MHV-DVIM, and MHV-A59. Enzymatic activity was measured by hydrolysis of p-nitrophenylacetate and colorimetric determination of the yellow cleavage product, p-nitrophenol. Purified virus (5 μg) was incubated at room temperature in 1 ml of PBS containing 1mM p-nitrophenylacetate in PBS with 1% acetonitrile. The accumulation of p-nitrophenol was monitored using a spectrophotometer at an optical density of 400 ($O.D._{400}$). The figure presents the average and standard deviation for three measurements per point.

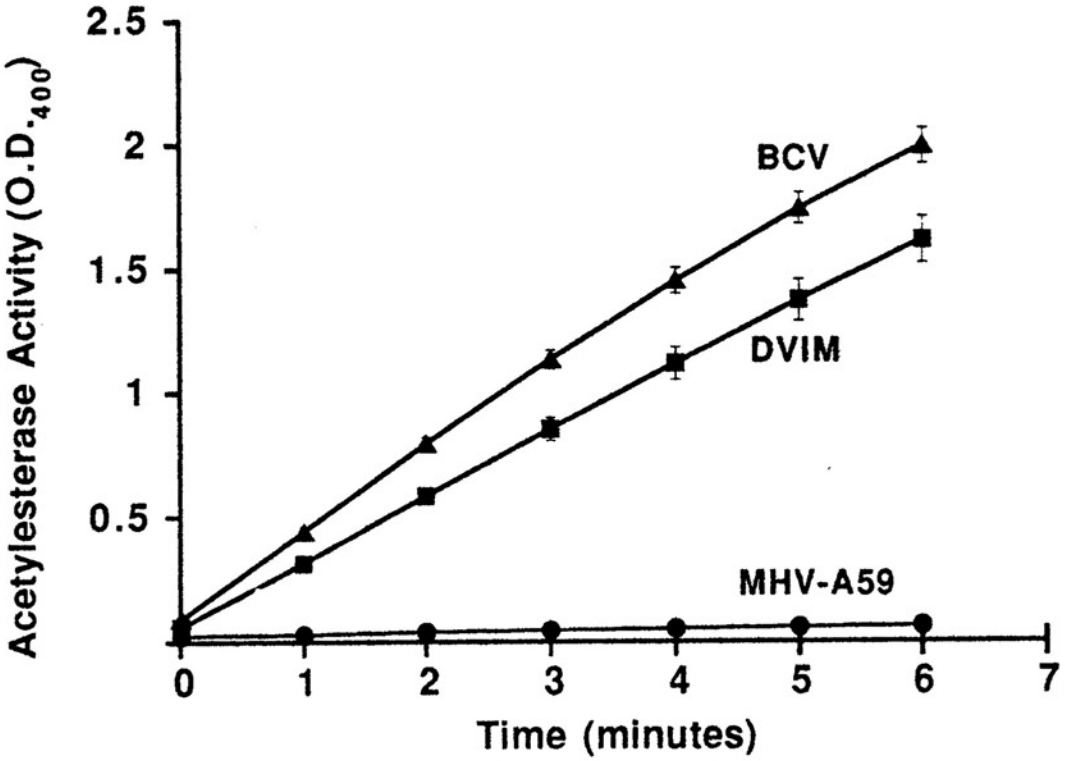
Acetylesterase Activity (O.D.400)
2.5
2
1.5
1
0.5
BCV
DVIM
MHV-A59
0
1
2
3
4
5
6
7
Time (minutes)

The results of the hemagglutination, hemadsorption, and acetylesterase assays showed that our MHV-DVIM expressed a functional HE glycoprotein with both receptor binding and receptor destroying activities.

Comparison of Viral Structural Proteins

The structural proteins of MHV-DVIM, MHV-A59, and BCV were analyzed by sodium dodecyl sulfate polyacrylamide gel electrophoresis with and without reduction followed by immunoblotting with convalescent mouse antiserum prepared against gradient purified MHV-DVIM (Figure 6). Under non-reducing conditions we found that the antiserum recognized five proteins of MHV-DVIM which probably correspond to uncleaved S, cleaved S, HE dimer, N, and M. On the other hand, this antiserum recognized only one protein on MHV-A59 and four on BCV. This could be because the MHV-DVIM proteins differ more from MHV-A59 than from BCV. Under reducing conditions, an additional MHV-DVIM polypeptide, probably the monomeric for of HE, was detected, but the S and the HE dimer were not. This antibody probably reacted better with the unreduced forms of the S and HE glycoproteins than with the reduced forms because it was raised against whole virions.

To identify the 140 and 70 kDa bands as the monomeric and dimeric forms of HE and the 180 and 90 kDa bands as the

Figure 6. Immunoblotting of MHV-DVIM, MHV-A59, and BCV with anti-DVIM antiserum. Gradient purified virions, 6 μg of protein per lane, were electrophoresed in an 8% polyacrylamide gel under nonreducing (-2ME) and reducing (+2ME) conditions and blotted to nitrocellulose. Virion proteins were detected with mouse anti-DVIM antiserum followed by ^{125}I-SPA. HE_u, unreduced hemagglutinin esterase; HE_r, reduced hamagglutinin esterase; S_0, uncleaved spike glycoprotein; S_1S_2, cleaved spike glycoprotein fragments; 2ME, 2-mercaptoethanol. Molecular weight markers in kilodaltons are shown on the right.

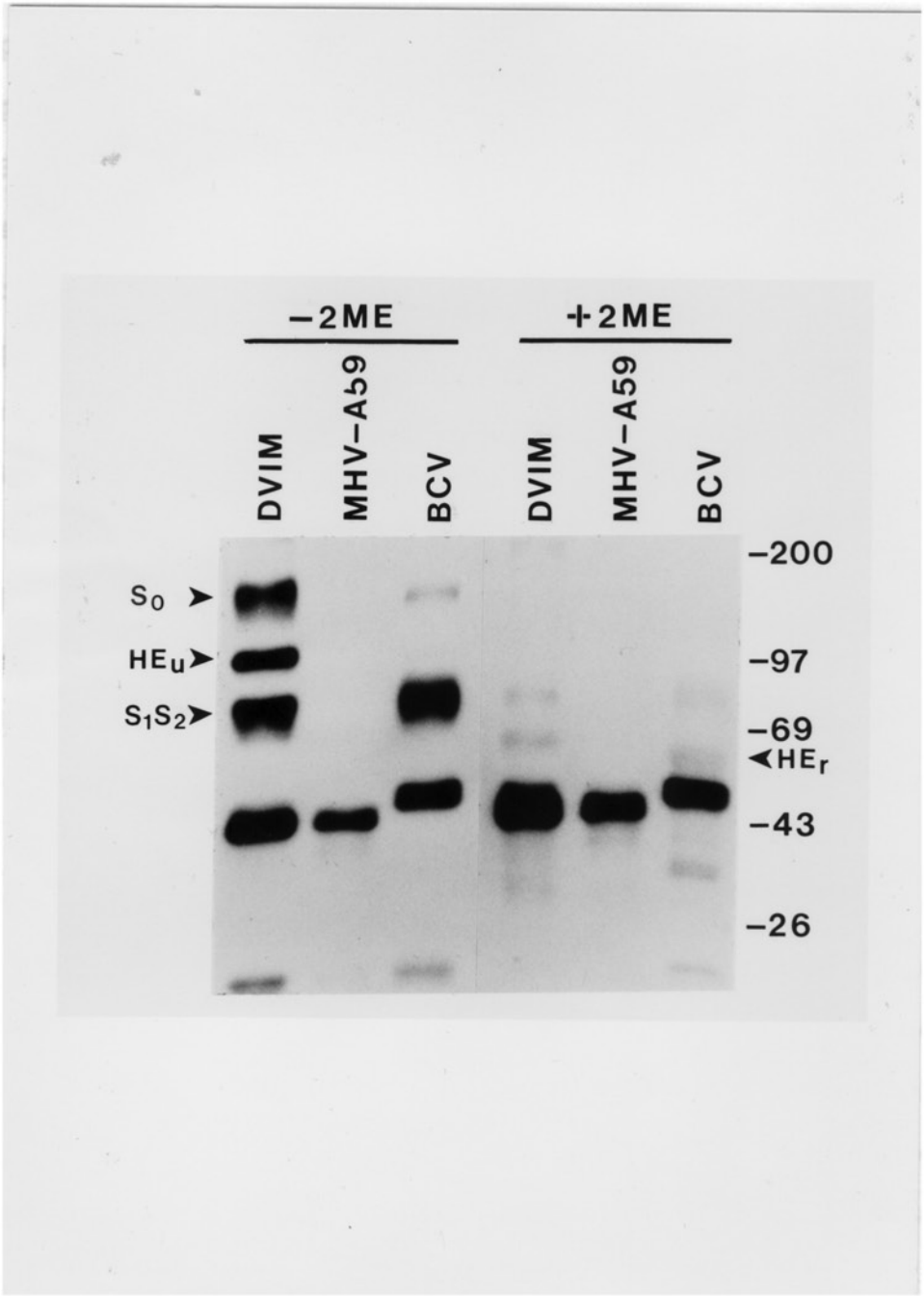
−2ME
+2ME
DVIM
MHV−A59
BCV
DVIM
MHV−A59
BCV
S0
HEu
S1S2
−200
−97
−69
HEr
−43
−26

uncleaved and cleaved forms of S, we immunoblotted these viral proteins with antisera specific for HE of BCV or for S of MHV-A59. The anti-HE antibody detected the 140 kDa glycoproteins of unreduced MHV-DVIM and BCV and the 70 kDa glycoproteins of reduced MHV-DVIM and BCV (Figure 7). The anti-S goat antiserum identified the uncleaved (180 kDa) and cleaved (90kDa) forms of S on the three virions in the absence of reducing agent. In the presence of mercaptoethanol, both forms of S were detected on MHV-A59, but only the cleaved forms of S glycoprotein were detected on MHV-DVIM or BCV (Figure 8).

Receptor Blockade

To determine whether interaction of HE with cell surface carbohydrate can lead to infection independently of the S glycoprotein, we used a monoclonal antibody to the receptor (MAb-CC1) which blocks binding of MHV-A59 virions to the 110 kDa glycoprotein receptor by the S glycoprotein (Williams et al., 1990; Dveksler et al., 1991). We asked, whether an HE-expressing virus can use HE to bind to cells and initiate infection when binding through S is blocked by the anti-receptor antibody. Since MAb-CC1 only recognizes MHVR in the carcinoembryonic antigen family of glycoproteins, and experiments with labeled MAb-CC1 indicate that few MHVR molecules are present on the surface of mouse

Figure 7. Immunoblotting of MHV-DVIM, MHV-A59, and BCV with antiserum against gp65 protein of BCV. Gradient purified virions, 6 μg of protein per lane, were electrophoresed in an 8% polyacrylamide gel under nonreducing (-2ME) and reducing (+2ME) conditions and blotted to nitrocellulose. Virion proteins were detected with rabbit antiserum against the gp65 glycoprotein of BCV followed by ^{125}I-SPA. MHV-DVIM and MHV-A59 lanes were exposed to autoradiographic film for 24 hours and BCV lane was exposed for 6 hours. HE_u, unreduced hemagglutinin-esterase; HE_r, reduced hemagglutinin-esterase; 2ME, 2-mercaptoethanol. Molecular weight markers in kilodaltons are shown on the right.

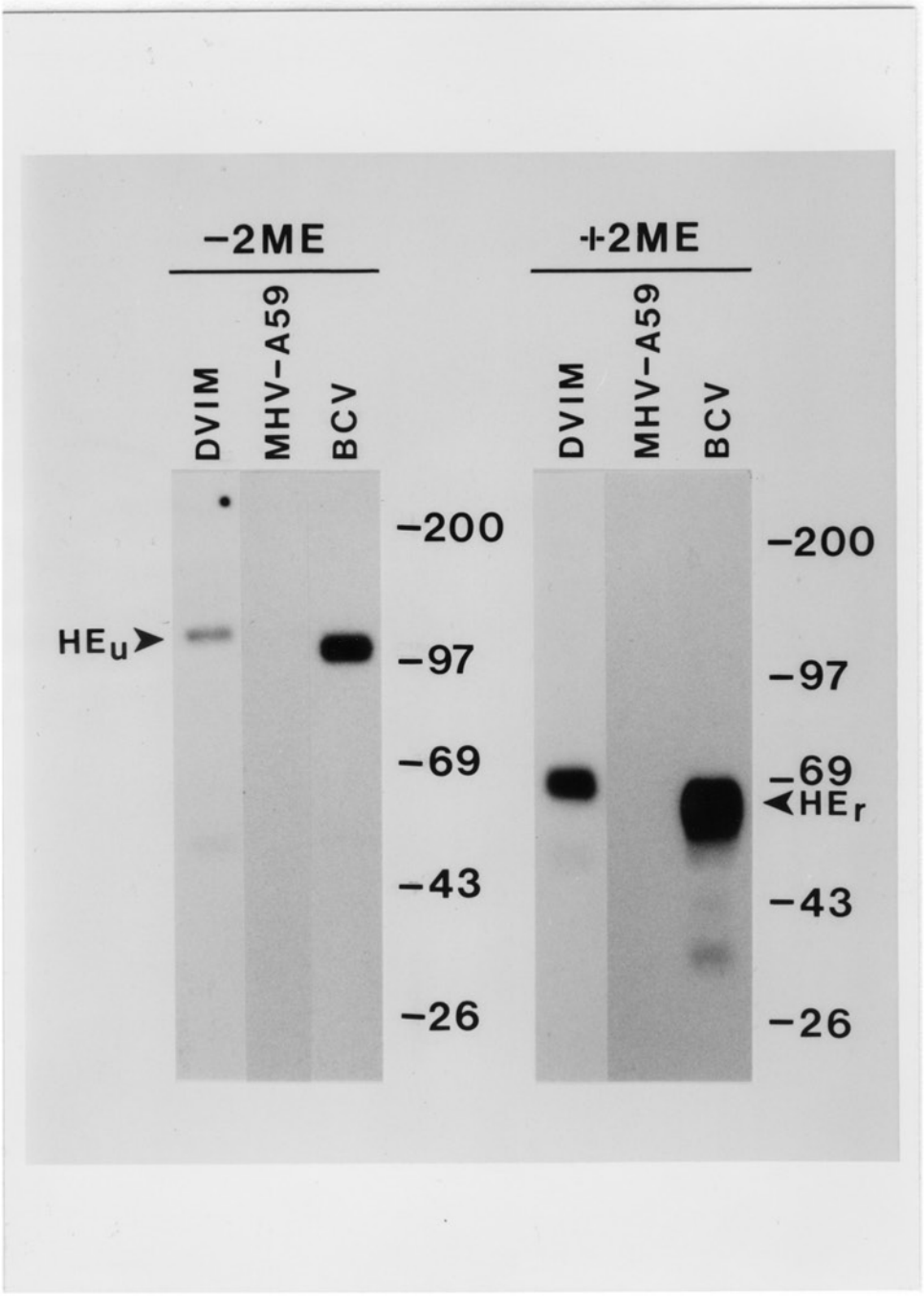
−2ME
+2ME
DVIM
MHV-A59
BCV
DVIM
MHV-A59
BCV
HEu
HEr
−200
−97
−69
−43
−26
−200
−97
−69
−43
−26

Figure 8. Immunoblotting of MHV-DVIM, MHV-A59, and BCV with antiserum against the S glycoprotein of MHV-A59. Purified virions, 6 μg of protein per lane, were electrophoresed in an 8% polyacrylamide gel under nonreducing (-2ME) and reducing (+2ME) conditions and blotted to nitrocellulose. Virion proteins were detected with goat antiserum against the S glycoprotein of MHV-A59 followed by ^{125}I-SPA. S_o, uncleaved spike glycoprotein; S_1S_2, cleaved spike glycoprotein fragments; 2ME, 2-mercaptoethanol. Molecular weight markers in kilodaltons are shown on the right.

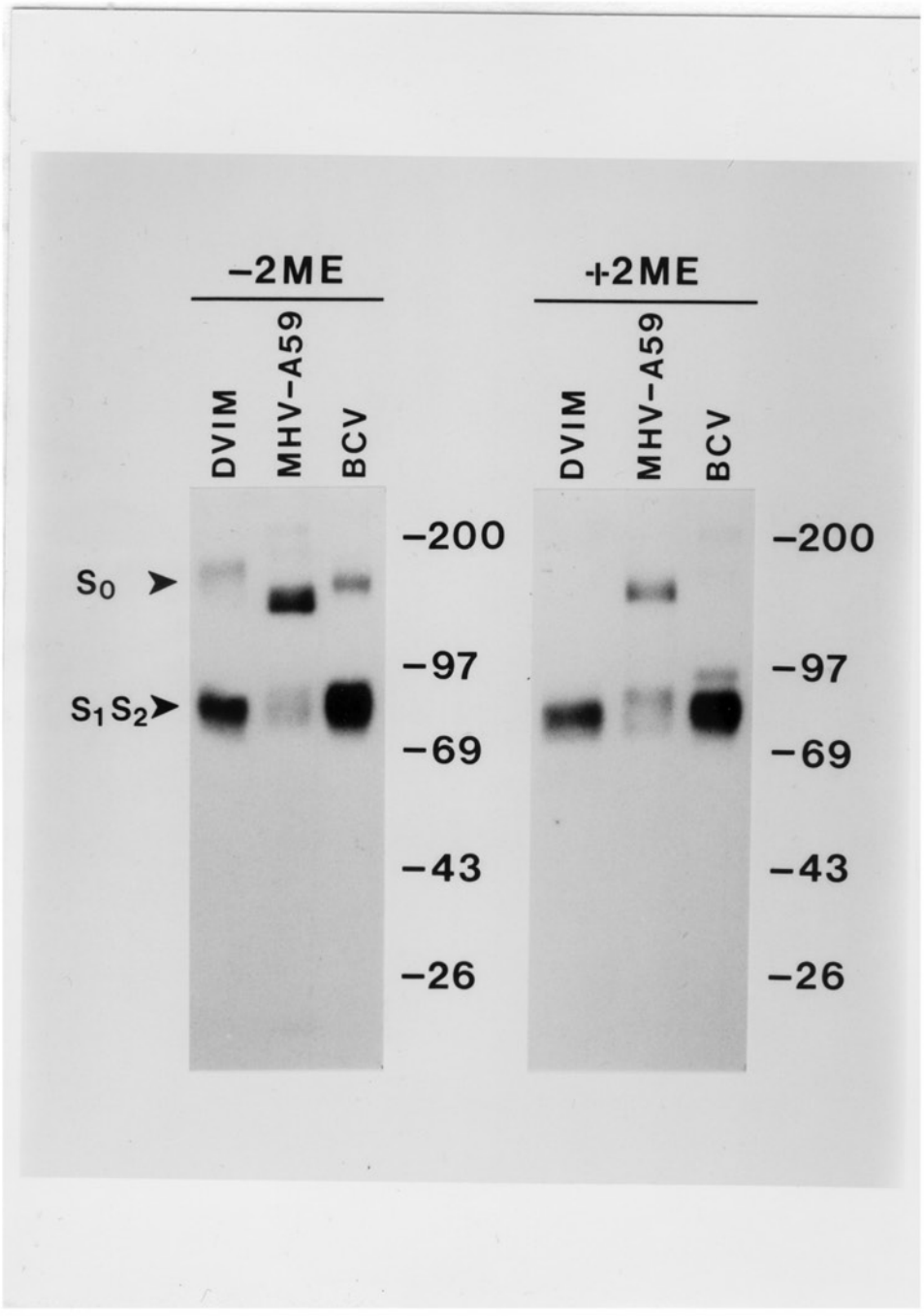
−2ME
+2ME
DVIM
MHV-A59
BCV
DVIM
MHV-A59
BCV
S0
S1 S2
−200
−97
−69
−43
−26
−200
−97
−69
−43
−26

fibroblasts, it is not likely that binding of MAb-CC1 would occlude other plasma membrane molecules which might be recognized by HE. In the experiments that follow, prior to virus challenge, we treated cells in culture with MAb-CC1 or with an unrelated monoclonal antibody of the same isotype, directed against cholera toxin, as a control (MAb-CT). The antibodies were either removed just before inoculation, or kept in culture throughout the course of the infection.

In the receptor blockade experiment, DBT cells were incubated with serial 2 fold dilutions of the MAb-CC1 or control MAb for 1 hour at 37°C. The antibodies were then removed and the cells were challenged with infectious MHV-DVIM or MHV-A59. When the infection had advanced sufficiently so that virus-induced syncytia and/or cell death could be seen in the culture, cell viability was measured using the MTT colorimetric reaction (Figure 9). The anti-receptor antibody protected the DBT cells against infection with MHV-A59 and with MHV-DVIM. After challenge with either MHV-DVIM or MHV-A59, survival of the population of cells decreased with decreasing concentrations of MAb-CC1, but the degree of protection conferred by each antibody concentration was similar for both strains of virus. Control cells similarly treated with an irrelevant monoclonal antibody of the same isotype as MAb-CC1, were not protected by any antibody concentration.

Figure 9. Protection of DBT cells from infection with MHV-DVIM or MHV-A59 by pretreatment of cells with anti-receptor MAb-CC1. DBT cells on a 96 well plate, were pretreated with a 1:2 serial dilution of MAb-CC1 (Anti-R) or a control MAb of the same isotype (Anti-CT) for 1 hour at 37°C. Antibodies were removed and the cells were challenged with an equal amount of MHV-DVIM or MHV-A59 (10^5 PFU per well diluted in cell culture media) for 1 hour at 37°C. Inoculum was removed and cultures were incubated at 37°C. When the infection had advanced sufficiently (16 hours for MHV-A59 and 36 hours for MHV-DVIM), cell survival was measured using the MTT colorimetric assay.

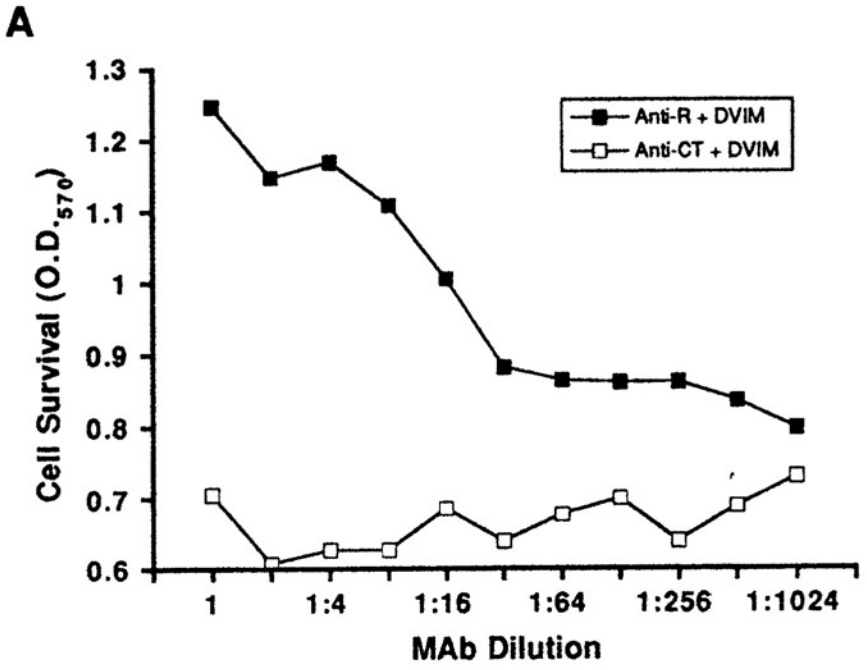
A
Anti-R + DVIM
Anti-CT + DVIM
Cell Survival (O.D.570)
1.3
1.2
1.1
1
0.9
0.8
0.7
0.6
1
1:4
1:16
1:64
1:256
1:1024
MAb Dilution

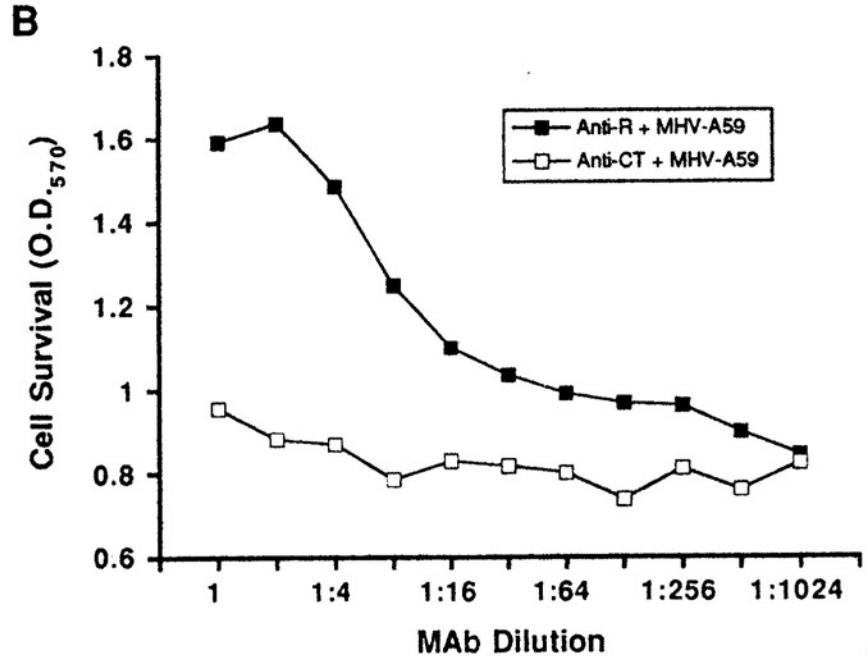
B
Anti-R + MHV-A59
Anti-CT + MHV-A59
Cell Survival (O.D.570)
1.8
1.6
1.4
1.2
1
0.8
0.6
1
1:4
1:16
1:64
1:256
1:1024
MAb Dilution

Reduction of Plaque Formation

It was important to determine whether the MHV-DVIM stock contained a subpopulation of virions resistant to receptor blockade with MAb-CC1. We therefore compared the ability of MHV-DVIM and MHV-A59 to form plaques on cells that had been pretreated with MAb-CC1. Table 3 (Expt. I) and Table 4 show that for two cell lines, L2 and DBT, pre-treatment with anti-receptor MAb-CC1 caused a greater than 99% reduction in plaque formation by both MHV-DVIM and MHV-A59. In a similar experiment in which the protective antibody was not removed before viral challenge but was kept in the culture media throughout the infection, neither MHV-DVIM nor MHV-A59 was able to form any plaques on protected DBT cells (Table 3, Expt II and Figure 10). The reason for the appearance of minute plaques in the first experiment may be that when cells were pre-treated with protective antibody, the antibody bound mainly to the receptors on the apical surface of the cells. If the antibody is removed and the cells migrate or receptor molecules regenerate on the cell membranes, unprotected receptor molecules would be exposed to residual virus particles which may then be capable of infecting these cells and forming a minute plaque. Note that in all cases plaques produced by MHV-A59 were substantially larger than those produced by MHV-DVIM, possibly also due to the better adaptation of MHV-A59 to

TABLE 3

Inhibition of MHV Plaque Formation on DBT Cells by MAb-CC1

	Expt.#	Virus	MAb-CT[a]	MAb-CC1[b]	%Inhibition[c]
Virus Titer (PFU/ml)	I[d]	MHV-DVIM	5.9×10^5	4.2×10^2	99.9
		MHV-A59	1.0×10^8	1.5×10^5	99.9
	II[e]	MHV-DVIM	1.3×10^5	< 7	> 99.9
		MHV-A59	5.3×10^7	< 7	> 99.9
Plaque Size (mm)	I	MHV-DVIM	0.9±0.3	minute[f]	
		MHV-A59	3.3±0.3	0.9±0.3	
	II	MHV-DVIM	1.1±0.3	none	
		MHV-A59	2.3±0.4	none	

a. MAb-CT, an IgG1 MAb directed against cholera toxin, CT, and irrelevant MAb.

b. MAb-CC1, anti-receptor MAb directed against MHVR, the 110 kDa receptor for MHV.

c. % Inhibition = 100 - [100(PFU/ml in MAb-CC1/PFU/ml in MAb-CT)]

d. DBT cells were pre-treated with MAb-CC1 or with MAb-CT for 1 hour. Antibodies were removed and the virus dilutions were added. After 1 hour, the unabsorbed virus was removed and an agar overlay was added. The plaques were developed at 37^0 and counted 72 hours p.i.

e. DBT cells were pre-treated with MAb-CC1 or with MAb-CT for 1 hour. Antibodies were removed and virus dilutions were mixed with an equal volume of MAb-CC1 or control MAb and added onto cells. After 1 hour unabsorbed virus was removed and an agar overlay containing 10% MAb-CC1 or control MAb was added. The plaques were developed and counted 48 hours p.i.

f. minute, < 0.3mm

TABLE 4

Inhibition of MHV Plaque Formation on L2 Cells by MAb-CC1

	Virus	MAb-CT[a]	MAb-CC1[b]	%Inhibition[c]
Virus[d] Titer (PFU/ml)	MHV-DVIM	2.1×10^5	2.1×10^2	99.9
	MHV-A59	5.2×10^8	1.0×10^6	99.8
Plaque Size (mm)	MHV-DVIM	1.0 ± 0.6	minute[e]	
	MHV-A59	4.7 ± 0.5	1.3 ± 0.8	

a. MAb-CT, an IgG1 irrelevant MAb directed against cholera toxin, CT, an irrelevant MAb.

b. MAb-CC1, anti-receptor MAb directed against MHVR, the 110 kDa receptor for MHV.

c. %Inhibition, 100-[100(PFU/ml in MAb-CC1/PFU/ml in MAb-CT)].

d. L2 cells were pretreated with MAb-CC1 or with MAb-CT for 1 hour. Antibodies were removed and the virus dilutions were added. After 1 hour the unabsorbed virus was removed and an agar overlay was added. The plaques were developed and counted 72 hours p.i.

e. minute, < 0.3mm

Figure 10. Plaque assay of MHV-DVIM and MHV-A59 in the presence and absence of anti-receptor MAb-CC1. DBT cells were treated for 1 hour with MAb-CC1 (plates at right) or with a control MAb-CT (plates at left). Antibodies were removed and a MHV-DVIM (A) or a MHV-A59 (B) inoculum (MOI, 0.2 PFU/cell) was mixed with an equal volume of MAb-CC1 or control MAb-CT and added to the plates, and virus was let to adsorb for 1 hour. At this time supernatants were removed and an agar overlay containing 10% MAb-CC1 or MAb-CT was added. The plaques were developed and counted 48 hours p.i. The virus dilutions on the photographed plates are the following: A: left, 10^{-3}; right, 10^{-1}; B: left, 10^{-6}; right, 10^{-1}.

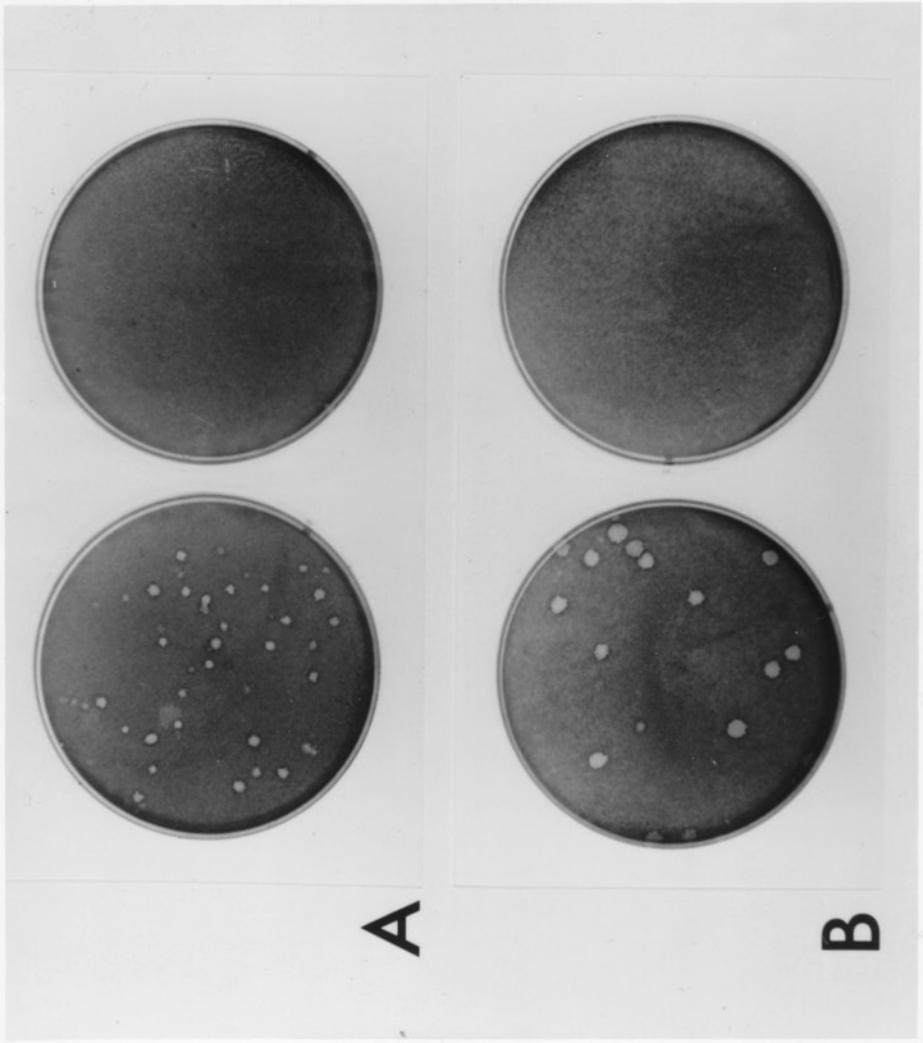
A
B

culture conditions. Also, MHV-DVIM showed greater plaque variability since these virions were not plaque purified whereas MHV-A59 virions were.

Fluorescent-Antibody Staining to Detect Infection of Single Cells

Since immunostaining allows the detection of infection on single cells we used this method to try to determine whether in the presence of the anti-receptor MAb-CC1, infection by MHV-DVIM could be occurring at a very low level, or without causing CPE. In addition, in this experiment we included MHV-JHM because this strain also can express HE (Yokomori et al., 1989). However, in the MHV-JHM strain the level of HE-expression varies among different isolates (Yokomori et al., 1991), and our isolate did not cause hemadsorption of RBC's in infected cultures. We thought that should the MHV-JHM in our hands be a low expressor of HE, MHV-JHM infection through HE attachment was still possible. In such a case, this infection would be detectable using immunofluorescence staining. As for the two previous experiments MHV-A59 was also included to enable a comparison between the two HE bearing strains (MHV-DVIM and MHV-JHM) and MHV-A59 which lacks HE. When cells were pretreated with MAb-CC1, and then challenged with MHV-DVIM, MHV-A59, or MHV-JHM, and the protective antibody was kept in

the media throughout the infection, no infected cells could be detected (Figure 11). Since the MOI that we used in this experiment was relatively low (MOI = 0.2 PFU/cell), we did not find antigen positive cells in every microscope field. In cells treated with the control monoclonal antibody, the average number of nuclei in antigen positive cells for the 30 fields that were randomly screened was 3.3 for MHV-DVIM, 9.4 for MHV-A59, and 7.4 for MHV-JHM. However, when the cells were treated with MAb-CC1, we did not find any antigen positive cells for any of the three viruses after screening 50 random fields.

These three protection experiments on cultured mouse cell lines: the receptor blockade on a 96 well plate, the reduction of plaque formation, and the immunofluorescent staining to detect infected cells, showed clearly that the HE glycoprotein alone is not sufficient to initiate MHV-DVIM infection on L2 and DBT cells. Therefore, interaction of S with its receptor is needed for MHV-DVIM infection to occur.

Challenge of BHK and MDCK Cells with MHV-DVIM

While this work was in progress, our lab identified and cloned the 110 kDa receptor for the S glycoprotein of MHV-A59 (MHVR) (Williams et al., 1991; Dveksler et al., 1991). We used fluorescent immunostaining to detect MHV-DVIM infection on BHK cells transfected with MHVR. BHK cells

Figure 11. Fluorescent-antibody staining of DBT cells protected with anti-receptor MAb-CC1 and challenged with MHV-DVIM, MHV-A59, or MHV-JHM. Prior to infection DBT cells were treated with MAb-CC1 (A, B, and C) or with MAb-CT, a control MAb of the same isotype (D, E, and F) for 1 hour at 37°C. These antibodies were kept in the media throughout the course of the infection. The cells were challenged with inoculum containing 50% MAb-CC1 or control MAb and MHV-DVIM (A and D), MHV-A59 (B and E) or MHV-JHM (C and F) at a MOI of 0.2 PFU/cell for the three strains. After 1 hour at 37°C the inoculum was removed and fresh media with 10% MAb-CC1 or control MAb was added. Cultures were fixed 10 hours p.i. and immunofluorescent staining was performed.

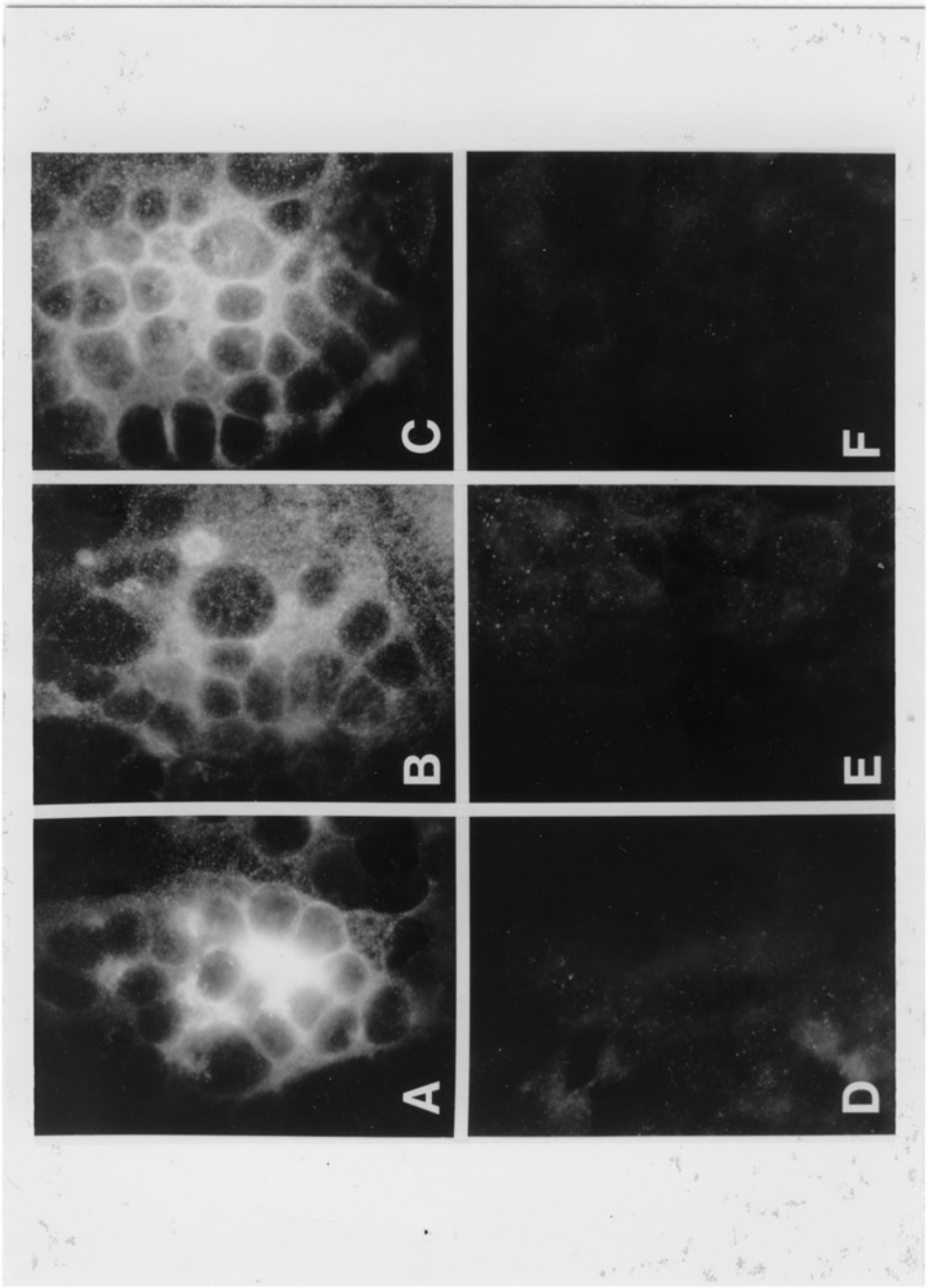
A
B
C
D
E
F

were resistant to MHV-DVIM infection unless the cells were transfected with MHVR. When the transfected cells were treated with anti-receptor MAb and challenged with MHV-DVIM, the cells were fully protected from MHV-DVIM infection (Figure 12). Since MHV-DVIM was able to infect BHK cells transfected with MHVR, it is possible that this receptor is sufficient for MHV-DVIM to initiate infection, and this virus strain probably utilizes the same receptor as MHV-A59.

Since BCV binds to Neu5,9Ac_2 to infect MDCK cells (Schultze and Herrler, 1992), it is clear that these cells express this sialic acid. If MHV-DVIM, not MHV-A59, could infect MDCK cells, this would imply that HE can lead to infection. We tested whether MHV-DVIM, which like BCV expresses HE, could infect these cells. Using immunofluorescence staining, we did not detect MHV-DVIM infection of MDCK cells. Therefore, it is likely that binding of the HE of MHV-DVIM to Neu5,9Ac_2 on MDCK cells did not permit this virus to initiate infection.

Infection of Mixed Glial Cell Cultures with MHV-DVIM, MHV-A59, and MHV-JHM

We conducted studies on mixed glial cell cultures to compare the infectivity pattern of MHV-DVIM, an HE-bearing strain of MHV, with that of the neurotropic MHV-JHM strain and the hepatotropic MHV-A59. We used three color

Figure 12. MAb-CC1 protection of BHK cells transfected with MHVR and challenged with MHV-DVIM. BHK cells transfected with MHVR were pretreated with anti-receptor MAb-CC1 (B) or MAb-CT a control antibody of the same isotype (A) for 1 hour at 37°C. The cells were then challenged with an MHV-DVIM (MOI, 0.2 PFU/cell) inoculum containing 50% anti-receptor MAb-CC1 or control MAb. After 1 hour the virus was removed and replaced by fresh media containing 10% of the same antibodies. Cultures were fixed 10 hours p.i. and immunofluorescent staining was performed.

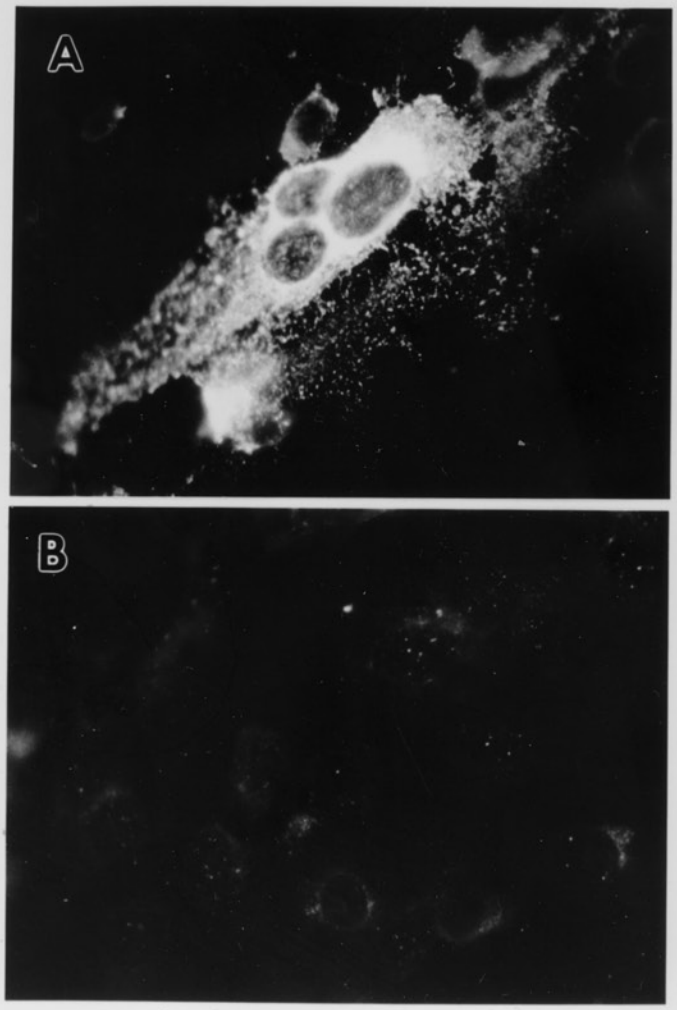
A
B

immunofluorescence staining to determine whether MHV-DVIM, MHV-A59, and MHV-JHM were capable of infecting glial cells of different lineages on primary glial cell cultures prepared from two-day-old C57BL/6 mice. We identified infected cells with antibodies to MHV-DVIM or MHV-A59, oligodendrocytes with an antibody to galactocerebroside, oligodendrocyte-type 2 astrocyte (O-2A) progenitor cells with the O4 monoclonal antibody, and the astrocytes with an antibody to glial fibrillary acidic protein. O-2A progenitors bind O4 in the absence of GC or GFAP labeling. Oligodendrocytes are recognized by both O4 and anti-GC but not by anti-GFAP and astrocytes are recognized by O4 and anti-GFAP but not by anti-GC (Armstrong et al., 1990). The fixed cells were labeled with antibody to MHV and with either of two different combinations of immunofluorescent cell markers. The first set of immunofluorescent markers was used to identify infected cells, oligodendrocytes, and astrocytes (Figure 13). The second set allowed the identification of infected cells, O2-A progenitor cells, and astrocytes (Figure 14). In most cases, it was not possible to determine the phenotype of the infected cells. This could occur if the virus was infecting other minor non-labelled cell types in these primary cultures such as microglia, fibroblasts, and ependymal cells. Another possible reason for failure to identify most infected cells would be if coronavirus infection reduces the expression of

Figure 13. Viral and cellular antigens in primary mouse brain cultures infected with various MHV strains. Primary brain cell cultures from 2 day old C57BL/6 mice were grown in culture for 12 days. Cells were pre-treated with control MAb-CT for 1 hour at 37°C. MHV-DVIM (A, B, C), MHV-A59 (D, E, F), MHV-JHM (G, H, I), or medium control (J, K, L,) inocula mixed with equal volumes of the control MAb were used to inoculate cells. After 1 hour at 37°C, the inocula were removed and fresh medium containing 10% control MAb was added. Cultures were fixed 10 hours p.i. Immunofluorescent staining was performed as follows: MHV antigens (A, D, G, J) were detected with mouse convalescent anti-MHV-DVIM; oligodendrocytes (B, E, H, K) were identified with rabbit polyclonal anti-galactocerebroside; astrocytes (C, F, I, L) were identified with rat polyclonal anti-glial fibrillary acidic protein followed by secondary antibodies conjugated to rhodamine to visualize viral antigens, fluorescein to visualize oligodendrocytes and coumarin to visualize astrocytes.

A
B
C
D
E
F
G
H
I
J
K
L

Figure 14. Viral and cellular antigens in primary mouse brain cultures infected with various MHV strains. Primary brain cell cultures from 2 day old C57BL/6 mice were grown in culture for 12 days. Cells were pre-treated with control MAb-CT for 1 hour at 37°C. MHV-DVIM (A, B, C), MHV-A59 (D, E, F), MHV-JHM (G, H, I), or media control (J, K, L,) inocula mixed with equal volumes of the control MAb were used to inoculate cells. After 1 hour at 37°C, the inocula were removed and fresh medium containing 10% control MAb was added. Cultures were fixed 10 hours p.i. Immunofluorescent staining was performed as follows: MHV antigens (A, D, G, J) were detected with rabbit polyclonal anti-MHV-DVIM; O-2A progenitor cells (B, E, H, K) were identified with MAb 04; astrocytes (C, F, I, L) were identified with rat polyclonal anti-glial fibrillary acidic protein followed by secondary antibodies conjugated to fluorescein to visualize viral antigens, rhodamine to visualize O-2A progenitors, and coumarin to visualize astrocytes.

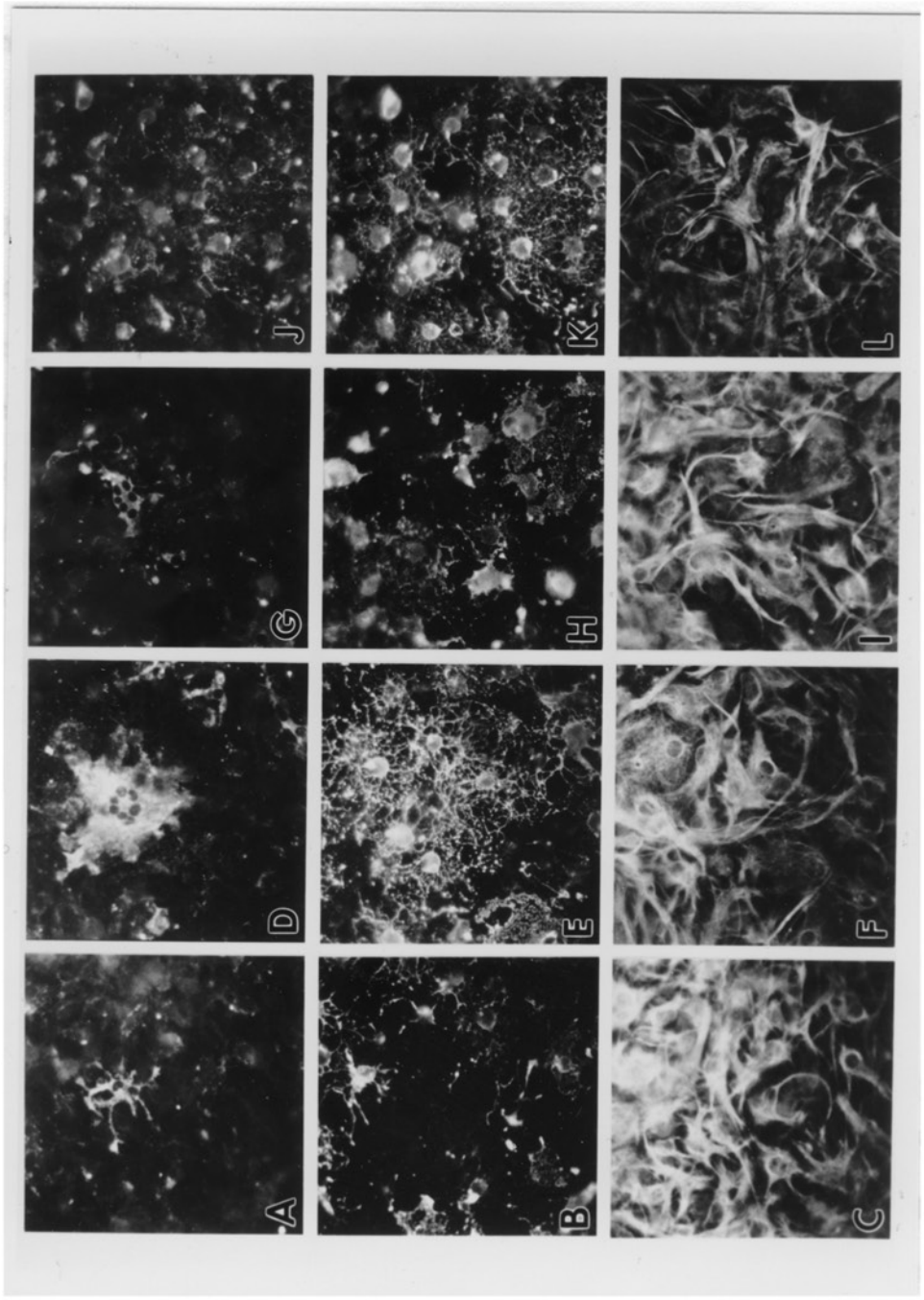
A
B
C
D
E
F
G
H
I
J
K
L

differentiation markers of the central nervous system cells. Figure 15 and Table 5 show some examples of cases in which we were able to identify the phenotype of the infected cell. In this cases, MHV-DVIM and MHV-JHM were found to infect both O-2A progenitor cells and oligodendrocytes.

To determine whether anti-receptor monoclonal antibody could protect central nervous system cells from virus infection, this experiment was done in the presence and absence of the anti-receptor MAb-CC1 (Figure 16, 17). To get a numerical assessment of the degree of protection conferred by this monoclonal antibody, we counted the number of nuclei in antigen positive cells that had been treated with MAb-CC1 and compared it to the same number in cells that had not been treated with MAb-CC1 (Table 5).

Since only a fraction of the infected cells could be identified using three color immunofluorescence we were not able to assess whether the three MHV strains tested infect predominantly the same or different glial cell types. Nevertheless, we were able to demonstrate that the three MHV strains all infected progenitor cells, MHV-A59 and MHV-JHM infected oligodendrocytes, and MHV-JHM infected astrocytes. Similarly to the results obtained on cultured mouse DBT cells, the anti-receptor MAb-CC1 blocked infection of MHV-DVIM, MHV-A59, and MHV-JHM on primary brain cells. This data suggest that MHV-DVIM cannot use the HE glycoprotein to gain entry to and infect mouse brain primary cell cultures.

Figure 15. Phenotype of MHV infected glial cells. Primary brain cell cultures from 2 day old C57BL/6 mice were grown in culture for 12 days. Cells were pre-treated with control MAb-CT for 1 hour at 37°C. MHV-DVIM (A, B, E, F), MHV-A59 (C, D), or MHV-JHM (G, H) inocula mixed with equal volumes of the control MAb were used to inoculate cells. After 1 hour at 37°C, the inocula were removed and fresh medium containing 10% control MAb was added. Cultures were fixed 10 hours p.i. Immunofluorescent staining was performed as follows: MHV antigens were detected with mouse convalescent anti-MHV-DVIM (E, G) or with rabbit polyclonal anti-MHV-A59 (A, C); O-2A progenitor cells (B, D) were identified with MAb O4; oligodendrocytes (F,H) were identified with rabbit polyclonal anti-galactocerebrosyde followed by secondary antibodies conjugated to fluorescein to visualize viral antigens (A, C) or oligodendrocytes (F, H), rhodamine to visualize O-2A progenitors (B, D) or viral antigens (E, G).

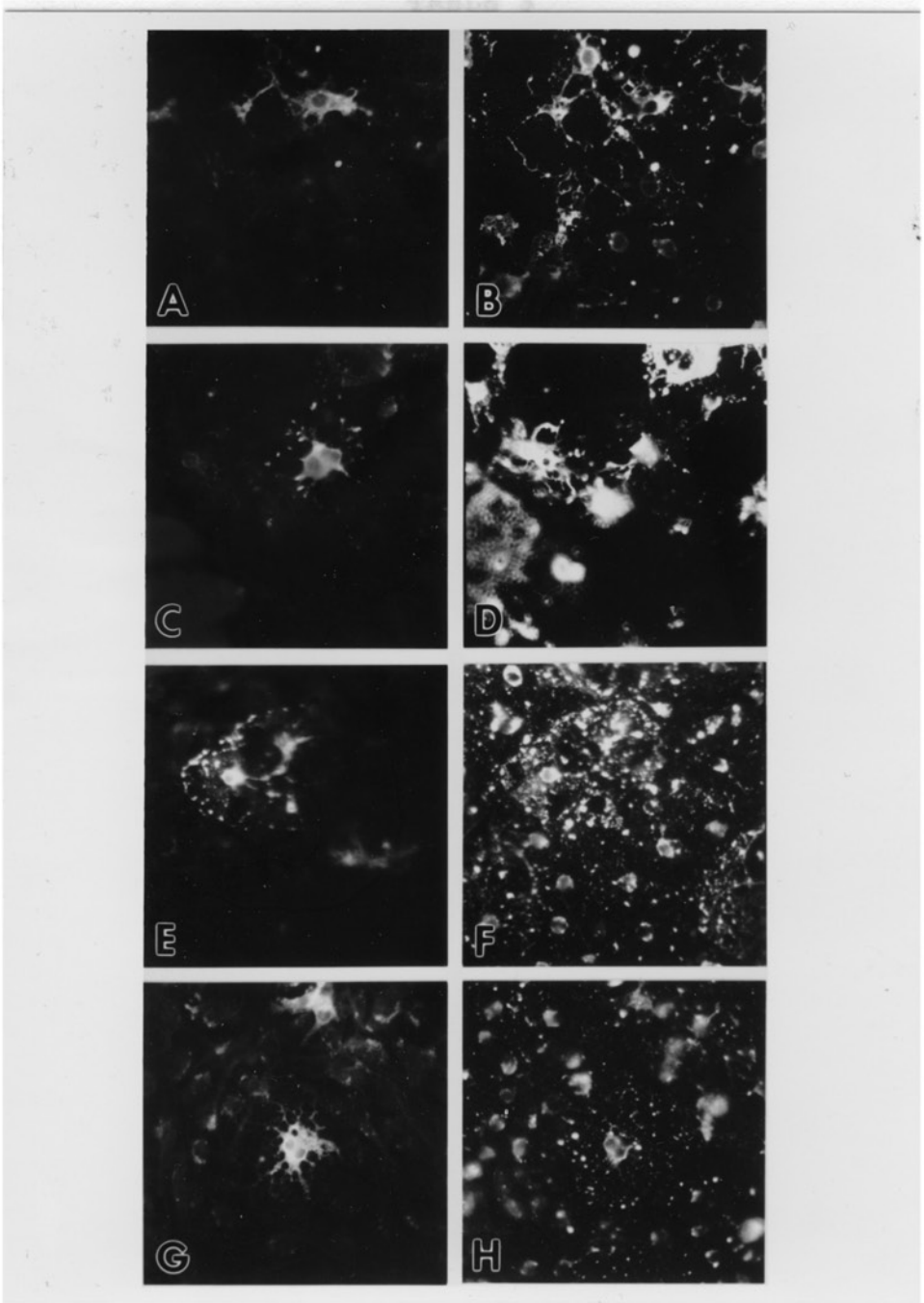
A
B
C
D
E
F
G
H

TABLE 5

Identification of MHV-Infected Cells in Primary C57BL/6 Mouse Central Nervous System Cultures

Detecting Antibody	Antibody Pretreatment of Cells	Number of cells positive for viral antigen[a] MHV-DVIM	MHV-A59	MHV-JHM
α MHV[b]	MAb-CT	60	1176	384
	MAb-CC1	1	1	0

	Cell Type	Number of virus positive cells identified with anti-cell antibodies MHV-DVIM	MHV-A59	MHV-JHM
O4[c]	Progenitors	3	4	5
α GC[d]	Oligodendrocytes	8	3	3
α GFAP[e]	Astrocytes	0	0	3

a. Primary brain cells from C57BL/6 mice were pretreated with anti-receptor MAb-CC1 or a control MAb-CT for 1 h at 37°C. Antibodies were removed and virus inoculum $5x10^5$ PFU/ well of 24 well plate containing 50% control or anti-receptor MAb was added and incubated for 1 hour at 37°. At this time the unabsorbed virus was removed and fresh media containing 10% MAb was added. Cells were fixed with 2% paraformaldehyde. Staining of O2-A progenitor or oligodendrocytes surface antigens was performed followed by permeabilization with ethanol and staining of the viral and astrocyte internal antigens. For cells treated with MAb-CT, numbers of positive cells, represent the average number of infected cells per microscope field on 30 random fields. For cells treated with MAb-CC1, numbers of positive cells represent the average number of infected cells per microscope field in 50 random fields.

b. α MHV: mouse anti-MHV-DVIM or rabbit anti-MHV-A59 serum.

c. O4: supernatant of hybridoma cultures, identifies O-2A progenitor cells.

d. α GC: rabbit anti-galactocerebroside serum, identifies oligodendrocytes.

e. α GFAP: rabbit anti-glial fibrillary acidic protein serum, identifies astrocytes.

Figure 16. Protection of mouse primary brain cells with MAb-CC1 from infection with various MHV strains. Primary brain cell cultures from 2 day old C57BL/6 mice were grown in culture for 12 days. Cells were pre-treated with MAb-CC1 or with control MAb-CT for 1 hour at 37°C. MHV-DVIM (A, B), MHV-A59 (C, D), or MHV-JHM (E, F) inocula mixed with equal volumes of MAb-CC1 (B, D, F) or control MAb (A, C, E) were used to inoculate cells. After 1 hour at 37°C, the inocula were removed and fresh medium containing 10% MAb-CC1 or control MAb-CT was added. Cultures were fixed 10 hours p.i. Immunofluorescent staining was performed as follows: MHV antigens were detected with mouse convalescent anti-MHV-DVIM followed by secondary antibodies conjugated to rhodamine to visualize viral antigens.

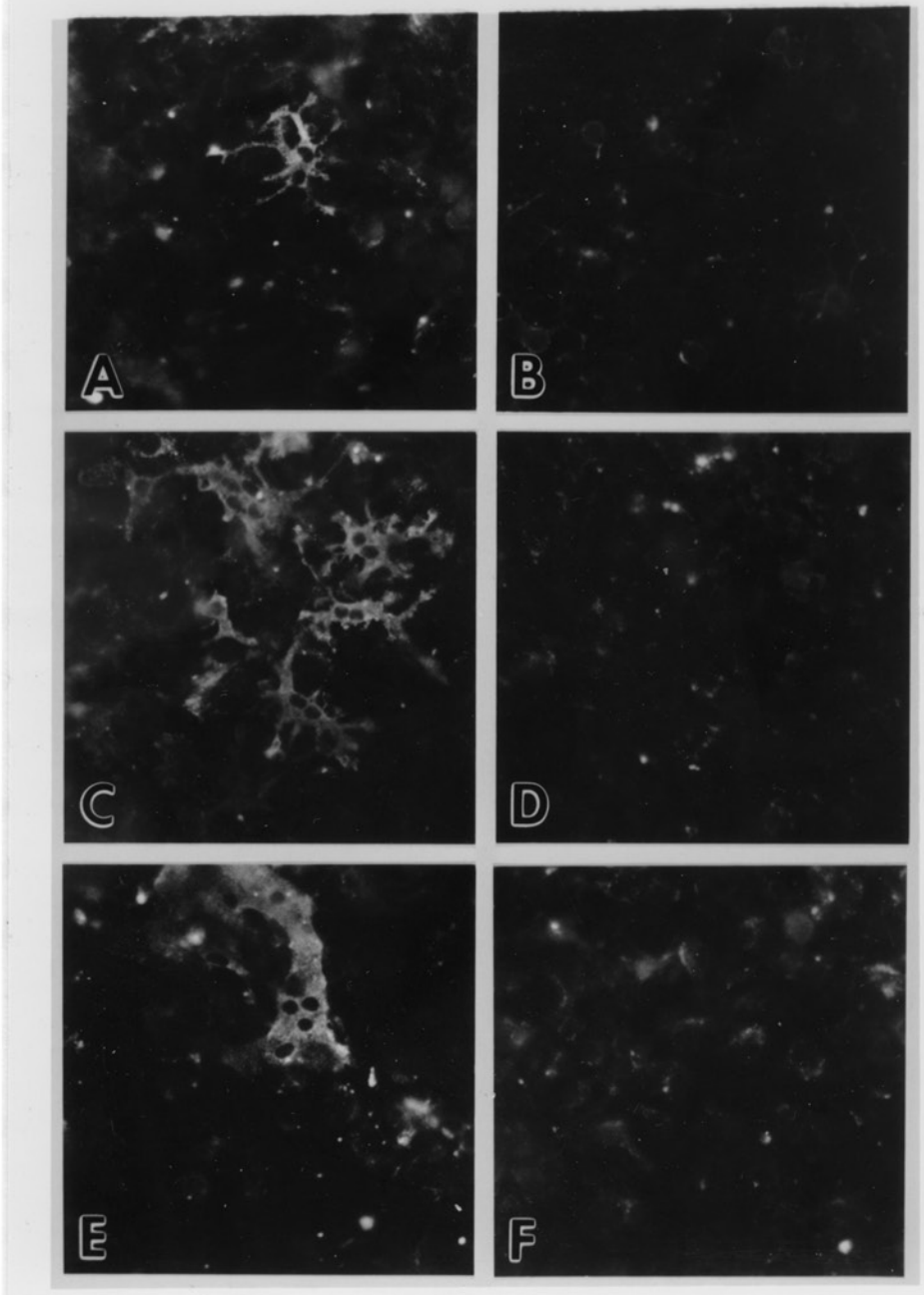
A
B
C
D
E
F

Figure 17. Protection of mouse primary brain cells with MAb-CC1 from infection with MHV-DVIM and MHV-A59. Primary brain cell cultures from 2 day old C57BL/6 mice were grown in culture for 12 days. Cells were pre-treated with MAb-CC1 for 1 hour at 37°C. MHV-DVIM (D, E), MHV-A59 (A, B, C), inocula mixed with equal volumes of MAb-CC1 were used to inoculate cells. After 1 hour at 37°C, the inocula were removed and fresh medium containing 10% MAb-CC1 was added. Cultures were fixed 10 hours p.i. Immunofluorescent staining was performed as follows: MHV antigens were detected with mouse convalescent anti-MHV-DVIM (D) or with rabbit polyclonal anti-MHV-A59 (A); O-2A progenitor cells were identified with MAb O4 (B); oligodendrocytes were identified with rabbit polyclonal anti-galactocerebrosyde (E); astrocytes were identified with rat polyclonal anti-glial fibrillary acidic protein (C); followed by secondary antibodies conjugated to fluorescein to visualize viral antigens (A) or oligodendrocytes (E), rhodamine to visualize O-2A progenitors (B) or viral antigens (D) and coumarin to visualize astrocytes (C).

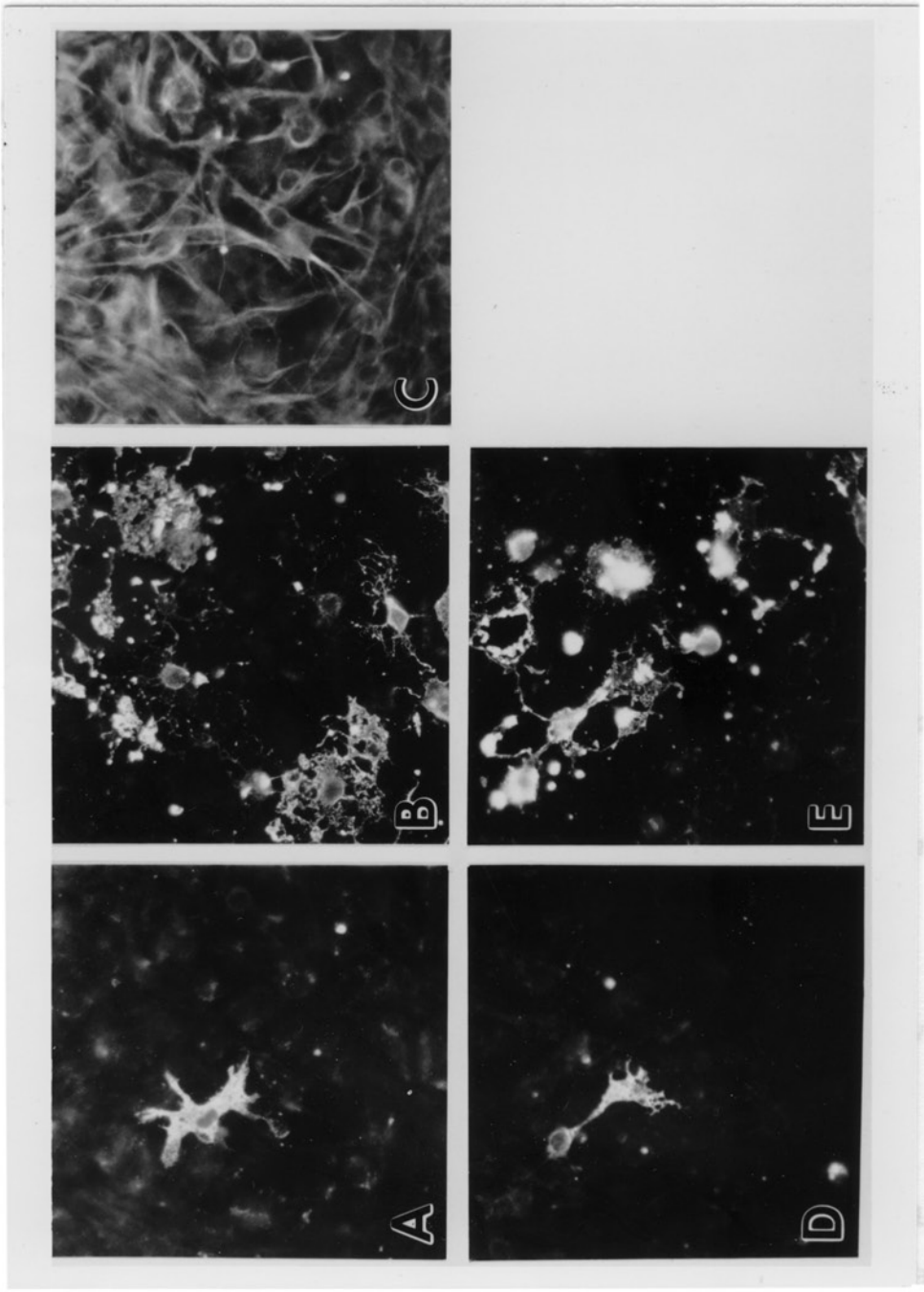
C
B
E
A
D

Virus Overlay Protein Blot Assay of MHV-DVIM and MHV-A59 Binding to Intestinal Brush Border Membranes from BALB/c Mice

The HE glycoprotein of MHV-DVIM like that of BCV and HCV-OC43 recognizes glycoproteins containing Neu5,9Ac_2 acid as a sugar residue. To determine whether MHV-DVIM would bind to many different glycoproteins that express this carbohydrate moiety on murine intestinal brush border membranes (BBM) we performed virus overlay blots with MHV-A59 or MHV-DVIM (Figure 18). Proteins of intestinal BBM were separated in an SDS-PAGE, blotted on to nitrocellulose membrane and then exposed to a suspension of MHV-A59 or MHV-DVIM. As it has been previously shown in our lab (Boyle et al., 1987), on this membrane preparation MHV-A59 binds to a 110 kDa glycoprotein. MHV-DVIM binds to the same glycoprotein of 110 kDa, but contrary to what we expected it did not bind to any additional brush border membrane proteins. When we exposed similar BBM preparations on nitrocellulose to MAb-CC1 prior to incubation with the virus suspension, MAb-CC1 blocked binding by both MHV-A59 and MHV-DVIM. Since we do not expect SDS-PAGE to affect sugar moieties, we may have not detected binding to additional glycoproteins because the sugar is not present on the BBM preparations or it is there in very small amounts. Alternatively, it could be that the binding of HE to sialic

Figure 18. Binding of MHV-DVIM and MHV-A59 to intestinal brush border membrane proteins from BALB/c mice. 200 μg of BBMs prepared from 4-6 week old BALB/c mice were analyzed on SDS-PAGE gels and transferred to nitrocellulose. Lanes were incubated with MAb-CC1 (marked +) or with control buffer (marked -). Samples were then probed with: MHV-DVIM followed by anti-MHV-DVIM antibody (lanes D), MHV-A59 followed by anti-MHV-A59 (lanes A), or no virus or antibody (lanes -). ^{125}I-SPA was used to detect bound antibody. Molecular weight markers in kilodaltons are shown on the right.

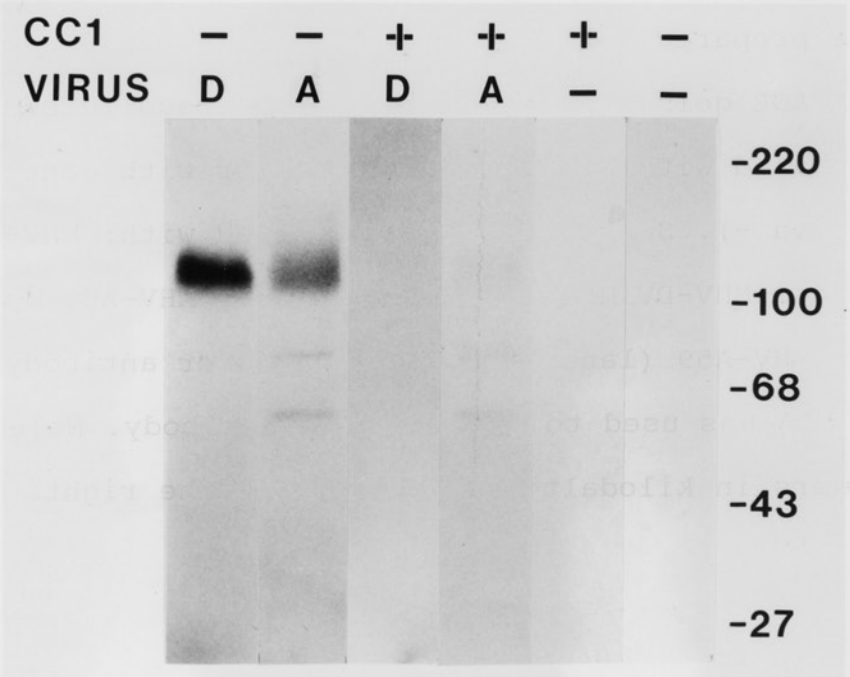
CC1 – – + + + –
VIRUS D A D A – –
-220
-100
-68
-43
-27

acid is weaker than that of S-receptor binding and did not sustain the conditions of the washes in this experiment.

DISCUSSION

Hemadsorption, hemagglutination, and acetylesterase assays show that the HE glycoprotein of MHV-DVIM binds to receptors on erythrocytes and possesses a receptor destroying enzyme comparable to the HE glycoprotein of influenza C virus. The HE of MHV-DVIM probably binds to Neu5,9Ac_2 as has been demonstrated for BCV, HCV-OC43, and HEV (Schultze et al., 1990; Vlasak et al., 1988b), and its receptor-destroying activity is probably due to the release of the acetyl group from position C-9 of this molecule (Vlasak et al., 1988b; Vlasak et al., 1988a; Schultze et al., 1991b). A 70 and 130-140 kDa structural proteins that cross react with the HE of BCV have been detected on MHV-DVIM but not on MHV-A59. Therefore, these MHV-DVIM proteins probably correspond to the reduced and unreduced forms of HE. On MHV-A59, the second ORF of the unique region of mRNA2 encodes for a protein which shares 30% homology with HA1 of influenza C virus but, lacks a translation initiation codon for the correct expression of this protein (Luytjes et al., 1988).

To determine whether HE could alone initiate infection by MHV-DVIM, we used the anti-receptor MAb-CC1 to block

binding of S to its receptor on cultured cells and then challenged these cells with HE bearing virions. Antibody to the 110 kDa MHV receptor protected mouse cell lines from infection with mouse coronavirus strains expressing HE and strains not expressing HE equally. As demonstrated using immunofluorescence staining of viral antigens, HE could not lead to infection of single cells. Antibody to the MHV receptor also protected primary mouse brain cultures from MHV-DVIM infection. This suggests that probably binding of HE to cell membrane molecules containing Neu5,9Ac_2 is not sufficient to intiate infection on cultured mouse fibroblasts and primary brain cells and that S must interact with MHVR to infect these cells.

Since in most cases we were not able to identify the phenotype of the glial cells infected by MHV-DVIM, MHV-A59, or MHV-JHM, we were not able to determine whether the cell tropism of MHV strains that express HE is different from those that do not.

The presence of Neu5,9Ac_2 on DBT cells and primary brain cells still needs to be demonstrated to prove that these putative receptor determinants were indeed available for HE attachment. However even the MDCK I cells, which are known to express sialic acid and are susceptible to BCV infection, did not show signs of infection using immunofluorescence when challenged with MHV-DVIM.

Because the level of expression of HE varies among

different MHV isolates, it has been proposed that in contrast to the other three structural proteins, N, M, and S, which are expressed in all virions, the HE of MHV may be an accessory protein without a distinct function in replication (Yokomori et al., 1991). It is possible that the presence of the HE gene in the MHV genome may have been derived from a random RNA-RNA recombination event, for example between MHV and influenza ancestors. Yet, as for influenza virus (Coleman and Ward, 1985), the esterase activity of HE may aid MHV-DVIM in the release of newly formed virions in the final stage of the replication cycle. This is in contrast to BCV were it has been demonstrated that Neu5,9Ac_2 is used by BCV to infect MDCK I cells (Schultze and Herrler, 1992). Futhermore, it has been shown that both the S and HE glycoproteins of BCV recognize Neu5,9Ac_2 on plasma membrane molecules. Similar to the hemagglutinin of influenza A virus, the S glycoprotein of BCV has receptor binding and fusion activity and HE of BCV has hemagglutimating and receptor destroying activities (Schultze et al., 1991a). The authors of this work propose that attachment may occur in two steps which involve different receptors. HE and the hemagglutinin on S could be involved in an initial binding step to sialic acid receptors, while interaction of S with a second receptor may lead to fusion. Based on our work on the HE glycoprotein of MHV-DVIM, we conclude that although HE may cause the virus

to adsorb to carbohydrate moieties on cellular membranes, interaction of S with its receptor is always required for the initiation of infection.

IV. CHARACTERIZATION OF RAT CORONAVIRUS STRUCTURAL PROTEINS AND STUDIES ON THE RAT CORONAVIRUS RECEPTOR

INTRODUCTION

Although murine coronaviruses (MHV) and rat coronaviruses cause common infections in colonies of laboratory rodents (Lindsey, 1986) and are closely related antigenically (Bhatt et al., 1972; Maru and Sato, 1982), each virus is restricted to a single host species under natural conditions, and the target tissues of the viruses in mice and rats are different. For rat coronavirus, target tissues include salivary and lacrimal glands, and the respiratory and reproductive tracts. Until recently, no cell line that supports the growth of rat coronavirus had been identified. Recently, Percy and colleagues reported that the L2 line of C3H mouse fibroblasts supports the growth of two rat coronavirus strains, Parker's rat coronavirus (PRCV) (Percy and Williams, 1990) and sialodacryoadenitis virus (SDAV)(Percy et al., 1989). Because of this breakthrough and the development of solid phase corona virus receptor assays in our laboratory, we could begin studies on the rat coronavirus receptor.

As described in chapter I, MHV infects the liver, intestinal epithelium, and central nervous system. A 110 kDa CEA-related glycoprotein (MHVR) on these tissues and on L2

cells was identified as the receptor for MHV-A59 (Boyle et al., 1987; Williams et al., 1990; Williams et al., 1991; Dveksler et al., 1991). Since both MHV and rat coronavirus replicate in the same mouse fibroblast cell line, we asked whether these viruses use the same receptor to infect L2 cells. We used anti-MHVR antibodies to determine whether they could block rat coronavirus infection of L2 cells as they block MHV infection (Williams et al., 1990). We also explored the possibility that a rat CEA glycoprotein homologous to the MHV receptor may serve as a receptor for rat coronavirus.

Finally, we used solid phase receptor assays to study whether the species specificity and tissue specificity of rat coronavirus binding correlate with the natural host range and the natural target tissues of the virus. We then focussed on membranes of different rat tissues that bind rat coronavirus and studied the proteins to which virus attaches.

RESULTS

Replication of SDAV and PRCV on L2(Percy) Cells

The mouse L2 cell line, a subline of L-929, was shown to support the growth of SDAV and PRCV (Percy et al., 1989; Percy and Williams, 1990). Since we acquired this cell line

from Dr. D. Percy we called it L2(Percy) to differentiate it from the L2 cells in our lab. Our L2 cells support the growth of several MHV strains (e.g. MHV-A59, MHV-JHM, MHV-DVIM) which cause marked CPE including formation of syncytial giant cells and destruction of the cell monolayer. However SDAV and PRCV caused only exceedingly rare foci of viral antigen or CPE on our L2 cells. L2(Percy) cells are susceptible to both MHV and rat coronavirus infection, and both viruses cause CPE on these cell cultures. Because coronaviruses generally have narrow host ranges and usually infect cell lines from their normal host, we wondered whether L2(Percy) cells may represent an accidental mixture of mouse and rat fibroblasts or an accidental somatic cell hybrid. We cloned single cells from L2(Percy) cultures and subcloned them twice. Forty five subclones were challenged with MHV-A59, PRCV, or SDAV. At 24 hours p.i., the cultures were observed for the development of CPE. If the L2(Percy) cultures represented an homogeneous cell population, we expected that both MHV and rat coronavirus would grow on all subclones. If this culture was composed of a mixture of cells of different origins, we expected that MHV might grow on the murine subclones and rat coronavirus on others potentially of rat origin. Each of the 45 subcloned populations showed CPE after infection with all three coronaviruses, although the degree of cell fusion and cell death varied markedly among the cloned cell lines. Figure 19

Figure 19. L2, L2(Percy), and L2(Percy) clonal cells infected with MHV-A59 or SDAV. Cultures were inoculated with MHV-A59 (MOI, 2 PFU/cell) or SDAV (MOI, 2 PFU/cell). After 1 hour at 37°C the inoculum was replaced by fresh media. Approximately 20 hours p.i. cultures were photographed. Cells: L2, A and B; L2(Percy), C and D; L2(Percy) 12.a, E and F; L2(Percy) 29.a, G and H; L2(Percy) 30.a, I and J; L2(Percy) 41.a, K and L. Viruses: MHV-A59, A, C, E, G, I, K; SDAV, B, D, F, H, J, L.

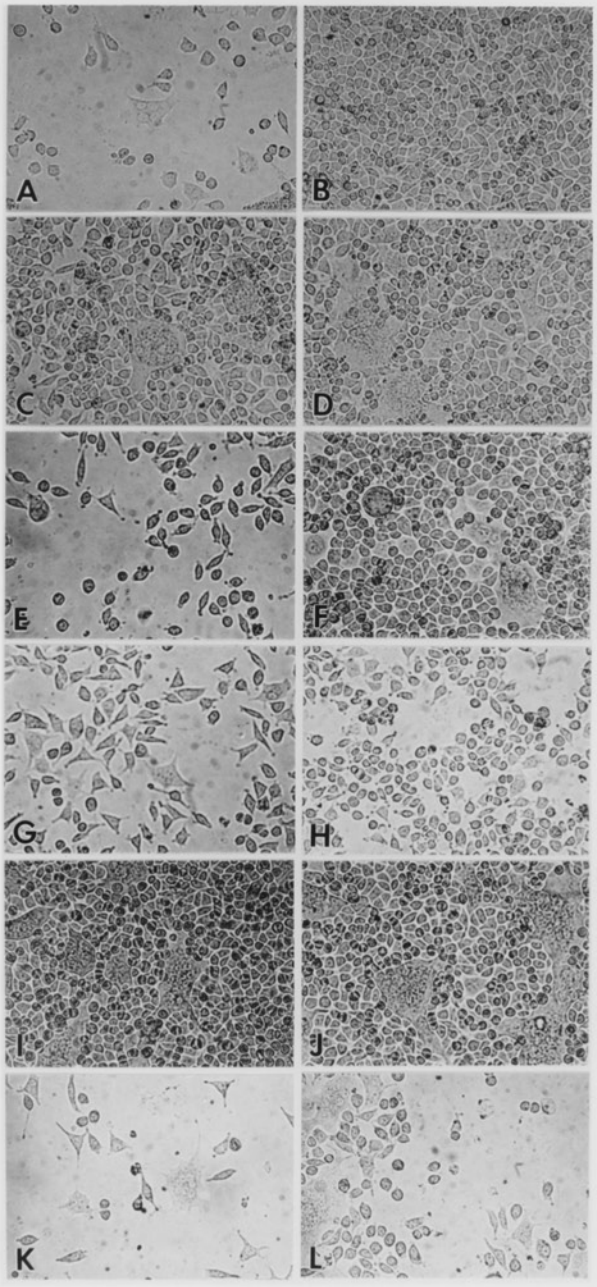
A
B
C
D
E
F
G
H
I
J
K
L

compares the CPE caused by MHV and SDAV on four subclones of the L2(Percy) cell line and on our L2 cells. Subclone 12.a showed high CPE with MHV-A59 but low CPE with SDAV; subclone 29.a showed low CPE with MHV-A59 and high CPE with SDAV; subclone 30.a showed low CPE with MHV-A59 and SDAV; and subclone 41.a showed high CPE with both viruses.

To quantitate these differences we compared the plaquing efficiency of MHV-A59, SDAV, and PRCV on these four L2(Percy)-derived cell lines (Figure 20 and Table 6). The same virus stocks were used to infect L2 cells and each of the four subclones of L2(Percy) cells. Both the titer of infectious virus and plaque sizes of the three viruses reflect our previous observations on the relative susceptibilities of these cell lines to the viruses. MHV-A59 produced the highest plaque titer on our L2 cells, while SDAV and PRCV produced the highest titers on the L2(Percy) 29.a and 41.a subclones. On all cell types PRCV formed only very small, turbid plaques that were very difficult to see. Gaertner and coworkers (1991), reported that SDAV growth on L2(Percy) cells was enhanced by treatment of cells with trypsin. We therefore repeated the plaque assay with PRCV following the same procedure as for the previous assays except that we added 3 μg/ml trypsin in the agar overlay. This treatment substantially increased the number and size of the PRCV plaques on the four L2(Percy) subclones. For example, on the 41.a cell line the number of plaques formed

Figure 20. Plaque assay of MHV-A59, SDAV, and PRCV on L2, L2(Percy) and L2(Percy) clonal cells. Serial dilutions of each virus were prepared and used to inoculate each one of the five cell lines on 60 mm plates on the same day. After 1 hour at 37°C the unadsorbed virus was removed and an agar overlay was added. For trypsin treatment of PRCV, 3 μg/ml trypsin were added to the agar overlay. Plaques were developed with neutral red and counted 48 hours p.i. and photographed 72 hours p.i.

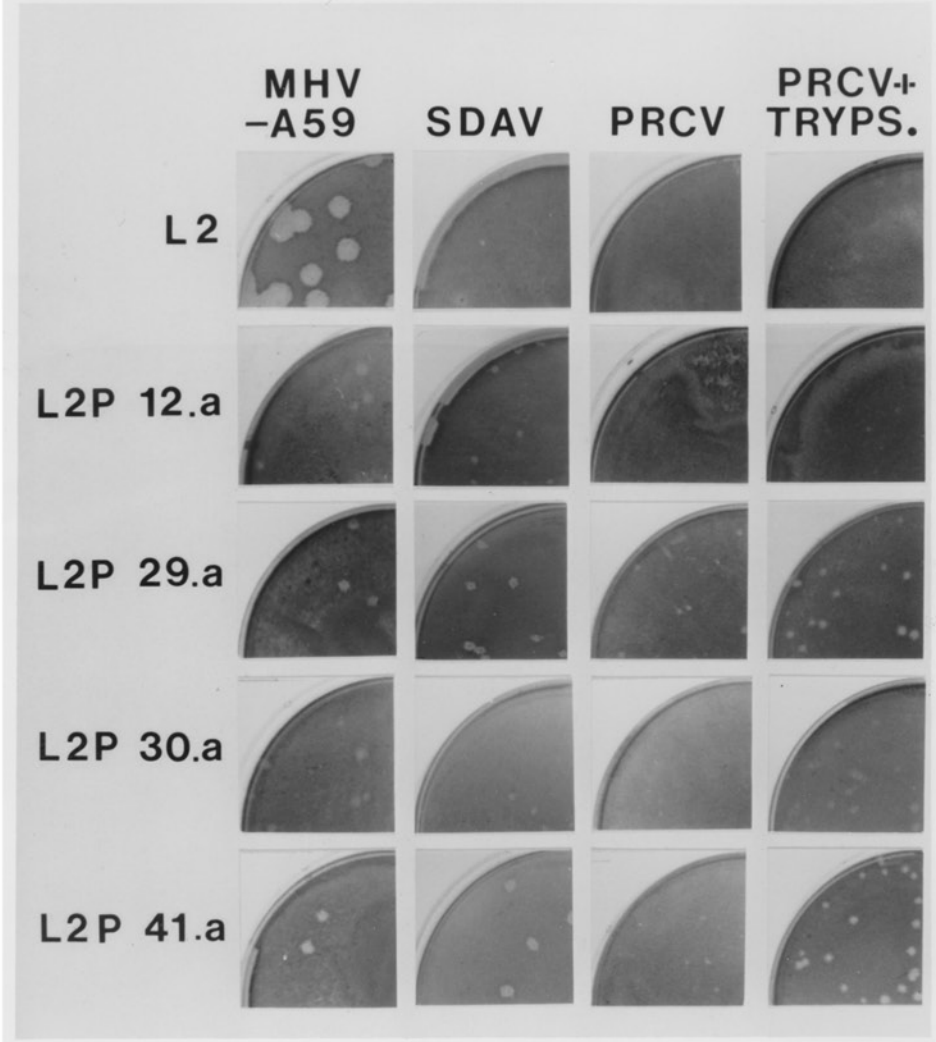
MHV
-A59
SDAV
PRCV
PRCV+
TRYPS.
L2
L2P 12.a
L2P 29.a
L2P 30.a
L2P 41.a

TABLE 6

Plaque Assay of MHV-A59, and Rat coronavirus strains SDAV and PRCV on L2 Cells and on Four Sublones of L2(Percy) Cells

	Cell Line	MHV-A59	SDAV	PRCV	PRCV + Trypsin
Virus Titer (PFU/ml)	L2	4.7×10^9	1.3×10^3	$< 6 \times 10^2$	$< 6 \times 10^2$
	L2P-12.a	4.0×10^9	8.0×10^6	$< 6 \times 10^2$	4.1×10^8
	L2P-29.a	5.3×10^8	8.5×10^7	6.5×10^7	1.1×10^9
	L2P-30.a	1.6×10^8	1.7×10^7	$< 6 \times 10^2$	3.5×10^8
	L2P-41.a	1.4×10^9	1.2×10^8	1.3×10^7	1.2×10^9
Plaque Size (mm)	L2	2.5±0.3	0.3	NA*	NA
	L2P-12.a	1.5±0.3	0.6±0.1	NA	0.6±0.2
	L2P-29.a	1.1±0.3	0.9±0.2	0.5±0.1	1.0±0.3
	L2P-30.a	1.0±0.2	0.6±0.2	NA	0.6±0.2
	L2P-41.a	1.3±0.3	1.0±0.1	0.5±0.1	0.9±0.3

*NA = not applicable

by PRCV in the presence of trypsin increased almost 100 fold to $1.2x10^9$ PFU/ml and plaque size almost doubled to 0.9 mm. The enhanced infectivity and CPE of PRCV in the presence of trypsin is likely to be due to the proteolytic cleavage of the viral S glycoprotein which enhances viral infectivity and cell fusing activity as found for BCV and some MHV strains (Sturman et al., 1985; Storz et al., 1981). For future experiments the 41.a cell line promises to be much better than the parental L2(Percy) cell line for the growth and assay of SDAV and PRCV.

Viral Structural Proteins

Since rat coronavirus has only recently been grown in tissue culture, characterization of its proteins and nucleic acids have been slow in comparison to other coronaviruses. To identify viral glycoproteins that might interact with cellular receptors, we characterized the proteins in purified SDAV virions. The structural proteins of SDAV were analyzed in immunoblots with mouse anti-SDAV, and compared to the proteins of MHV-A59 and BCV (Figure 21). Under non-reducing conditions this antibody could identify well only a 50 kDa polypeptide which on MHV and BCV corresponds to the nucleocapsid protein (N). The 100 kDa band that is seen weakly on SDAV could correspond to the cleaved form of the S glycoprotein or to the dimeric form of the HE. We could not

Figure 21. Immunoblotting of RCV-SDAV, MHV-A59, and BCV with anti-RCV-SDAV antiserum. Gradient purified virions, 6 μg of protein per lane, were electrophoresed in an 8% polyacrylamide gel under nonreducing (-2ME) and reducing (+2ME) conditions and blotted to nitrocellulose. Virion proteins were detected with mouse anti-RCV-SDAV antiserum followed by ^{125}I-SPA. 2ME, 2-βmercaptoethanol; RCV, RCV-SDAV; MHV, MHV-A59. Molecular weight markers in kilodaltons are shown on the right.

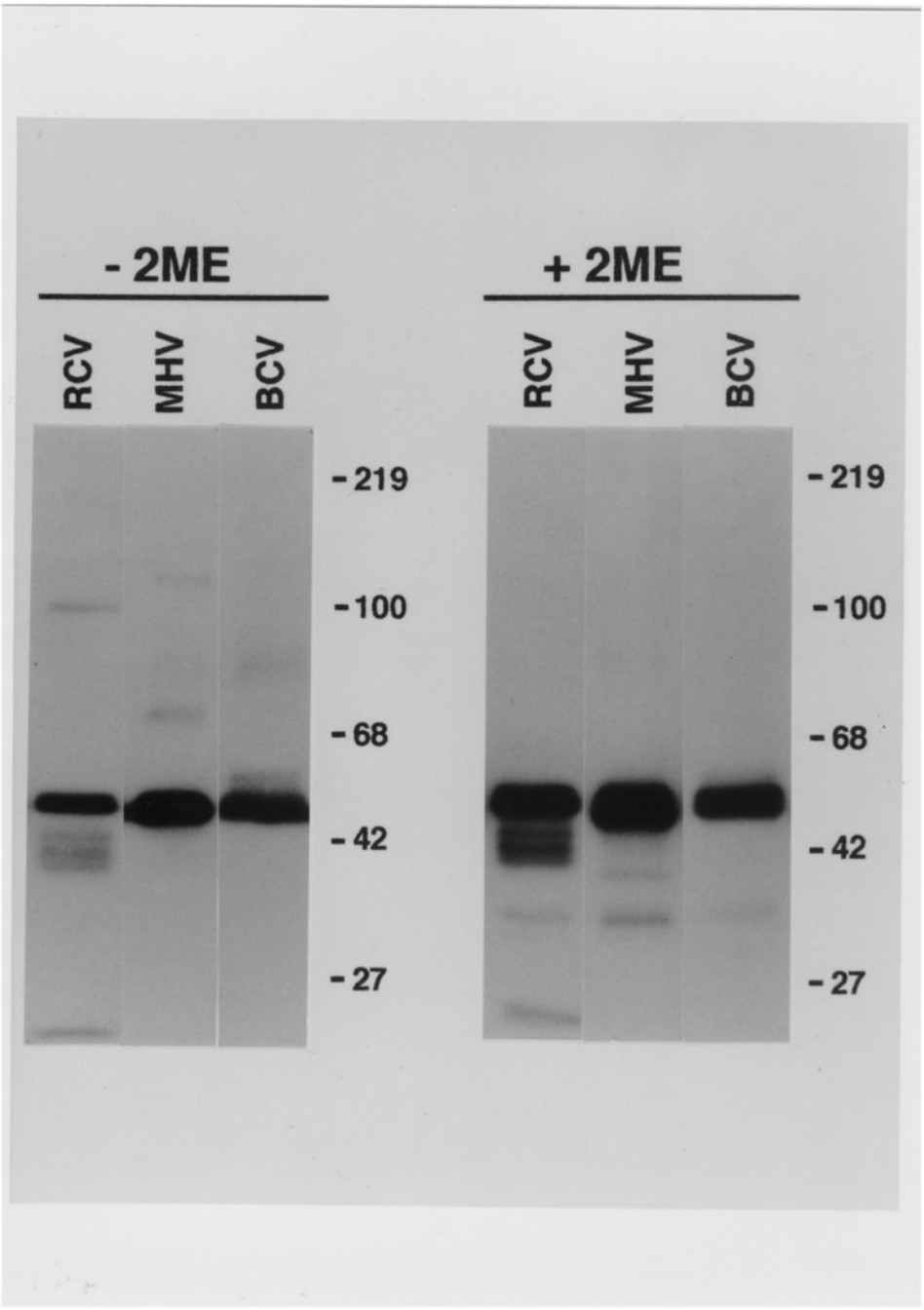
- 2ME
+ 2ME
RCV
MHV
BCV
RCV
MHV
BCV
- 219
- 100
- 68
- 42
- 27
- 219
- 100
- 68
- 42
- 27

establish the origin of the three 40-44 kDa bands detected on SDAV. On MHV-A59 the anti-SDAV antibody could recognize a polypeptide of about 120 kDa that could be a trimer of N (Robbins et al., 1986) and a 70 kDa protein which we could not identify.

Since this antibody could not recognize well the surface glycoproteins of SDAV, we tried to identify this molecules on immunoblots of viral proteins with antisera specific for S of MHV-A59 and antisera specific for HE of BCV. Figure 22 shows that the anti-S antiserum identified a 180-190 kDa protein under non reducing conditions and a 80-90 kDa protein under reducing conditions, which probably correspond to the uncleaved and cleaved forms of S respectively. On these blots we were also able to identify both forms of S on MHV-A59 and BCV. In addition, on MHV-A59 we saw a 240 kDa band in the absence of reducing agent and a similar band on BCV in its presence. This band may correspond to the trimeric form of S (Delmas and Laude, 1990).

To determine whether SDAV expresses HE, we immunoblotted these viral proteins with antisera specific for HE of BCV (Figure 23). In the presence of reducing agent, this antibody identified a 70-75 kDa protein on rat coronavirus which would correspond to the monomeric HE glycoprotein. On BCV this antibody saw both the monomeric and the dimeric forms of HE. Since this glycoprotein is not

Figure 22. Immunoblotting of RCV-SDAV, MHV-A59, and BCV with antiserum against the S glycoprotein of MHV-A59. Gradient purified virions, 6 μg of protein per lane, were electrophoresed in an 8% polyacrylamide gel under nonreducing (-2ME) and reducing (+2ME) conditions and blotted to nitrocellulose. Virion proteins were detected with goat antiserum against the S glycoprotein of MHV-A59 followed by ^{125}I-SPA. 2ME, 2-βmercaptoethanol; RCV, RCV-SDAV; MHV, MHV-A59. Molecular weight markers in kilodaltons are shown on the right.

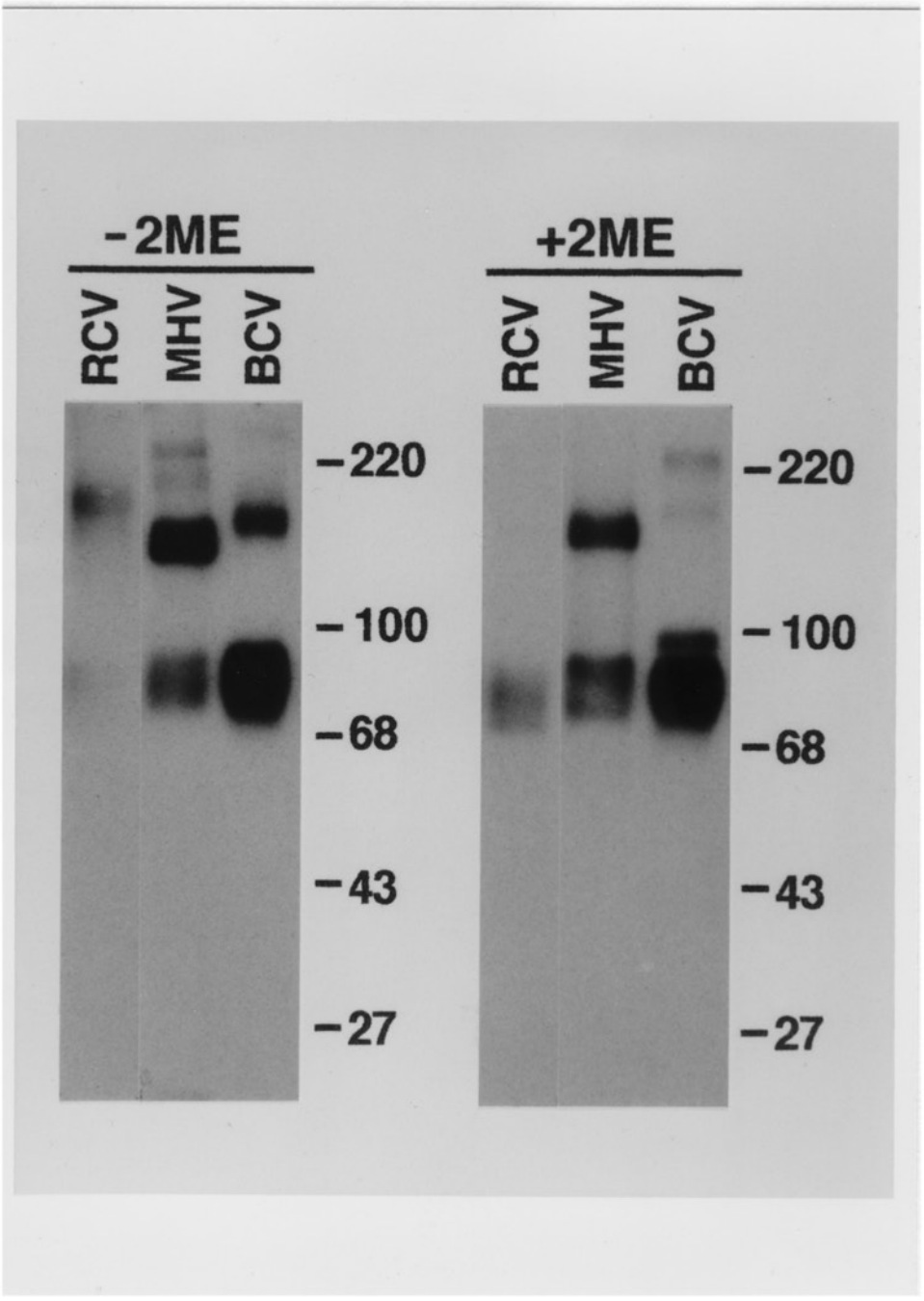
-2ME
+2ME
RCV
MHV
BCV
RCV
MHV
BCV
-220
-100
-68
-43
-27
-220
-100
-68
-43
-27

Figure 23. Immunoblotting of RCV-SDAV, MHV-A59, and BCV with anti-HE antiserum against HE glycoprotein of BCV. Gradient purified virions, RCV-SDAV 12 μg of protein per lane, and MHV-A59 and BCV 6 μg of protein per lane, were electrophoresed in an 8% polyacrylamide gel under nonreducing (-2ME) and reducing (+2ME) conditions and blotted to nitrocellulose. Virion proteins were detected with rabbit antiserum against the gp65 glycoprotein of BCV followed by ^{125}I-SPA. RCV and MHV lanes were exposed to autoradiographic film for 48 hours and BCV lane was exposed for 12 hours. 2ME, 2-mercaptoethanol; RCV, RCV-SDAV; MHV, MHV-A59. Molecular weight markers in kilodaltons are shown on the right.

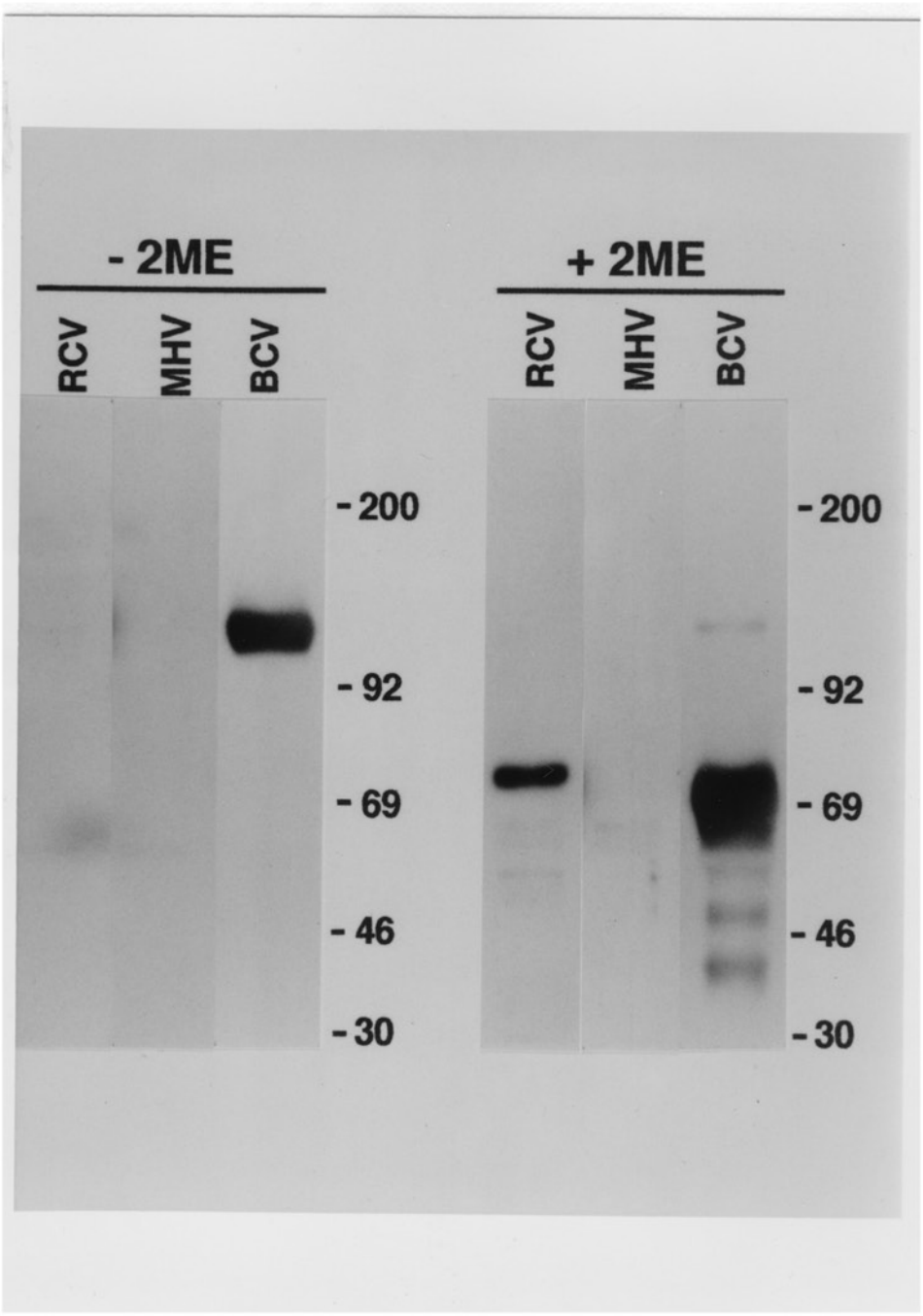
- 2ME
+ 2ME
RCV
MHV
BCV
RCV
MHV
BCV
- 200
- 92
- 69
- 46
- 30
- 200
- 92
- 69
- 46
- 30

expressed on MHV-A59 no bands were detected on this virus (Luytjes et al., 1988). Although these data suggest that SDAV expresses a glycoprotein related to BCV-HE, this molecule may be expressed at a relatively low level or may be non-functional because infected L2(Percy) cells did not hemadsorb BALB/c mouse erythrocytes, and we could not detect acetylesterase activity on purified virions (data not shown). Immunoblot analysis of SDAV virions showed that SDAV expresses two surface glycoproteins, S of 180-200 kDa and HE of 70-75 kDa.

Antibody Blockade of the MHV Receptor

The fact that MHV and rat coronavirus are antigenically related and that both viruses grow on the same mouse fibroblast cell line, L2(Percy), prompted us to determine whether the receptors for rat coronavirus and MHV are related. We used monoclonal antibody to the receptor (MAb-CC1) which blocks infection by MHV to learn whether this antibody also protects L2(Percy) cells from rat coronavirus infection. L2(Percy) 41.a cells were pretreated with serial 2 fold dilutions of the MAb-CC1 or a control MAb (MAb-CT) for 1 hour. The antibodies were then removed and the cells were challenged with infectious MHV-A59 or SDAV. When the infection had advanced sufficiently and syncytia and/or cell death could be observed in the culture, the cells were fixed

and stained with crystal violet (Figure 24). The anti-receptor MAb-CC1 protected the L2(Percy) 41.a cells from infection with MHV-A59, and cell survival decreased with decreasing concentrations of anti-receptor antibody. But when these cells were treated with the same antibodies and challenged with SDAV, MAb-CC1 did not protect the cultures from infection.

MAb-CC1 is very species-specific and probably only binds to the region of the receptor molecule to which MHV binds or close to it (Compton, 1988). We therefore tried to protect cells with a polyclonal anti-MHV receptor antibody. This antibody was raised in our lab against the purified denatured form of the MHV receptor and on immunoblots of rat liver membranes it identifies a rat homologue of the MHV receptor and protects mouse fibroblasts against MHV infection (Dvekslar et al., 1991). L2(Percy) cells were incubated with this polyclonal anti-MHV receptor antibody for 1 hour. The antibodies were removed and the cells were inoculated with SDAV or PRCV. After 1 hour the inoculum was replaced with fresh medium containing 10% anti-MHV receptor antibody. Cultures were fixed 8 and 24 hours p.i. and viral antigens were detected by immunofluorescence. Infection on the cells treated with anti-MHV polyclonal antibody appeared to be similar to infection on the control cells. Antibody to the MHV receptor did not block rat coronavirus infection of L2(Percy) cells (data not shown). These results strongly

Figure 24. Blocking of coronavirus infection of L2(Percy) subclone 41.a cells by anti-receptor MAb-CC1. L2(Percy) 41.a cells were pretreated with 2 fold serial dilutions of MAb-CC1 (Anti-R) or a control MAb of the same isotype (Anti-CT) for 1 hour at 37°C (rows 1 to 11, from left to right). Antibodies were removed and the cells were challenged with $5x10^5$ PFU/well of MHV-A59 (upper plate) or RCV-SDAV (lower plate) for 1 hour at 37°C. When the infection had advanced sufficiently (16 hours for MHV-A59 and 24 hours for RCV-SDAV), cells were stained with crystal violet. In each of the two 96 well plates upper wells of column 12 received neither antibodies nor virus; 4 lower wells of column 12 received no antibodies but were inoculated with MHV-A59 (upper plate) or RCV-SDAV (lower plate).

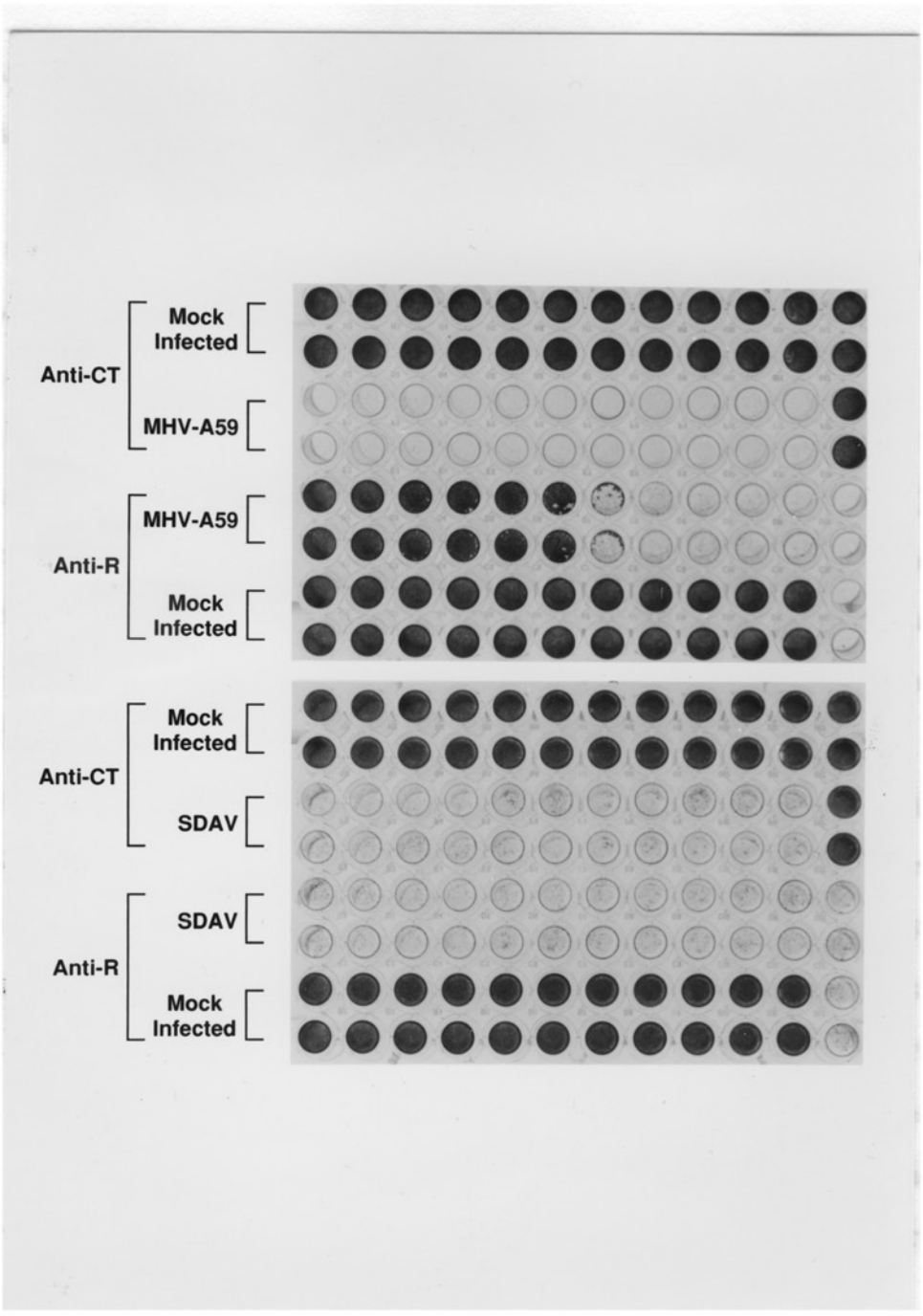
Anti-CT
Mock Infected
MHV-A59
Anti-R
MHV-A59
Mock Infected
Anti-CT
Mock Infected
SDAV
Anti-R
SDAV
Mock Infected

indicate that MHV-A59 and rat coronavirus use different receptors to infect the same cell line.

Studies on Interaction of Rat Coronavirus with Rat Homologs of the MHV Receptor

The cellular receptor for murine coronavirus MHV-A59 has been cloned and found to be a member of the carcinoembrionic antigen (CEA) family of glycoproteins (Williams et al., 1991; Dveksler et al., 1991), with a 67 % identity at the amino acid level with rat ecto-ATPase (Lin and Guidotti, 1989). To determine whether this member of the rat CEA family serves as a receptor for rat coronavirus we used COS cells transiently transfected with ecto-ATPase (kindly provided by Dr. S. H. Lin, Houston, TX). Two antibodies to this molecule, antibody 669 to the denatured form of the molecule and antibody 708 to the native form of the molecule were also provided by Dr. Lin. Antibody 669 was used in an immunoblot analysis of membrane preparations of different rat tissues, to determine whether rat ecto-ATPase is expressed in the natural target tissues of SDAV infection (Figure 25). Ecto-ATPase is expressed in several rat and mouse tissues (e.g. rat parotid, submandibular and lacrimal exorbital glands and lung, and mouse and rat liver and intestine). Expression of ecto-ATPase in the different rat tissues does not always correlate with the target tissues of

Figure 25. Immunoblotting of membrane preparations of mouse and rat tissues with anti-ectoATPase. Crude membrane preparations of mouse and rat tissues, 200 μg of protein per lane, were electrophoresed in an 8% polyacrylamide gel and transferred to nitrocellulose. Blots were incubated with rabbit anti-ectoATPase (No. 669) followed by ^{125}I-SPA. BL, BALB/c mouse liver; BI, BALB/c mouse intestine; Pa, parotid gland; Sm, submandibular gland; LE, lacrimal exorbital gland; LI, lacrimal intraorbital gland; Lu, lung; Li, liver; In, intestine. Molecular weight markers in kilodaltons are shown on the right.

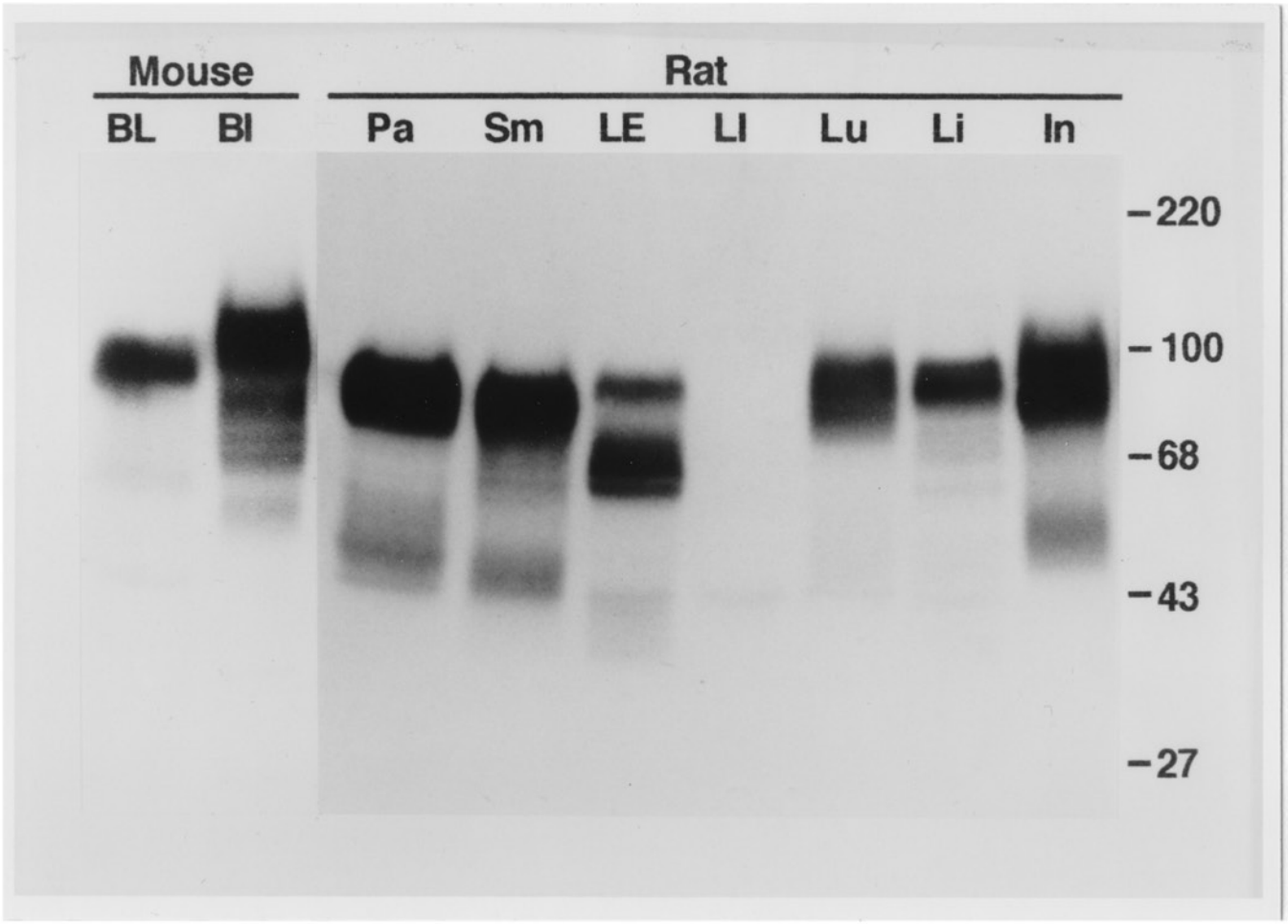
Mouse
Rat
BL
Bl
Pa
Sm
LE
Ll
Lu
Li
In
220
100
68
43
27

SDAV during natural course of infection. Rat coronavirus infects salivary and lacrimal glands and lung, but liver and intestine are not affected by this virus.

The transiently transfected COS cells were challenged with SDAV (MOI=5 PFU/ml) and fixed 8 and 24 hours p.i. We used double immunofluorescent labelling to detect both ecto-ATPase and viral antigens. Some of the transfected cells which were expressing ecto-ATPase were irregular in shape with prominent surface projections (Figure 26) but we did not find any of these cells to be infected with SDAV. Immunoblot analysis of cellular extracts of ecto-ATPase-transfected COS cells showed a high level of expression of ecto-ATPase (Figure 27, lane 1) but no viral antigens were detected on ecto-ATPase-transfected cells infected with SDAV (data not shown). In control COS cells only a relatively small amount of protein that cross reacts with antibody to rat ecto-ATPase could be detected (Figure 27, lane 2). Since expression of this candidate receptor in COS cells might not be sufficient for SDAV to overcome the species barrier and viral replication might be blocked in these cells after viral attachment, we repeated this experiment on BHK cells, because they are of rodent origin and are resistant to rat coronavirus infection. We subcloned the ecto-ATPase cDNA given to us by Dr. S. Lin in a cdm8 vector into a pRSV-neo vector, which we used to electroporate BHK cells. These transiently transfected cells were inoculated

Figure 26. COS cells transiently transfected with rat ecto-ATPase and challenged with SDAV. COS cells transfected with ecto-ATPase were challenged with SDAV (MOI, 0.2 PFU/cell). After 1 hour the virus was removed and replaced by fresh media. Cultures were fixed 8 and 24 hours p.i. and immunofluorescent staining was performed as follows: SDAV antigens were detected with mouse anti-SDAV (not shown); ecto-ATPase was detected with rabbit anti-ecto-ATPase (No. 708) (A, B); followed by secondary antibodies conjugated to rhodamine to visualize SDAV antigens (not shown), and fluorescein to visualize ecto-ATPase.

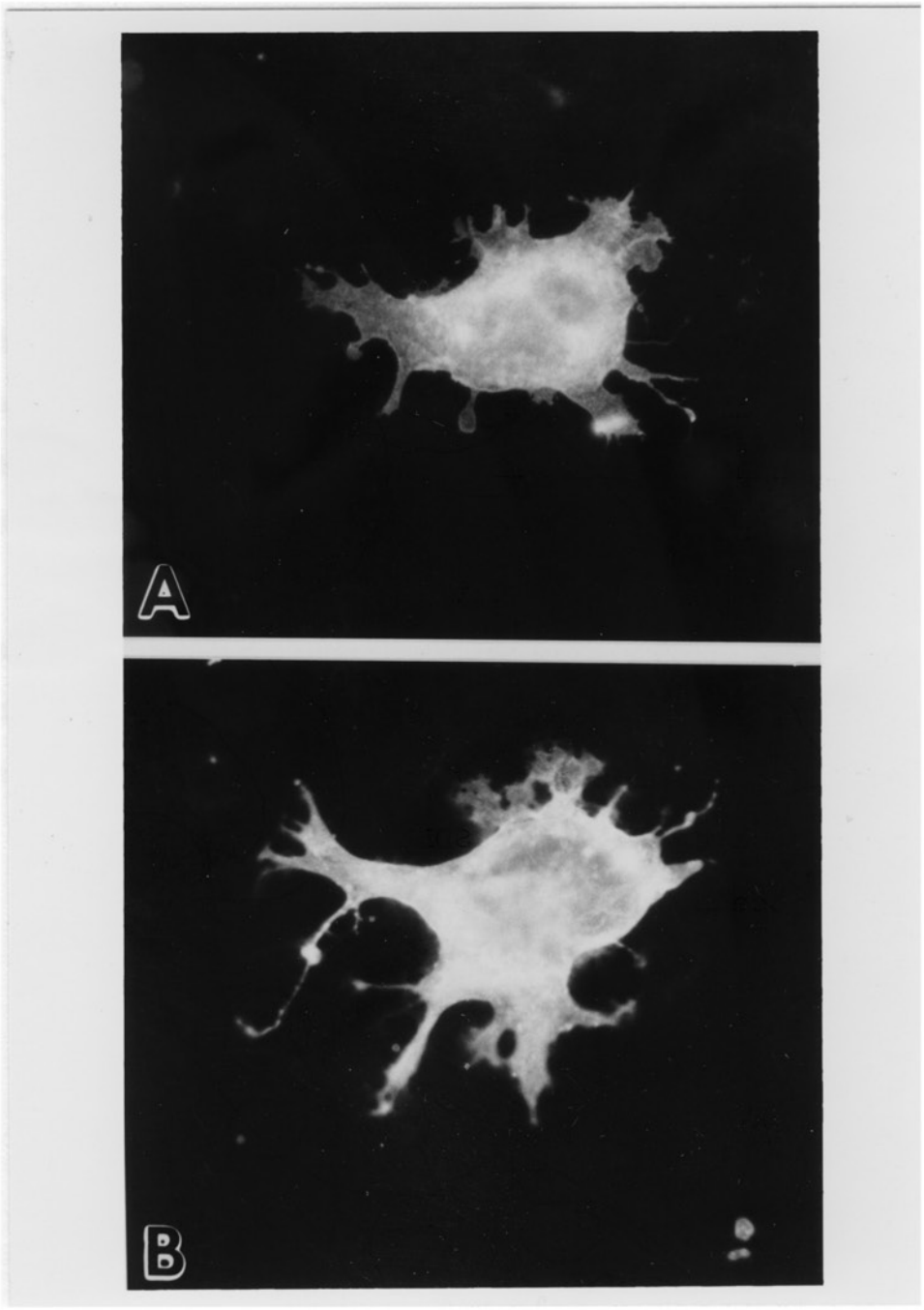
A
B

Figure 27. Immunoblotting of cellular extracts of COS cells transfected with ecto-ATPase. Cellular extracts of COS cells (lane 2) and cellular extracts of COS cells transfected with ecto-ATPase (lane 1) were electrophoresed in an 8% polyacrylamide gel under reducing conditions and blotted to nitrocellulose. Ecto-ATPase proteins were detected with rabbit anti-ecto-ATPase antiserum followed by ^{125}I-SPA. Molecular weight markers in kilodaltons are shown on the right.

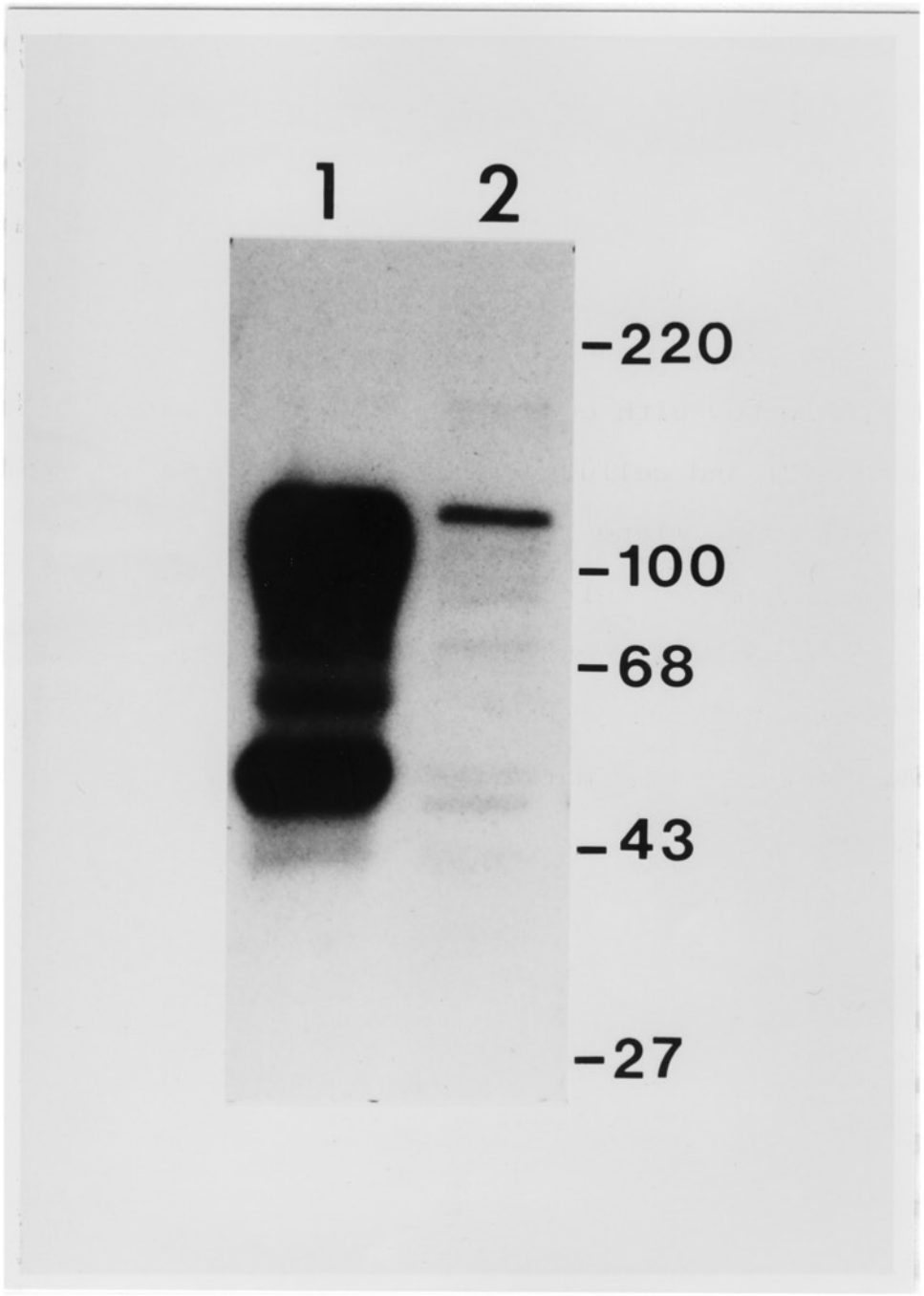
1
2
-220
-100
-68
-43
-27

with SDAV (MOI=10 PFU/ml) and PRCV (MOI=100 PFU/ml) and fixed 8 hours p.i. and double immunofluorescent staining was performed in order to detect ecto-ATPase and viral antigens. Neither SDAV antigens nor ecto-ATPase was detected on cells transiently transfected with ecto-ATPase. We conclude that in these experiments expression of ecto-ATPase was either too low to detect or transfection was not efficient. Further experiments in which cells expressing ecto-ATPase are selected for challenge with rat coronavirus will be required to determine whether ecto-ATPase can serve as a receptor for rat coronaviruses.

Virus Overlay Protein Blot Assays (VOPBA) of rat coronavirus and MHV on membrane tissues of different organs

Receptors for MHV-A59, of 100-120 kDa, are expressed on intestinal and liver membranes of adult MHV-A59-susceptible BALB/c mice but not adult MHV-A59-resistant SJL/J mice (Boyle et al., 1987). We wanted to determine if SDAV shows strong tissue specificity and to compare this specificity to that of MHV-A59. VOPBAs were performed on crude membrane preparations of tissues which SDAV infects under natural conditions: rat lacrimal glands, rat salivary glands, and rat lung, and of tissues which SDAV does not infect: mouse and rat intestine, and mouse liver (Figure 28). Blotting with MHV-A59 confirmed the previous observation that this

Figure 28. Virus overlay protein blot assay (VOPBA) of MHV-A59 binding to membrane preparations of mouse and rat tissues. Crude membrane preparations of mouse liver and intestine and rat lung, intestine, and parotid and lacrimal glands, 200 μg of protein per lane, were electrophoresed in an 8% polyacrylamide gel and transferred to nitrocellulose. Blots were incubated with MHV-A59 supernatants of infected cells containing 25 mM hepes, followed by goat antiserum against S of MHV-A59, and then ^{125}I-SPA. BL, BALB/c mouse liver; BI, BALB/c mouse intestine; Lu, rat lung; LE, rat lacrimal exorbital gland; Pa, rat parotid gland; In1, intestine of adult rat; In2 and In3, intestine of 10 and 5 day old rats, respectively. Molecular weight markers in kilodaltons are shown on the right.

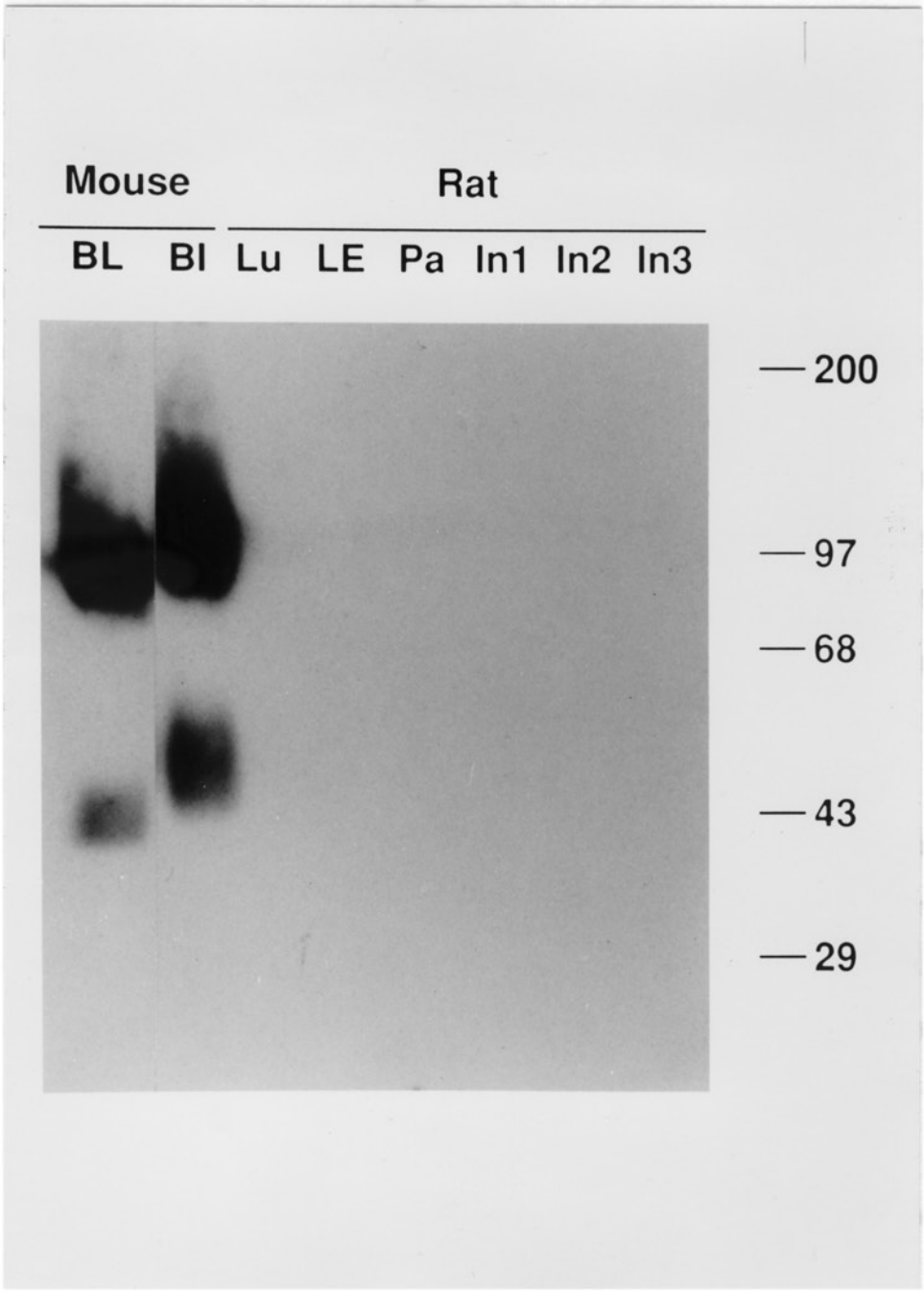
Mouse
Rat
BL
Bl
Lu
LE
Pa
In1
In2
In3
200
97
68
43
29

virus binds to the 100-120 kDa receptor on mouse intestine and liver membrane preparations (Boyle et al., 1987). MHV-A59 which did not bind to any of the rat tissue showed a strong species specificity. Unlike MHV-A59, SDAV did not bind to one major protein but to several different proteins on each tissue (Figure 29, upper panel). SDAV binds to proteins on all susceptible rat tissues: it binds to membranes of rat parotid, submandibular lacrimal exorbital, and lacrimal intraorbital glands, and lung. SDAV did not significantly bind to any membrane proteins in rat intestine or to mouse liver or intestine, which are not target tissues for this virus. The control for this VOPBA used conditioned medium from uninfected cells in place of supernatant medium from SDAV-infected cells (Figure 29, lower panel). In this experiment, the anti-SDAV antibody recognized a protein of 50 kDa in lacrimal exorbital and partoid glands. This protein is probably the nucleocapsid protein of SDAV. The rats from which these membrane preparatins were made were probably infected with SDAV. Because one of the animals from this batch had inflamed submandibular glands, its tissues were not included in the preparation and SDAV infection of this animal was confirmed by histopathology. Apparently, other animals in the batch had inapparant infection. The 50 kDa bands were not observed in membranes from different batches of rats.

SDAV, thus showed a degree of tissue specificity though

Figure 29. Virus overlay protein blot assay (VOPBA) of RCV-SDAV binding to membrane preparations of mouse and rat tissues. Crude membrane preparations of mouse and rat tissues, 200 μg of protein per lane, were electrophoresed in an 8% polyacrylamide gel and transferred to nitrocellulose. Blots were incubated with supernatant medium from SDAV-infected cells containing 25 mM Hepes, followed by mouse anti-RCV-SDAV ascites and then ^{125}I-SPA (upper panel). Blots were incubated with conditioned supernatant medium from uninfected cells containg 25 mM Hepes, followed by anti-RCV-SDAV ascites and then ^{125}I-SPA (lower panel). BL, BALB/c mouse liver; BI, BALB/c mouse intestine; P, parotid gland; Sm, submandibular gland; LE, lacrimal exorbital gland; LI, lacrimal intraorbital gland; Lu, lung; In, intestine. Molecualr weight markers in kilodaltons are shown on the right.

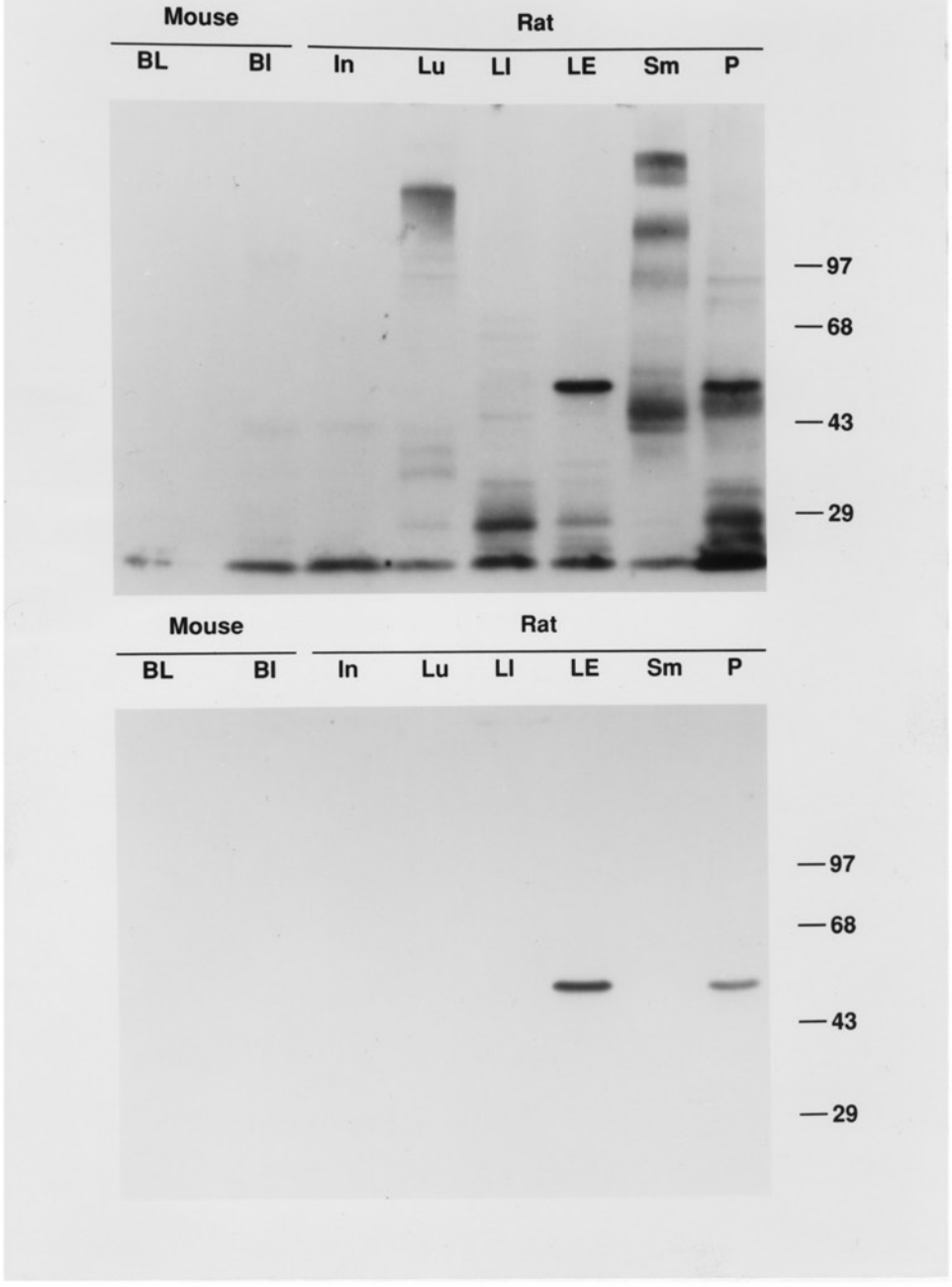
Mouse
Rat
BL
Bl
In
Lu
Ll
LE
Sm
P
97
68
43
29
Mouse
Rat
BL
Bl
In
Lu
Ll
LE
Sm
P
97
68
43
29

it is not as marked as the tissue specificity of MHV-A59. The binding of the virus to several proteins indicates that the receptor for rat coronavirus could be a member of a family of proteins with different MWs all of which bind virus. Alternatively the SDAV receptor might be a rare or labile molecule of cellular membranes which would be difficult to detect using the VOPBA. In this case, detection of non-specific attachment to non-receptor proteins might be favored.

DISCUSSION

The ability to study the biochemical characteristics of rat coronaviruses and their interaction with receptors was dependent upon being able to grow the viruses in cell culture. Although the L2 mouse fibroblast cell line in our lab is not susceptible to infection with SDAV and PRCV, the L2(Percy) variant of this cell line obtained from Dr. Percy's laboratory is susceptible to infection with both PRCV and SDAV. A subpopulation of the cells is susceptible and undergoes fusion with SDAV. This is surprising because the rat viruses cannot be grown in other mouse cell lines. The difference between L2 and L2(Percy) cells is not understood. No mutagenesis or selective growth conditions had been used by Dr. Percy. It therefore, was important to determine whether the L2(Percy) cells had been inadvertently

contaminated with rat cells. We therefore subcloned the L2(Percy) cell line. All subclonal lines of the L2(Percy) cells were susceptible to infection with MHV and with both strains of rat coronavirus. Thus the L2(Percy) cell line probably does not represent a mixture of rat and mouse fibroblasts. If a contaminating rat cell initiated the rat coronavirus susceptibility of L2(Percy) cells, then the rat cell could have fused with the mouse cells to make a subpopulation of mouse-rat hybrids that would be susceptible to both rodent viruses.

In the four subclones of L2(Percy) cells infection by SDAV and PRCV causes different degrees of CPE. Based on their plaquing efficiency, the L2(Percy) 29.a and 41.a sublines are probably the best lines for the growth and assay of PRCV and SDAV because they produced the largest plaques and the highest plaque titers. In addition, we found that trypsin treatment of PRCV substantially increased the size and number of plaques which would otherwise be very small and difficult to see.

Since little is known about the structural proteins of rat coronavirus, it was important for us to determine which glycoproteins are expressed on the virion surface, and might participate in receptor-virus interaction. Immunoblots of purified virions showed that SDAV expresses a 180-200 kDa S glycoprotein, that when proteolytically cleaved yields two subunits of 90-100 kDa. On the surface of the SDAV virions,

the S glycoproteins are probably in their cleaved form held together by disulfide bonds because under reducing conditions, S appeared mostly as a 90-100 kDa band. For several coronaviruses it has been shown that proteolytic cleavage of S greatly increases virus infectivity in culture Under reducing conditions we identified a second protein of 70 kDa which probably corresponds to the monomeric form of the HE surface glycoprotein. It appears that HE is not highly expressed on SDAV because infected cells did not adsorb mouse RBC's and acetylesterase activity, although detectable, was much lower than for BCV and MHV-DVIM. Yet, it is important to remember that SDAV virions may express HE which could cause non-specific binding to the same carbohydrate moieties on different membrane glycoproteins.

Since rat coronavirus and MHV are antigenically related and infect the same cell line, I wanted to determine whether rat coronavirus uses the same receptor as MHV, a rat homolog of the MHV receptor, or a different member of the CEA family of glycoproteins. During the course of this research the receptor for MHV-A59 was cloned and found to be a member of the carcinoembrionic antigen (CEA) family of glycoproteins in the immunoglobulin superfamily (Dveksler et al., 1991; Williams et al., 1991). Polyclonal and monoclonal antibodies to the MHV receptor that confer protection against MHV infection of L2(Percy) cells did not protect these cells against infection with SDAV or PRCV. Therefore, MHV and rat

coronavirus do not share the same receptor binding site.

Rat ecto-ATPase, which has a 67% identity at the amino acid level with the MHV receptor, does not appear to serve as a receptor for rat coronavirus either. COS cells transiently transfected with ecto-ATPase were not susceptible to SDAV infection, and antibodies to this molecule did not protect L2(Percy) cells from infection with SDAV or PRCV. Since the rat immunoglobulin superfamily contains several members which share sequence homology with the MHV receptor, perhaps a different member of the CEA family such as the rat pregnancy specific glycoprotein could serve as a receptor for rat coronavirus.

With the purpose of identifying proteins on target tissues which bind rat coronavirus I used the solid phase receptor binding assay. SDAV bound mainly to rat membrane preparations from natural target tissues such as lacrimal and salivary glands, but not to intestine. However, there was some SDAV binding on rat liver which is not known to be a target tissue for virus infection in vivo. In VOPBAS, virus bound to several different proteins in each tissue. The putative receptor could be a moiety expressed on several members of a family of related molecules. Alternatively rat coronavirus could be less species and tissue specific than MHV. MHV receptors are very species specific, being present only in mice; but receptors for other coronaviruses (e.g. HCV-229E, CCV, FIPV and TGEV) are less specific for binding

but may still be very specific for infection. In addition, this solid phase assay detects molecules on cellular membranes that bind virus which may not necessarily be viral receptors.

In summary, we have identified two sublines of the L2(Percy) cell line that will facilitate the growth of rat coronavirus. The 29.a and 41.a sublines which show marked CPE with extensive fusion and cell death upon PRCV and SDAV infection will aid in the assessment of infection vs. protection when testing anti-receptor antibody candidates or in the identification of protective anti-receptor monoclonal antibodies. Mouse polyclonal antiserum raised against rat coronavirus target tissues will be tested for its efficacy in protecting L2(Percy) cells from rat coronavirus infection. If protection occurs, then a anti-receptor monoclonal antibody could be raised and used for receptor purification. Such an antibody would be very helpful in understanding the nature of the receptor on L2(Percy) cells, its identity to the receptor in rat tissues and whether its tissue distribution corresponds to the tissues affected during the natural course of infection.

V. FUTURE DIRECTIONS

Viral receptors on the surface of host cells are the first molecules virus interact with, as they begin the infection cycle. Since they are the key to the initiation of infection virus-receptor interactions are studied for viral therapy, for the identification of compounds that block virus receptor interactions. Examples of compounds that could be effective therapeutic agents are ligand-mimics or receptor-mimics. The ligand mimics resemble the binding domain of the virus attachment protein and could compete with the virus for binding to the receptor. Compounds that mimic the virus binding domain are anti-receptor antibodies, anti-idiotypic antibodies directed against anti-bodies to the VAP's, synthetic peptides resembling the binding region of the VAP's, and natural ligands of the virus receptor. Anti-receptor antibodies that block virus binding have been raised against the receptors for HIV (Dalgleish et al., 1984, Klatzman et al., 1984b), poliovirus (Minor et al., 1984), and rhinovirus (Colonno et al., 1986). An anti-idiotypic antibody against an antibody that recognizes the reovirus hemagglutinin blocks binding of this virus to its receptor (Kauffman et al., 1983). Synthetic peptides resembling the binding domain of the Epstein-Barr virus (Nemerow et al., 1989) and the foot and mouth disease virus (Fox et al., 1989) inhibit virus binding. The natural ligand

of the vaccinia virus receptor, epidermal growth factor, blocks infection of murine L cells (Eppstein, 1985). The receptor mimics could bind to the virus attachment protein and impede the virus from interacting with the host cell receptor. Antibodies against regions of the virus that interact with receptors, such as antibodies against the binding domain of gp120 of HIV (Lasky et al., 1987) and viral receptors such as the secreted form of CD4, have been shown to neutralize infectivity of HIV <u>in vitro</u> (Smith et al., 1987).

Receptors are also fundamental in dictating viral tropism which produces selective damage to specific cells, tissues, or hosts. The importance of viral receptors in determining species specificity of certain viruses is demonstrated in experiments where transfection of non permissive cells with a receptor gene or with the viral genome is enough to overcome the specificity barrier. For example, when the receptor for MHV-A59 was transfected into receptor negative human or hamster cells, these cells became susceptible to MHV infection (Dveksler et al., 1991).

In addition to virus-receptor interaction, there are additional factors which determine the tropism of the virus. These could be accessory proteins needed for the replication of the virus after the initial attachment step as well as physiological conditions required for viral replication. A classical example is the receptor for influenza virus.

Although sialic acid carbohydrate moieties are present in lipids or proteins on cellular membranes of most tissues, influenza virus infects only the upper respiratory tract.

The importance of studying virus receptors and their role in determining tissue and host specificity is clearly demonstrated by the way this field of research has grown in the past four years. New biochemical techniques and the better understanding of the biology of the cell made possible the cloning and characterization of several virus receptors. For example the receptors for poliovirus, human rhinovirus, human coronavirus-229E, MHV-A59 and others have been cloned. Our laboratory has been involved in the study of receptors for coronaviruses and I have been interested in the receptor for the rat coronavirus and in the importance of the interaction of hemagglutinin-esterase, expressed in some coronaviruses, with Neu5,9Ac_2 as an alternative mechanism of viral entry.

For our future studies on the rat coronavirus receptor we will prepare membrane preparations from susceptible tissues, e.g. parotid or lacrimal glands, as immunogens for the identification of a monoclonal antibody that protects cells from infection. Such an antibody would be instrumental in the identification and purification of the receptor using methods such as gel filtration and monoclonal antibody affinity chromatography. Based on the amino acid sequence of the purified protein oligonucleotide probes would be

designed for the isolation of the cDNA encoding the receptor. The isolation of a full length receptor cDNA clone, would allow transfection of non permissive cells. Detection of virus attachment or infection on the transfected cells would provide proof that the cloned cDNA encodes for a functional rat coronavirus receptor.

At the same time we think it is worth testing whether the rat homologs of other identified coronavirus receptors could serve as receptors for rat coronavirus. For example, both HCV-229E and TGEV which are closely related serologically use the same molecule, aminopeptidase N, as a receptor in the host species they infect. Although MHV and rat coronavirus are in the same serologic group, the disease pattern they produce in their specific hosts is quite different. Since the beginning of this project, the MHV receptor has been identified and characterized as a member of the CEA family of glycoproteins. The pattern of expression of the different CEA family members on different tissues is complex and not completely understood in the rat and the mouse. It will be of interest to determine whether rat coronavirus uses a rat CEA-like molecule as its receptor.

The isolation of the rat coronavirus receptor would be of enormous help to answer many questions. Regarding the species specificity of the virus we would want to determine whether the restriction to one host is determined at the

level of virus attachment or at subsequent steps in the viral replication cycle. We could also determine whether tissue tropism follows the pattern of receptor expression in different organs. Finally, the virus-receptor complex could be studied to identify the parts of the receptor and the VAP that interact with each other. These studies on virus attachment will aid to the development of a mechanistic picture of the viral entry process.

VI. BIBLIOGRAPHY

Armstrong, R., Friedrich Jr., V. L., Holmes, K. V., Dubois-Daleq. M. (1990). In vitro analysis of the oligodendrocyte lineage in mice during demyelination and remyelination. J. Cell Biol. **111**, 1183-1195.

Bailey, O. T., Pappenheimer, A. M., Cheever, F. S., and Daniels, J. B. (1949). A murine virus (JHM) causing disseminated encephalomyelitis with extensive destruction of myelin. II. Pathology. J. Exp. Med. **90**, 195-212.

Bang, F. B. and Warwick, A. (1960). Mouse macrophages as host cells for the mouse hepatitis virus and the genetic basis of their susceptibility. Proc. Natl. Acad. Sci. U. S. A. **46**, 1065-1075.

Baric, R. S., Stohlman, S. A., Razavi, M. K., and Lai, M. M. C. (1985). Characterization of leader-related small RNAs in coronavirus-infected cells: further evidence for leader-primed mechanism of transcription. Virus Res. **3**, 19-33.

Barthold, S. W., Smith, A. L., Lord, P. F., Bhatt, P. N., Jacoby, R. O., and Main, A. J. (1982). Epizootic coronaviral typhlocolitis in suckling mice. Lab. Anim. Sci. **32**, 376-383.

Barthold, S. W. and Smith, A. L. (1984). Mouse hepatitis virus strain-related patterns of tissue tropism in suckling mice. Arch. Virol. **81**, 103-112.

Beaudette, F. R. and Hudson, C. B. (1937). Cultivation of the virus of infectious bronchitis. J. Am. Vet. Med. Assoc. **90**, 51-60.

Bhatt, P. N., Percy, D., and Jones, A. M. (1972). Characterization of the virus of sialodacryoadenitis of rats: A member of the coronavirus group. J. Infect. Dis. **126**, 123-130.

Boursnell, M. E., Brown, T. D., Foulds, I. J., Green, P. F., Tomley, F. M., and Binns, M. M. (1987). Completion of the sequence of the genome of the coronavirus avian infectious bronchitis virus. J. Gen. Virol. **68**, 57-77.

Boyle, J. F., Weismiller, D. G., and Holmes, K. V. (1987). Genetic resistance to mouse hepatitis virus correlates with absence of virus-binding activity on target tissues. J. Virol. **61**, 185-189.

Bradford, M. M.(1976). A rapid and sensitive method for the quantitation of protein utilizing the principle of protein dye binding. Anal. Biochem. **72**, 248-254.

Budzilowicz, C. J., Wilczynski, S. P., and Weiss, S. R. (1985). Three intergenic regions of coronavirus mouse hepatitis virus strain A59 genome RNA contain a common nucleotide sequence that is homologous to the 3' end of the viral mRNA leader sequence. J. Virol. **53**, 834-840.

Cavanagh, D., Brian, D. A., Enjuanes, L., Holmes, K. V., Lai, M. M., Laude, H., Siddell, S. G., Spaan, W., Taguchi, F., and Talbot, P. J. (1990). Recommendations of the Coronavirus Study Group for the nomenclature of the structural proteins, mRNAs, and genes of coronaviruses. Virology **176**, 306-307.

Cheever, F. S., Daniels, J. B., Pappenheimer, A. M., and Bailey, O. T. (1949). A murine virus (JHM) causing disseminated encephalomyelitis with extensive destruction of myelin I. Isolation and biological properties of the virus. J. Exp. Med. **90**, 181-194.

Coleman, P. M., and Ward, C. W. (1985). Structure and diversity of influenza virus neuraminidase. Curr. Top. Microbiol. Immunol. **11**, 177-255.

Collins, A. R., Knobler, R. L., Powell, H., and Buchmeier, M. J. (1982). Monoclonal antibodies to murine hepatitis

virus-4 (strain JHM) define the viral glycoprotein responsible for attachment and cell-cell fusion. Virology **119**, 358-371.

Colonno, R. J., Callahan, P. L., and Long, W. J. (1986). Isolation of a monoclonal antibody that blocks attachment of the major group of human rhinoviruses. J. Virol. **57**, 7-12.

Compton, S. R. (1988). Coronavirus Attachment and Replication, The Uniformed Services University of the Health Sciences, Bethesda, MD.

Compton, S. R., Rogers, D. B., Holmes, K. V., Fertsch, D., Remenick, J., and McGowan, J. J. (1987). In vitro replication of mouse hepatitis virus strain A59. J. Virol. **61**, 1814-1820.

Dalgleish, A. G., Beverly, P. C. L., Clapham, P. R., Crawford, D. H., Greaves, M. F. and Weiss, R. A. (1984). The CD4(T4) antigen is an essential component of the receptor for the AIDS retrovirus. Nature, **312**, 763-767.

Dalziel, R. G., Lampert, P. W., Talbot, P. J., and Buchmeier, M. J. (1986). Site-specific alteration of murine hepatitis virus type 4 peplomer glycoprotein E2 results in reduced neurovirulence. J. Virol. **59**, 463-471.

Delmas, B. and Laude, H. (1990). Assembly of coronavirus spike protein into trimers and its role in epitope expression. J. Virol. **64**, 5367-5375.

Denison, M. and Perlman, S. (1987). Identification of putative polymerase gene product in cells infected with murine coronavirus A59. Virology **157**, 565-568.

Deregt, D., Sabara, M., and Babiuk, L. A. (1987). Structural proteins of bovine coronavirus and their intracellular processing. J. Gen. Virol. **68**, 2863-2877.

Dick, G. W. A., Niven, J. S. F., and Gledhill, A. W. (1956). A virus related to that causing hepatitis in mice (MHV). Br. J. Exp. Pathol. **37**, 90-98.

Doyle, L. P. and Hutchings, L. M. (1946). A transmissible gastroenteritis in pigs. J. Am. Vet. Assoc. **108**, 257-259.

Dubois-Dalcq, M. E., Doller, E. W., Haspel, M. V., and Holmes, K. V. (1982). Cell tropism and expression of mouse hepatitis viruses (MHV) in mouse spinal cord cultures. Virology **119**, 317-331.

Dveksler, G. S., Pensiero, M. N., Cardellichio, C. B., Williams, R. K., Jiang, G. S., Holmes, K. V., and

Dieffenbach, C. W. (1991). Cloning of the mouse hepatitis virus (MHV) receptor: expression in human and hamster cell lines confers susceptibility to MHV. J. Virol. **65**, 6881-6891.

Dyer, C. A. and Benjamins, J. A. (1988). Redistribution and internalization of antibodies to galactocerebroside by oligodendroglia. J. Neurosci. **8**, 833-891.

Ebner, D., Raabe, T., and Siddell, S. G. (1988). Identification of the coronavirus MHV-JHM mRNA 4 product. J. Gen. Virol. **69**, 1041-1050.

Eppstein, D. A., Marsh, Y.V., Schreiber, A. B., Newman, S. R., Todaro, G. J., and Nestor, J. J. (1985). Epidermal growth factor receptor occupying inhibits vaccinia virus infection. Nature **318**, 663-665.

Fingeroth, J. D., Weis, J. J., Tedder, T. F., Strominger, J. L., Biro, P. A. and Fearon, D. T. (1984). Epstein-Barr virus receptor of human B lymphocytes is the C3d receptor CR2. Proc. Nat. Acad. Sci., U.S.A., **81**, 4510-4514.

Fleming, J. O., Trousdale, M. D., el-Zaatari, F. A., Stohlman, S. A., and Weiner, L. P. (1986). Pathogenicity of antigenic variants of murine coronavirus JHM selected with

monoclonal antibodies. J. Virol. **58**, 869-875.

Fox, G., Parry, N. R., Barnett, P. V., McGinn B., Rowlands, D. J., and Brown, F. (1989). The cell attachment site on foot and mouth disease virus includes the amino acid sequence RGD (arginine-glycine-aspartic acid). J. Gen. Virol. **70**, 625-637.

Frana, M. F., Behnke, J. N., Sturman, L. S., and Holmes, K. V. (1985). Proteolytic cleavage of the E2 glycoprotein of murine coronavirus: host-dependent differences in proteolytic cleavage and cell fusion. J. Virol. **56**, 912-920.

Gaertner, D. J., Smith, A. L., Paturzo, F. X., and Jacoby, R. O. (1991). Susceptibility of rodent cell lines to rat coronaviruses and differential enhancement by trypsin or DEAE-dextran. Arch. Virol. **118**, 57-66.

Gledhill, A. W. and Andrewes, C. H. (1951). A hepatitis virus of mice. Brit. J. Exp. Path. **32**, 559.

Greve, J. G., Davis, G., Meyer, A. M., Forte, C. P., Yost, S. C., Marlov, C. W., Kamarck, M. E., and Mc Clelland, A. (1989). The major human rhinovirus receptor is ICAM-1. Cell **56**, 839-847.

Herrler, G., Rott, R., Klenk, H. -D., Muller, P., Shukla, A. K., and Schauer, R. (1985). The receptor-destroying enzyme of influenza C virus is neuraminate-O-acetylesterase. EMBO. J. **4**, 1503-1506.

Herrler, G. and Klenk, H. D. (1987). The surface receptor is a major determinant of the cell tropism of influenza C virus. Virology **159**, 102-108.

Hirano, N., Murakami, T., Taguchi, F., Fujiwara, K., and Matumoto, M. (1981). Comparison of mouse hepatitis virus strains for pathogenicity in weanling mice infected by various routes. Arch. Virol. **70**, 69-73.

Hirano, N., Takamaru, H., Ono, K., Murakami, T., and Fujiwara, K. (1986). Replication of sialodacryoadenitis virus of rat in LBC cell culture. Brief report. Arch. Virol. **88**, 121-125.

Holmes, K. V. (1989). Virology (Fields, B. N., Ed.) 2nd edition. Raven Press, New York.

Holmes, K. V., Doller, E. W., and Sturman, L. S. (1981). Tunicamycin resistant glycosylation of coronavirus glycoprotein: demonstration of a novel type of viral glycoprotein. Virology **115**, 334-344.

Homsy, J., Meyer, M., Tateno, M., Clarkson, S., and Levy, J. A. (1989). The Fc and not CD4 receptor mediates antibody enhancement of HIV infection in human cells. Science **244**, 1357-1360.

Innes, J. R. M. and Stanton, M. F. (1961). Acute disease of the submaxillary gland and Harderian glands (sialodacryoadenitis) of rats with cytomegaly and no inclusion bodies. Am. J. Pathol. **38**, 455-468.

Jacobs, L., Spaan, W. J., Horzinek, M. C., and van der Zeijst, B. A. M. (1981). Synthesis of subgenomic mRNA's of mouse hepatitis virus is initiated independently: evidence from UV transcription mapping. J. Virol. **39**, 401-406.

Jacoby, R. O. (1986). Viral and Mycoplasmal Infections of Rodents (Bhatt, P. N., Jacoby, R. O., Morse, H. C., and New, A. E. , Eds.) Academic Press, New York. 625-638.

Jubelt, B. G., Gallez-Hawkins, O., Naranyan, H., and Johnson, R. T. (1980). Pathogenesis of human poliovirus infection in mice. I. Clinical and pathological studies. J. Neuropath. Exp. Neurol. **39**, 138-149.

Kauffman, R. S., Noseworthy, J. H., Nepom, J. T., Finberg, R., Fields, B. N., and Greene, M. I. (1983). Cell receptors

for the mammalian reovirus. II. Monoclonal anti-idiotypic antibody blocks viral binding to cells. J. Immunol. **131**, 2539-2541.

Keck, J. G., Matsushima, G. K., Makino, S., Fleming, J. O., Vannier, D. M., Stohlman, S. A., and Lai, M. M. C. (1988a). In vivo RNA-RNA recombination of coronavirus in mouse brain. J. Virol. **62**, 1810-1813.

Keck, J. G., Soe, L. H., Makino, S., Stohlman, S. A., and Lai, M. M. C. (1988b). RNA recombination of murine coronaviruses: recombination between fusion-positive mouse hepatitis virus A59 and fusion-negative mouse hepatitis virus 2. J. Virol. **62**, 1989-1998.

Kessler, M., Acuto, O., Storelli, C., Murer, H., Muller, M., and Semenza, G. (1978). A modified procedure for the rapid preparation of efficiently transporting vesicles from small intestinal brush border membranes. Their use to investigate some properties of D-glucose and choline transport systems. Biochem. Biophys. Acta. **506**, 136-154.

King, B. and Brian, D. A. (1982). Bovine coronavirus structural proteins. J. Virol. **42**, 700-707.

King, B., Potts, B. J., and Brian, D. A. (1985). Bovine

coronavirus hemagglutinin protein. Virus. Res. **2**, 53-59.

Klatzmann, D., Barrë-Sinoussi, F., Nugeyre, M. T., Danquet, C., Vilmer, E., Griscelli, C., Brun-Veziret, F., Rouzioux, C., Gluckman, J. C., and Chermann, J. C. (1984a). Selective tropism of lymphadenopathy associated virus (LAV) for helper-inducer T lymphocytes. Science **225**, 59-63.

Klatzmann, D., Champagne, E., Chamaret, S., Gruest, J., Guetard, D., Hercend, T., Gluckman, J. C., and Montagnier, L. (1984b). T-lymphocyte T4 molecule behaves as the receptor for human retrovirus LAV. Nature **312**, 767-768.

Knobler, R. L., Haspel, M. V., and Oldstone, M. B. (1981). Mouse hepatitis virus type 4 (JHM strain)-induced fatal central nervous system disease. I. Genetic control and murine neuron as the susceptible site of disease. J. Exp. Med. **153**, 832-843.

Kraft, L. M.(1962). An apparently new lethal virus disease of infant mice. Science **137**, 282-283.

La Monica, N., Banner, L. R., Morris, V. L., and Lai, M. M. (1991). Localization of extensive deletions in the structural genes of two neurotropic variants of murine coronavirus JHM. Virology **182**, 883-888.

Lai, M. M. C., Makino, S., Soe, L. H., Shieh, C. -K., Keck, J. G., and Fleming, J. O. (1987). Coronavirus: A jumping RNA transcription. Cold Spring Harbor Symposia on Quantative Biology **42**, 359-365.

Lapps, W., Hogue, B. G., and Brian, D. A. (1987). Sequence analysis of the bovine coronavirus nucleocapsid and matrix protein genes. Virology **157**, 47-57.

Lasky, L. A., Nakamura, G., Smith, D. H., Fence, C., Shimasaki, C., Patzer, E., Berman, P., Gregory, T. and Capon, D. J. (1987). Delineation of a region of the human immunodeficiency virus type 1 gp120 glycoprotein critical for interaction with the CD4 receptor. Cell **50**, 975-985.

Laude, H., Rasschaert, D., and Huet, J. C. (1987). Sequence and N-terminal processing of the transmembrane protein E1 of the coronavirus transmissible gastroenteritis virus. J. Gen. Virol. **68**, 1687-1693.

Lavi, E., Gilden, D. H., Highkin, M. K., and Weiss, S. R. (1984a). Persistence of mouse hepatitis virus A59 RNA in a slow virus demyelinating infection in mice as detected by in situ hybridization. J. Virol. **51**, 563-566.

Lavi, E., Gilden, D. H., Wroblewska, Z., Rorke, L. B., and

Weiss, S. R. (1984b). Experimental demyelination produced by the A59 strain of mouse hepatitis virus. Neurology **34**, 597-603.

Lavi, E., Gilden, G. H., Wroblewska, Z., Rorke, L. B., and Weiss, S. R. (1984c). Molecular biology and pathogenesis of coronaviruses (Rottier, P. J., van der Zeijst, B. A. M., Spaan, W. J. M., and Horzinek, M. , Eds.) Plenum Publishing Corp., New York. 237-246.

Le Prevost, C., Levy-Leblond, E., Virelizier, J. L., and Dupuy, J. M. (1975a). Immunopathology of mouse hepatitis virus type 3 infection. Role of humoral and cell-mediated immunity in resistance mechanisms. J. Immunol. **114**, 221-225.

Le Prevost, C., Virelizier, J. L., and Dupuy, J. M. (1975b). Immunopathology of mouse hepatitis virus type 3 infection. III Clinical and virologic observation of a persistent viral infection. J. Immunol. **115**, 640-643.

Leibowitz, J. L., Perlman, S., Weinstock, G., DeVries, J. R., Budzilowicz, C., Weissemann, J. M., and Weiss, S. R. (1988). Detection of a murine coronavirus nonstructural protein encoded in a downstream open reading frame. Virology **164**, 156-164.

Lentz, T. L. (1990). The recognition event between virus and host cell receptor: a target for antiviral agents. J. Gen. Virol **71**, 751-766.

Lin, S. H. and Guidotti, G. (1989). Cloning and expression of a cDNA coding for a rat liver plasma membrane ecto-ATPase. The primary structure of the ecto-ATPase is similar to that of the human biliary glycoprotein I. J. Biol. Chem. **264**, 14408-14414.

Lindsey, J. R. (1986). Viral and Mycoplasmal Infections of Rodents (Bhatt, P. N., Jacoby, R. O., Morse, H. C., and New, A. E. , Eds.) Academic Press, New York. 801-808.

Lucas, A., Flintoff, W., Anderson, R., Percy, D., Coulter, M., and Dales, S. (1977). In vivo and in vitro models of demyelinating diseases: Tropism of the JHM strain of murine hepatitis virus for cells of glial origin. Cell **12**, 553-560.

Luytjes, W., Bredenbeek, P. J., Noten, A. F., Horzinek, M. C., and Spaan, W. J. (1988). Sequence of mouse hepatitis virus A59 mRNA 2: Indications for RNA recombination between coronaviruses and influenza C virus. Virology **166**, 415-422.

Macnaughton, M. R., Davies, H. A., and Nermut, M. V. (1978). Ribonucleoprotein-like structures from coronavirus

particles. J. Gen. Virol. **39**, 545-549.

Maddon, P. J., Dalgleish, A. G., McDougal, J. S., Clapham, P. R., Weiss, R. A., and Axel, R. (1986). The T4 gene encodes the AIDS virus receptor and is expressed in the immune system and the brain. Cell **47**, 333-348.

Makino, S., Keck, J. G., Stohlman, S. A., and Lai, M. M. C. (1986). High-frequency RNA recombination of murine coronaviruses. J. Virol. **57**, 729-737.

Manaker, R. A., Piczak, C. V., Miller, A. A., and Stanton, M. F. (1961). A hepatitis complicating studies with mouse leukemia. J. Natl. Cancer Inst. **27**, 29-51.

Maru, M. and Sato, K. (1982). Characterization of a coronavirus isolated from rats with sialoadenitis. Arch. Virol. **73**, 33-43.

McDougal, J. S., Kennedy, M. S., Sligh, J. M., Cort, S. P., Mawle, A., and Nicholson, J. K. (1986). Binding of HTLV-III/LAV to T4+ T cells by a complex of the 110K viral protein and the T4 molecule. Science **231**, 382-385.

Mendelsohn, C. L., Wimmer, E., and Racaniello, V. R. (1989). Cellular receptor for poliovirus: molecular cloning,

nucleotide sequence, and expression of a new member of the immunoglobulin superfamily. Cell **56**, 855-865.

Menezes, J., Seigneurin, J. M., Patel, P., Bourkas, A., and Lenoir, G. (1977). Presence of Epstein-Barr virus receptors, but absence of virus penetration, in cells of an Epstein-Barr virus genome-negative human lymphoblastoid T line (Molt 4). J. Virol. **22**, 816-821.

Minor, P. D., Pipkin, P. A., Hockley, D., Schild, G. C., and Almond, J. W. (1984). Monoclonal antibodies which block cellular receptors of poliovirus. Virus Res. **1**, 203-212.

Morris, V. L., Tieszer, C., Mackinnon, J., and Percy, D. (1989). Characterization of coronavirus JHM variants isolated from Wistar Furth rats with a viral-induced demyelinating disease. Virology **169**, 127-136.

Nagashima, K., Wege, H., Meyermann, R., and ter Meulen, V. (1978). Corona virus induced subacute demyelinating encephalomyelitis in rats: a morphological analysis. Acta Neuropathol. (Berl) **44**, 63-70.

Nakada, S., Creager, R. S., Krystal, M., Aaronson, R. P., and Palese, P. (1984). Influenza C virus hemagglutinin: comparison with influenza A and B virus hemagglutinins. J.

Virol. **50**, 118-124.

Nelson, J. B.(1952). Acute hepatitis associated with mouse leukemia. I. pathological features and transmission of the disease. J. Exp. Med. **96**, 293-303.

Nemerow, G. R., Houghten, R. A., Moore, M. D., and Cooper, N. R. (1989). Identification of an epitope in the major envelope protein of Eppstein-Barr virus that mediates viral binding to the B lymphocyte EBV receptor (CR2). Cell **56**, 369-377.

Neville, D. M.,Jr. (1976). Biochemical analysis of membranes (Maddy, A. H., Ed.) John Wiley and Sons, New York. 27-54.

Palese, P. and Schulman, J. L. (1976). Mapping of the influenza virus genome: identification of the hemagglutinin and the neuraminidase genes. Proc. Natl. Acad. Sci. U. S. A. **73**, 2142-2146.

Parker, J. S., Cross, S. S., and Rowe, W. R. (1970). Rat coronavirus (RCV), a prevelant naturally occuring pneumotropic virus of rats. Arch. Gesamte. Virusforsch. **31**, 293-302.

Parker, M. D., Cox, G. J., Deregt, D., Fitzpatrick, D. R.,

and Babiuk, L. A. (1989). Cloning and in vitro expression of the gene for the E3 haemagglutinin glycoprotein of bovine coronavirus. J. Gen. Virol **70**, 155-164.

Pasick, J. M. M., and Dales, S. (1991). Infection by Coronavirus JHM of rat neurons and oligodendrocyte-type-2 astrocyte lineage cells during distinct developmental stages. J. Virol. **65**, 5013-5028.

Paulson, J. C. (1985). The Receptors, vol. 2 (Conn P.M. Ed.) Academic Press, New York. 131-219.

Paulson, J. C., Sadler, J. E., and Hill, R. L. (1979). Restoration of specific myxovirus receptors to asialoerythrocytes by incorporation of sialic acid with pure sialyltransferases. J. Biol. Chem. **254**, 2120-2124.

Percy, D. H., Hanna, P. E., Paturzo, F. X., and et.al., (1984). Comparison of strain susceptibility to experimental sialodacryoadenitis in rats. Lab. Anim. Sci. **34**, 255-260.

Percy, D., Bond, S., and MacInnes, J. (1989). Replication of sialodacryoadenitis virus in mouse L-2 cells. Arch. Virol **104**, 323-333.

Percy, D. H. and Williams, K. L. (1990). Experimental

Parker's coronavirus infection in Wistar rats. Lab. Anim. Sci. **40**, 603-607.

Percy, D. H., Williams, K. L., Bond, S. J., and MacInnes, J. I. (1990). Characteristics of Parker's rat coronavirus (PRC) replicated in L-2 cells. Arch. Virol. **112**, 195-202.

Pfleiderer, M., Routledge, E., and Sidell, S. G. (1990). Coronaviruses and their Diseases (Cavangh, D. and Brown, T. D. K. , Eds.) Plenum, New York. 21-31.

Pfleiderer, M., Routledge, E., Herrler, G., and Siddell, S. G. (1991). High level transient expression of the murine coronavirus haemagglutinin-esterase. J. Gen. Virol. **72(6)**, 1309-1315.

Robbins, S. G., Frana, M. F., McGowan, J. J., Boyle, J. F., and Holmes, K. V. (1986). RNA-binding proteins of coronavirus MHV: detection of monomeric and multimeric N protein with an RNA overlay-protein blot assay. Virology **150**, 402-410.

Rogers, G. N., Herrler, G., Paulson, J. C., and Klenk, H. D. (1986). Influenza C virus uses 9-O-acetyl-N-acetylneuraminic acid as a high affinity receptor determinant for attachment to cells. J. Biol. Chem. **261**, 5947-5951.

Rottier, P. J., Welling, G. W., Welling-Wester, S., Niesters, H. G., Lenstra, J. A., and van der Zeijst, B. A. M. (1986). Predicted membrane topology of the coronavirus protein E1. Biochemistry. **25**, 1335-1339.

Sawicki, S. G. and Sawicki, D. L. (1986). Coronavirus minus-strand RNA synthesis and effect of cycloheximide on coronavirus RNA synthesis. J. Virol. **57**, 328-334.

Schalk, A. F. and Hawn, M. C. (1931). An apparently new respiratory disease of baby chicks. J. Am. Vet. Med. Assoc. **78**, 413-422.

Schultze, B., Gross, H. J., Brossmer, R., Klenk, H. D., and Herrler, G. (1990). Hemagglutinating encephalomyelitis virus attaches to N-acetyl-9-O-acetylneuraminic acid-containing receptors on erythrocytes: comparison with bovine coronavirus and influenza C virus. Virus. Res. **16**, 185-194.

Schultze, B., Gross, H. J., Brossmer, R., and Herrler, G. (1991a). The S protein of bovine coronavirus is a hemagglutinin recognizing 9-O-Acetylated sialic acid as a receptor determinant. J. Virol. **65**, 6232-6237.

Schultze, B., Wahn, K., Klenk, H. D., and Herrler, G. (1991b). Isolated HE-protein from hemagglutinating

encephalomyelitis virus and bovine coronavirus has receptor-destroying and receptor-binding activity. Virology. **180**, 221-228.

Schultze, B. and Herrler, G. (1992). Bovine coronavirus uses N-acetyl-9-0-acetylneuraminic acid as a receptor determinant to initiate the infection of cultured cells. J. Gen. Virol. **73**, 901-906.

Sethna, P. B., Hung, S. L., and Brian, D. A. (1989). Coronavirus subgenomic minus-strand RNAs and the potential for mRNA replicons. Proc. Natl. Acad. Sci. U. S. A. **86**, 5626-5630.

Siddell, S. (1982). Coronavirus JHM: tryptic peptide fingerprinting of virion proteins and intracellular polypeptides. J. Gen. Virol. **62**, 259-269.

Siddell, S.(1983). Coronavirus JHM: coding assignments of subgenomic mRNAs. J. Gen. Virol. **64**, 113-125.

Siddell, S., Wege, H., and ter Meulen, V. (1982). The structure and replication of coronaviruses. Curr. Top. Micro. Imm. **99**, 131-163.

Smith, M. S., Click, R. E., and Plagemann, P. G. (1984).

Control of mouse hepatitis virus replication in macrophages by a recessive gene on chromosome 7. J. Immunol. **133**, 428-432.

Smith, D. H., Byrn, R. A., Marsters, S. A., Gregory, T., Groopman, J. E. and Capon, D. J. (1987). Blocking of HIV-1 infectivity by a soluble secreted form of the CD4 antigen. Science **238**, 1704-1707.

Soe, L. H., Shieh, C. K., Baker, S. C., Chang, M. F., and Lai, M. M. C. (1987). Sequence and translation of the murine coronavirus 5'-end genomic RNA reveals the N-terminal structure of the putative RNA polymerase. J. Virol. **61**, 3968-3976.

Sorensen, O., Perry, D., and Dales, S. (1980). In vivo and in vitro models of demyelinating diseases. III. JHM virus infection of rats. Arch. Neurol. **37**, 478-484.

Spaan, W., Cavanagh, D., and Horzinek, M. C. (1988). Coronaviruses: structure and genome expression. J. Gen. Virol. **69**, 2939-2952.

Staunton, D. E., Merluzzi, V. J., Rothlein, R., Barton, R., Marlin, S. D., and Springer, T. A. (1989). A cell adhesion molecule, ICAM-1, is the major surface receptor for

rhinoviruses. Cell **56**, 849-853.

Stern, D. F. and Sefton, B. M. (1982). Coronavirus proteins: structure and function of the oligosaccharides of the avian infectious bronchitis virus glycoproteins. J. Virol **44**, 804-812.

Stohlman, S. A. and Frelinger, J. A. (1978). Resistance to fatal central nervous system disease by mouse hepatitis virus strain JHM. I. Genetic analysis. Immunogenetics **6**, 277-281.

Stohlman, S. A., Frelinger, J. A., and Weiner, L. P. (1980). Resistance to fatal central nervous system disease by mouse hepatitis virus, strain JHM. II. Adherent cell-mediated protection. J. Immunol. **124**, 1733-1739.

Storz, J., Rott, R., and Kaluza, G. (1981). Enhancement of plaque formation and cell fusion of an enteropathogenic coronavirus by trypsin treatment. Infect. Immun. **31**, 1214-1222.

Stuhler, A., Wege, H., and Siddell, S. G. (1991). Localization of antigenic sites on the surface glycoprotein of mouse hepatitis virus. J. Gen. Virol. **72**, 1655-1658.

Sturman, L. S. and Takemoto, K. K. (1972). Enhanced growth of a murine coronavirus in transformed mouse cells. Infect. Immun. **6**, 501-507.

Sturman, L. S. and Holmes, K. V. (1983). The molecular biology of coronaviruses. Adv. Virus. Res. **28**, 35-112.

Sturman, L. S., Holmes, K. V., and Behnke, J. (1980). Isolation of coronavirus envelope glycoproteins and interaction with the viral nucleocapsid. J. Virol. **33**, 449-462.

Sturman, L. S., Ricard, C. S., and Holmes, K. V. (1985). Proteolytic cleavage of the E2 glycoprotein of murine coronavirus: Activation of cell-fusing activity of virions by trypsin and separation of two different 90K cleavage fragments. J. Virol. **56**, 904-911.

Sugiyama, K. and Amano, Y. (1980). Hemagglutination and structural polypeptides of a new coronavirus associated with diarrhea in infant mice. Arch. Virol. **66**, 95-105.

Sugiyama, K. and Amano, Y. (1981). Morphological and biological properties of a new coronavirus associated with diarrhea in infant mice. Arch. Virol. **67**, 241-251.

Sugiyama, K., Ishikawa, R., and Fukuhara, N. (1986). Structural polypeptides of the murine coronavirus DVIM. Arch. Virol. **89**, 245-254.

Swift, A. M. and Machamer, C. E. (1991). A Golgi retention signal in a membrane-spanning domain of coronavirus E1 protein. J. Cell Biol. **115**, 19-30.

Taguchi, F., Siddell, S. G., Wege, H., and ter Meulen, V. (1985). Characterization of a variant virus selected in rat brains after infection by coronavirus mouse hepatitis virus JHM. J. Virol. **54**, 429-435.

Taguchi, F., Massa, P. T., and ter Meulen, V. (1986). Characterization of variant virus isolated from neural cell culture after infection of mouse coronavirus JHMV. Virology **155**, 267-270.

Tardieu, M., Epstein, R. L., and Weiner, H. L. (1982). Interaction of viruses with cell surface receptors. Int. Rev. Cytol. **80**, 27-61.

Tomassini, J. E., Graham, D., De Witt, C. M., Lineberger, D. W., Rodkey, J. A., and Colonno, R. J. (1989). cDNA Cloning Reveals that the Major Group Rhinovirus Receptor on HeLa Cells is Intercellular Adhesion Molecule 1. Proc. Natl.

Acad. Sci. U. S. A. **86**, 4907-4911.

Tooze, S. A., Tooze, J., and Warren, G. (1988). Site of addition of N-acetyl-galactosamine to the E1 glycoprotein of mouse hepatitis virus-A59. J. Cell Biol. **106**, 1475-1487.

Tschachler, E., Groh, V., Popovic, M., Mann, D. L., Konrad, K., Safai, B., Eron, L., diMarzo Veronese, F., Wolff, K., and Stingl, G. (1987). Epidermal Langerhans cells--a target for HTLV-III/LAV infection. J. Invest. Dermatol. **88**, 233-237.

Tyrrell, D. A., Almeida, J. D., Berry, D. M., Cunningham, C. H., Hamre, D., Hofstad, M. S., Mallucci, L., and McIntosh, K. (1968). Coronaviruses. Nature **220**, 650.

Tyrrell, D. A., Almeida, J. D., Cunningham, C. H., Dowdle, W. R., Hofstad, M. S., McIntosh, K., Tejima, M., Zakstelskaya, L. Y. A., Easterday, B. C., Kapikian, A. Z., and Bingham, R. W. (1975). Coronaviridae. Intervirology **5**, 76-82.

Vlasak, R., Krystal, M., Nacht, M., and Palese, P. (1987). The influenza C virus glycoprotein (HE) exhibits receptor-binding (hemagglutinin) and receptor-destroying (esterase) activities. Virology **160**, 419-425.

Vlasak, R., Luytjes, W., Leider, J., Spaan, W., and Palese, P. (1988a). The E3 protein of bovine coronavirus is a receptor-destroying enzyme with acetylesterase activity. J. Virol. **62**, 4686-4690.

Vlasak, R., Luytjes, W., Spaan, W., and Palese, P. (1988b). Human and bovine coronaviruses recognize sialic acid-containing receptors similar to those of influenza C viruses. Proc. Natl. Acad. Sci. U. S. A. **85**, 4526-4529.

Wege, H., Sidell, S., and ter Meulen, V. (1982). The biology and pathogenesis of coronaviruses. Curr. Top. Microbiol. Immun. **99**, 165-200.

Wege, H., Winter, J., and Meyermann, R. (1988). The peplomer protein E2 of coronavirus JHM as a determinant of neurovirulence: definition of critical epitopes by variant analysis. J. Gen. Virol. **69**, 87-98.

Weiner, L. P.(1973). Pathogenesis of demyelination induced by a mouse hepatitis virus (JHM virus). Arch. Neurol. **28**, 293-303.

Weir, E. C., Jacoby, R. O., Paturzo, F. X., Johnson, E. A., and Ardito, R. B. (1990). Persistence of sialodacryoadenitis virus in athymic rats [published erratum appears in Lab Anim

Sci 1991 Jun;41(3):291]. Lab. Anim. Sci. **40**, 138-143.

Weis, W., Brown, J. H., Cusack, S., Paulson, J. C., Skehel, J. J., and Wiley, D. C. (1988). Structure of the influenza virus haemagglutinin complexed with its receptor, sialic acid. Nature **333**, 426-431.

Williams, R. K., Jiang, G. S., Snyder, S. W., Frana, M. F., and Holmes, K. V. (1990). Purification of the 110-kilodalton glycoprotein receptor for mouse hepatitis virus (MHV)-A59 from mouse liver and identification of a nonfunctional, homologous protein in MHV-resistant SJL/J mice. J. Virol. **64**, 3817-3823.

Williams, R. K., Jiang, G. S., and Holmes, K. V. (1991). Receptor for mouse hepatitis virus is a member of the carcinoembryonic antigen family of glycoproteins. Proc. Natl. Acad. Sci. U. S. A. **88**, 5533-5536.

Woyciechowska, J. L., Trapp, B. D., Patrick, D. H., Shekarchi, I. C., Leinikki, P. O., Sever, J. L., and Holmes, K. V. (1984). Acute and subacute demyelination induced by mouse hepatitis virus strain A59 in C3H mice. J. Exp. Pathol. **1**, 295-306.

Yokomori, K., La Monica, N., Makino, S., Shieh, C. K., and

Lai, M. M. (1989). Biosynthesis, structure, and biological activities of envelope protein gp65 of murine coronavirus. Virology **173**, 683-691.

Yokomori, K., Banner, L. R., and Lai, M. M. (1991). Heterogeneity of gene expression of the hemagglutinin-esterase (HE) protein of murine coronaviruses. Virology **183**, 647-657.